UNIVERSITEIT VAN PRETORIA
UNIVERSITY OF PRETORIA
YUNIBESITHI YA PRETORIA

Probing the Effects of Retinoblastoma Binding Protein 6 (RBBP6) Knockdown on the sensitivity of Cisplatin in Cervical Cancer cells

Harshini Mehta

(16025483)

Submitted in partial fullfillment of the requirements for the degree:

MSc Genetics

Faculty of Natural and Agricultural Sciences

Department of Biochemistry Genetics and Microbiology

Division of Genetics

University of Pretoria

Pretoria

2 March 2022

UNIVERSITEIT VAN PRETORIA
UNIVERSITY OF PRETORIA
YUNIBESITHI YA PRETORIA

Submission declaration

I, **HARSHINI MEHTA** declare that this dissertation, which I hereby submit for the degree **MSC GENETICS** at the University of Pretoria, is my own work and has not previously been submitted by me for a degree at this or any other tertiary institution.

Signature: Harshini Mehta

Date: 2 March 2022

UNIVERSITEIT VAN PRETORIA
UNIVERSITY OF PRETORIA
YUNIBESITHI YA PRETORIA

Plagiarism declaration

University of Pretoria

Faculty of Natural and Agricultural Sciences

Department of Biochemistry, Genetics and Microbiology

Division of Genetics

Full name: **Harshini Mehta** Student number: **16025483**

Title of work: **Probing the effects of Retinoblastoma Binding Protein 6 (RBBP6) knockdown on the sensitivity of cisplatin in cervical cancer cells.**

1. I understand what plagiarism entails and am aware of the University's policy in this regard.
2. I declare that this MSc. Dissertation is my own original work. Where someone else's work was used (whether from a printed source, the internet, or any other source) due acknowledgement was given and reference was made according to departmental requirements.
3. I did not make use of another student's previous work and submit it as my own.
4. I did not allow and will not allow anyone to copy my work with the intention of presenting it as his or her own work.

Signature: 

Date: 2 March 2022

TABLE OF CONTENTS

Abbreviations

ABC	ATP-Binding Cassette
Ago2	Argonaute 2
AIDS	Acquired Immune Deficiency Syndrome
APAF-1	Apoptotic Protease Activating Factor-1
ATM	Ataxia Telangiectasia Mutated
ATP7A/B	Adenosine Triphosphatase-7-Alpha/Beta
Bad	Bcl-xL/BCL-2-Associated Death protein
Bax	BCL-2-Associated Death protein
Bcl-2	B-Cell Leukaemia-2
BH3	Bcl-2 Homology 3
BVZ	Bevacizumab
Ca^{2+}	Calcium Ion
CaSki	Cervical cancer cell line
Caspase	Cysteine Aspartic-Specific Proteases
CD4	Cluster of Differentiation-4
CDDP	Cisplatin
CDK1	Cyclin-Dependent Kinase-1
cDNA	Complementary DNA
Chl	Chloroform
CI	Cell Index
CIN 1	Grade 1 Cervical Intraepithelial Neoplasia
Cl^-	Chloride Ion
CO_2	Carbon dioxide
CPT	Camptothecin
CRB	Carboplatin
CTR1	Copper Transporter Receptor 1

Cyt c	Cytochrome c
dH_2O	Distilled water
DMEM	Dulbecco's Modified Eagle's Medium
DMSO	Dimethyl Sulfoxide
DNA	Deoxyribonucleic Acid
DNase	Deoxyribonuclease
dNTP	Deoxy-Nucleotide-Triphosphate
DWNN	Domain With No Name
E	Early (Region)
E. coli	*Escherichia coli*
E2F	E2 Transcription Factor
E6AP	E6-Associated Protein
EGFR	Epidermal Growth Factor Receptor
EP	European Pharmacopoeia
ER	Endoplasmic Reticulum
ERCC1	Excision Repair Cross-Complementation 1
EtBr	Ethidium Bromide
EtOH	Ethanol
FBS	Fetal Bovine Serum
FDA	Food and Drug Administration
FITC	Fluorescein Isothiocyanate
G1/2	Growth Phase 1/2
GABA	Gamma Amino Butyric Acid
GAPDH	Glyceraldehyde 3-Phosphate Dehydrogenase
GITC	Guanidinium Isothiocyanate
GSH	Glutathione
HCK1T	Human Cervical Keratinocytes
HeLa	Henrietta Lacks

HIV	Human Immunodeficiency Virus
HPV	Human Papillomavirus
HR-HPV	High Risk-Human Papillomavirus
IC_{50}	Inhibitory Concentration
IDT	Integrated DNA Technologies
IFO	Ifosfamide
IP3	Inositol 1,4,5-Trisphosphate
IPOH	Isopropyl Alcohol
IRI	Irinotecan
IV	Intravenous
L	Late (Region)
LCR	Long Control Region
LR-HPV	Low Risk-Human Papillomavirus
M	Mitotic Phase
Mad2	Mitotic Arrest Deficient-2
MCF-7	Michigan Cancer Foundation-7
MDM2	Mouse Double Minute 2
MDR	Multi-Drug Resistance
Mg^{2+}	Magnesium Ion
$MgCl_2$	Magnesium Chloride
MMR	Mismatch Repair
MOMP	Mitochondrial Outer Membrane Permeability
MRC-5	Human Fetal Lung Fibroblast
mRNA	Messenger Ribonucleic Acid
MRP	Multi-Drug Resistant Protein
MSH2	MutS Homolog 2
MTT	Methyl Thiazolyl Tetrazolium
NCR	National Cancer Registry

NER	Nucleotide Excision Repair
NH_3	Amine Group
NIBIOHN	National Institute of Biomedical Innovation, Health, and Nutrition
NSCLC	Non-Small Cell Lung Cancer
OMM	Outer Mitochondrial Membrane
ORF	Open Reading Frame
ORR	Overall Response Rate
OS	Overall Survival
p21	Cyclin-dependent kinase inhibitor 1
P2P-R	Proliferation Potential Protein-Related
p53	Tumor Suppressor Protein 53
PACT	p53-Associated Cellular protein Testis-derived
PAP	Papanicolaou
PBS	Phosphate Buffered Saline
PCD	Programmed Cell Death
PCR	Polymerase Chain Reaction
PI	Propidium Iodide
PMS2	Post-Meiotic Segregation 2
pRB	Retinoblastoma protein
PRO	Proline
PS	Phosphatidylserine
Pt	Platinum
PTX	Paclitaxel
qPCR	Quantitative Polymerase Chain Reaction
RBBP6	Retinoblastoma Binding Protein 6
RBQ-1	Retinoblastoma Binding Protein Q-1
RING	Really Interesting New Gene

RIPK	receptor Interacting Protein Kinase
RISC	RNA-Induced Silencing Complex
RNA	Ribonucleic Acid
RNAi	Ribonucleic Acid Interference
RNase	Ribonuclease
RNP	RNA-Protein
rRNA	Ribosomal Ribonucleic Acid
RT	Reverse Transcription
RTase	Reverse Transcriptase
RTCA	Real Time Cell Analyzer
RT-qPCR	Real Time Quantitative PCR
SEM	Standard Error of the Mean
SER	Serine
SiHa	Cervical cancer cell line
siRBBP6	Small Interfering RBBP6
siRNA	Small Interfering Ribonucleic Acid
Sirt1	Silent Information Regulator 1
SSCC	Small Cell Cervical Cancer
STS	Staurosporine
SYBR	Synergy Brands
T_a	Annealing temperature
Taq	*Thermus aquaticus*
T_m	Melting Temperature
TOPI	Topoisomerase I
TOPO	Topotecan
TP53	Tumor Suppressor Protein 53
TPB	Topoisomerase, Paclitaxel, Bevacizumab
tRNA	Transfer Ribonucleic Acid

TXR1	Taxol Resistance Gene 1
Vero	Non-cancerous African Green Monkey cell line
VIA	Visual Inspection using Acetic acid
WHO	World Health Organization
WT	Wild-Type
YB-1	Y-box-Binding protein 1
β2-AR	β2-Adrenergic Receptor

List of Tables

List of Figures

Acknowledgements

I would like to express my sincerest appreciation to my supervisor, Dr. Pontsho Moela, for giving me the opportunity to pursue my passion for genetics within her research group. I have learnt a great deal from her and am thankful for the endless support, encouragement, and guidance she has shown me these past four years. I would also like to extend my deepest gratitude to my co-supervisor, Dr. Melvin Ambele, for his invaluable insights and constructive criticism. I feel privileged to have had the honor of being mentored by two knowledgeable and highly experienced researchers in the field.

My success would not have been possible without the care and nurturing from my parents, Vijay and Jagruti Mehta. Despite living apart from them during my university years, their love, pride, and encouragement have never faltered. Even during trying times, they have supported me financially and allowed me to further my studies and pursue my master's degree. For that, I will always be indebted to them. I would like to thank my brother, Pranay Mehta, for always lending a patient and persistent hand with any IT issues that I struggled to solve, and my sister, Binal Mehta, who has continued to be my guide and my inspiration and who has pushed me to further better myself in all aspects of life. I cannot begin to express my thanks to my partner, Frikkie du Toit, for his unconditional love, and unwavering patience during some of the most stressful periods throughout this journey. His profound belief in my abilities has helped me stay positive and encouraged me to always do my best. I am also truly appreciative for his knowledge and expertise in resolving all my software-related issues. I would also like to extend my gratitude to his parents, Christo and Debbie du Toit, who have been as supportive and loving as my own parents and have been there for me when I needed them.

I would like to thank the University of Pretoria for granting me Merit Awards as well as a postgraduate bursary which covered my tuition fees. Their aid helped lessen a financial burden and enabled me to focus on my studies. Finally, I would like to acknowledge the National Research Foundation (NRF) and the South African Medical Research Council (SAMRC) for their funding that permitted me to conduct this study without any financial strain.

Abstract

RBBP6 is considered a potential cancer biomarker due to its association with cell proliferation and overexpression at cervical cancer sites where there is marked apoptosis and elevated p53. More information is emerging regarding the role of RBBP6 in cancer treatment, specifically its potential to sensitize cancer cells to radiation and certain chemotherapeutic agents via Bcl-2 regulation. Cisplatin is an FDA-approved chemotherapeutic agent that still presents with acquired resistance in certain cervical cancer cases through p53 repression and Bcl-2 up-regulation, which is why there is ongoing research to understand the molecular mechanisms involved in the response of cervical cancer cells to Cisplatin. The present study, therefore, investigates the relationship between Cisplatin and *RBBP6* gene expression in high-risk HPV-positive cervical cancer cells. *RBBP6* was silenced in Hela, CaSki and Vero cells using RNAi technology, followed by measurement of wild-type *p53* and *Bcl-2* at mRNA level through RT-qPCR. Cells co-treated with Cisplatin and siRBBP6 were then analyzed for apoptosis induction and real time growth monitoring using flow cytometry and the xCELLigence system, respectively. Co-treated HeLa cells showed a reduction in apoptosis compared to the Cisplatin-only group despite complete repression of *Bcl-2*. Furthermore, real time cell monitoring revealed delayed growth inhibition in *RBBP6*-knockdown HeLa cells treated with Cisplatin, suggesting that RBBP6 is necessary for sensitizing HeLa cells to Cisplatin. Co-treated CaSki cells up-regulated wild-type *p53* and down-regulated *Bcl-2*, and this was coupled with a higher percentage of apoptosis induction compared to the Cisplatin-only group. Cell growth analysis of CaSki cells also revealed delayed growth inhibition, but in the Cisplatin-only group where *RBBP6* was highly expressed, suggesting that RBBP6 limits Cisplatin sensitivity in CaSki cells. Overall, our findings reveal that silencing *RBBP6* enhances Cisplatin sensitivity in CaSki cells via *Bcl-2* repression and *p53* up-regulation, but absence of this gene desensitizes HeLa cells to Cisplatin and limits apoptosis induction and cell proliferation. This is the first study to reveal a possible relationship between *RBBP6* and Cisplatin in HPV-positive cervical cancer cells.

CHAPTER 1: LITERATURE REVIEW

1.1. Cervical Cancer

1.1.1. Epidemiology

Cancer is a genetic disease characterized by uncontrolled proliferation of abnormal cells, which potentially develop into malignant tumors within the body. According to the International Agency for Research on Cancer, there was an estimated 19.3 million new cancer cases and 10 million cancer-related deaths in 2020, therefore, positioning cancer as the leading cause of death worldwide (Sung *et al.* 2021). The leading cancer types in males and females differ in terms of incidence and mortality rates. Men are more frequently diagnosed with prostate cancer, followed by lung cancer, colorectal cancer, and liver cancer. However, lung cancer is the leading cause of cancer-related death in men, followed by the less fatal prostate cancer and liver cancer (Sung *et al.* 2021). In women, breast cancer is the most diagnosed and the leading cause of cancer-related deaths worldwide, followed by colorectal, lung, and cervical cancer (Bray *et al.* 2018; Sung *et al.* 2021).

Within the past five years, cervical cancer incidence and mortality rates have raised concerns. Despite being one of the best preventable forms of cancer (Petry 2014), this malignancy is still ranked as the fourth most diagnosed form and the fourth leading cause of cancer-related death in women worldwide (Tuohetimulati *et al.* 2018; Manikandan *et al.* 2019; Sung *et al.* 2021). There are three types of cervical cancers: squamous cell carcinoma occurring in squamous cells lining the outer cervix, adenocarcinoma occurring in glandular cells lining the cervical canal and adeno-squamous carcinoma occurring in both cell types (Wipperman *et al.* 2018; Jhingran *et al.* 2020). About 71% of global cervical cancer cases are squamous cell carcinomas, 25% are adenocarcinomas and 4% are adeno-squamous carcinomas (Wipperman *et al.* 2018; Lobo *et al.* 2020). Approximately 570 000 new cervical cancer cases and 311 000 deaths were reported globally in 2018 (Bray *et al.* 2018), which escalated to 604,000 and 342,000, respectively, in 2020 (Sung *et al.* 2021). In about 42 countries, most of

which are in Sub-Saharan Africa, South-Eastern Asia, Latin America and the Caribbean, cervical cancer is the leading cause of cancer-related deaths in females (Vaccarella *et al.* 2017; Bray *et al.* 2018; Sung *et al.* 2021).

In South Africa, a middle-income country, cervical cancer is the second leading cause of cancer-related deaths in woman (Denny and Kuhn 2017; Shrestha *et al.* 2018). The National Cancer Registry (NCR) of South Africa recently highlighted that black females have an increased risk of developing cervical cancer compared to women of other race groups (Singh *et al.* 2014; Singh 2019). A lifetime risk value of 1 in 36 was reported for black woman, 1 in 64 for white women, 1 in 73 for coloured women, and 1 in 118 for Asian women (Singh 2019). Furthermore, majority of cervical cancer cases were reported to occur in South African women who are between the ages of 35 and 60, with black women being affected at an earlier age than women of other races (Singh *et al.* 2014; Singh 2019).

Despite cervical cancer not being the leading cause of mortality in females presently, it is still a major health problem. While more transitioned countries have reported a drastic reduction in cervical cancer incidences and related deaths (Vaccarella *et al.* 2017; Sung *et al.* 2021), it still accounts for 80% of all cancer cases in developing countries, where women have limited access to a high standard of medical care and infrastructure (Mthembu 2013; Denny and Kuhn 2017; Moela 2018), effective screening facilities (Sung *et al.* 2021) and lack awareness of this disease (Mwaka *et al.* 2016). The World Health Organization (WHO) has predicted a drastic increase in the number of cervical cancer cases in developing countries from the previously reported rate of 8 cases per day to 12 per day by 2025 (Lukac *et al.* 2018). For this reason, the WHO emphasizes the immediate need to manage and eventually eradicate this malignancy globally (Brisson and Drolet 2019).

1.1.2. Risk and Causal Factors

1.1.2.1. Human Papilloma Virus

Of many factors that influence the development of cervical cancer, the Human Papillomavirus (HPV) plays a necessary role (Schiffman and Solomon 2013; Sung *et al.* 2021). HPV, belonging to the *Papillomaviridae* viral family, is a common sexually transmitted virus that infects the reproductive tract to eventually lead to tumor formation in females (Kombe *et al.* 2021). Over 200 different strains of HPV have been identified and classified into two forms: low-risk HPVs (LR-HPV) that are responsible for anogenital and cutaneous warts and high-risk HPVs (HR-HPV) that cause oropharyngeal, cervical, anal, vaginal, and penile cancers (Kombe *et al.* 2021). An estimated 85% of invasive cervical cancer cases are associated with HPV infection and 98% of cervical cancer-related deaths are attributed to HR-HPVs. Persistent primary infection of proliferating basal cells of the squamous epithelium with HR-HPV causes grade I cervical intraepithelial neoplasia (CIN I) which, if left untreated can progress to severe dysplasia and invasive carcinoma (Meijer *et al.* 2000). Two thirds of global cervical cancer cases arise from HR-HPV 16 and/or HR-HPV 18 infections, however, HR-HPV 31, 33, 35, 45, 52, 58, and 59 oncogenic strains also promote cancer in the cervix, vulvar, vagina and anus (Clifford *et al.* 2003; Guan *et al.* 2012; Kombe *et al.* 2021; Wilailak *et al.* 2021)

HPV exists as a non-enveloped capsid enclosing histone-associated, double-stranded, circular Deoxyribonucleic Acid (DNA). Only a single DNA strand transcribes the eight open reading frames (ORF) that fall within three functional regions. The Early (E) region encodes six proteins (E1, E2, E4, E5, E6 and E7) that are required for viral replication and carcinogenesis; the Late (L) region encodes two proteins (L1 and L2) that are required for structure and virion formation; and the remaining Long Control Region (LCR) contains *cis* elements required for viral DNA replication and transcription (Kombe *et al.* 2021; Santacroce *et al.* 2021). L1 and L2 are structural proteins that assemble into capsomers and form the icosahedral capsid that surrounds the viral genome. Proteins E1 and E2 activate viral replication by binding together and assembling at the origin of replication. E4 is involved in

viral maturation and release, while E5 promotes cell proliferation through an enhancing interaction with epidermal growth factor receptor (EGFR). E6 and E7 are oncogenic proteins that encourage tumorigenesis through viral-host DNA integration and negative regulation of tumor suppressor proteins (Santacroce *et al.* 2021).

During the early stages of viral infection, E2 inhibits transcription of the viral oncoproteins E6 and E7. However, upon integration of the viral genome into the host, expression of E2 is inactivated, allowing promotion of E6 and E7 transcription. E6 binds to and promotes degradation of the tumor suppressor protein, p53, through interaction with E6-associated protein (E6AP) ligase. This prevents activation of p53-mediated apoptosis induction due to limited p53 activity. E7 binds to and degrades tumor suppressor protein, pRB. This disrupts the regulatory interaction between E2F transcription factor and pRB and endorses the expression of E2F-responsive genes that promote continuous DNA synthesis and cell cycle progression. Ultimately, cells become immortal due to their ability to evade DNA and cell repair signals (Santacroce *et al.* 2021).

Although this virus is an important factor contributing to this malignancy, its presence alone is not sufficient for the development of cervical cancer and other environmental and lifestyle factors play a causal role (Lukac *et al.* 2018; Jhingran *et al.* 2020; Kombe *et al.* 2021).

1.1.2.2. Human Immunodeficiency Virus

Another important but indirect risk factor contributing to cervical cancer development is Human Immunodeficiency Virus (HIV) infection and Acquired Human Immunodeficiency Syndrome (AIDS). Research has proven that women with HIV have a six-fold increase in risk of cervical cancer compared to HIV-negative women, especially women in Southern African countries where this epidemic is common (Carter 2020). Due to diminished CD4 cell counts and a weakened immune system brought about by HIV infection, HIV-positive women are more susceptible to HPV infection and other diseases (Ferreira *et al.* 2017; Stelzle *et al.* 2021). Not only does HIV/AIDS increase the risk of cervical cancer, but it increases the risk of recurrence

after treatment and reduces life expectancy (Stelzle *et al.* 2021). In addition to HIV/AIDS, other sexually transmitted diseases such as chlamydia, gonorrhea, syphilis play a contributing role to HPV infection and cervical cancer development (Jhingran *et al.* 2020).

1.1.2.3. Other Risk Factors

Along with HIV and/or HPV infection, several behavioral and environmental factors are associated with increased prevalence of cervical cancer, including family history of this disease, poverty, obesity, having multiple sexual partners, continued use of oral contraceptives, cigarette smoking and having sexual intercourse or falling pregnant between young ages of 18-30 years (Burd 2003; Mwaka *et al.* 2016; Jhingran *et al.* 2020). HPV can be transmitted sexually, via vaginal and anal intercourse, or non-sexually, via the placenta or birth canal from mother to fetus and through contact with infected skin or surfaces (Sabeena *et al.* 2017). Alternatively, cervical cancer could prevail through mutational changes that spontaneously occur in DNA of cervical cells and ultimately promotes their uncontrollable growth and proliferation to form a tumor (Jhingran *et al.* 2020).

1.1.3. Preventative Measures

Cervical cancer, despite being associated with a persistent viral infection (Burd 2003), is still one of the best preventable malignancies compared to others due to its long pre-invasive period (Šarenac and Mikov 2019). Primary prevention methods involve raising awareness of sexually transmitted diseases and encouraging young teenagers to practice abstinence, limit their number of sexual partners, and to make use of condoms during sexual activity (Wilailak *et al.* 2021). HPV vaccination is the key primary prevention strategy for achieving long term control of cervical cancer. Currently, three highly effective Food and Drug Administration (FDA)-approved vaccines, Gardasil®, Gardasil9® and Cervarix™, have been developed within the last two decades, which are effective at reducing, but not eliminating, infection by a broad range of HR-HPV strains (Wang *et al.* 2013; Mbulawa *et al.* 2015; Kombe *et al.* 2021). HPV vaccination programs are however a major problem in middle-income countries such as

South Africa due to limited service platforms, lack of awareness and operational costs (Wilailak *et al.* 2021).

Secondary prevention strategies include screening programs and early detection of precancerous lesions, especially in unvaccinated women and those infected with less common HR-HPV strains (Wilailak *et al.* 2021). Gold standard approaches for screening include routine Papanicolaou (PAP) smear tests, liquid-based cytology or visual inspection using acetic acid (VIA) or Lugol iodine (Denny 2010; Wilailak *et al.* 2021). Tertiary prevention methods include treating cervical cancer patients to reduce mortality rates and providing quality post-treatment care and rehabilitation to improve their quality of life (Finocchario-Kessler *et al.* 2016; Mwaka *et al.* 2016).

1.2. Cervical Cancer Treatment

Patients with invasive cervical cancer rely on chemotherapy and radiotherapy-based treatment, however, other approaches involve surgery, immunotherapy, and more recently, gene and small interfering Ribonucleic Acid (siRNA) therapy (Cibula *et al.* 2011; Wipperman *et al.* 2018; Mahmoodi Chalbatani *et al.* 2019). The choice of treatment is, however, dependent on the stage of cancer, existing health problems or clinical history and potential risk factors that patients experience (Wipperman *et al.* 2018). Surgery is the preferred treatment option for early-stage cervical cancer where either the tumor, the cervix (trachelectomy) or both the uterus and cervix (hysterectomy) are removed, depending on tumor size. Chemotherapy, which involves intravenous (IV) or oral administration of anti-cancer drugs (Jhingran *et al.* 2020), has proven to be the most effective line of attack against advanced and recurrent metastatic cancers, especially in cases where patients are insusceptible to surgery and radiotherapy (Peralta-Zaragoza *et al.* 2012; Wipperman *et al.* 2018).

1.2.1. Chemotherapy

Several drugs for chemotherapy-based treatment of cervical cancer have shown promising activity when administered alone as single agents or in combination with other drugs, with

combination therapy yielding more favorable responses for recurrent and advanced cancer forms (Green and Lainakis 2006). Commonly administered drugs include platinum and non-platinum-based agents such as Cisplatin (CDDP), Paclitaxel (PTX), Irinotecan (IRI), and Topotecan (TOPO) (Yu and Garcia 2015; Lin *et al.* 2019; Jhingran *et al.* 2020). Platinum-based agents exhibit more promising anti-tumor activity compared to non-platinum drugs (Yu and Garcia 2015). TOPO, a Camptothecin (CPT) derivative (Pectasides *et al.* 2008), is a topoisomerase I (TOPI) inhibitor that when administered at a dose of 1.5 mg/m^2 for 5 successive days every 21 days resulted in a 12.5% overall response rate (ORR) in patients (Tsuda *et al.* 2016). PTX at a dose of 170 mg/m^2 for 24 hr. every 21 days yielded a 17% ORR (Tsuda *et al.* 2016). IRI, another CPT derivative, when administered at a dose of 125 mg/m^2 for 4 weeks yielded a 21% ORR (Pectasides *et al.* 2008). These rates demonstrate the moderate anti-tumor activity and efficacy of single-use agents in treating cervical cancer.

This is further demonstrated in a study by Frumovitz et al. (2017), which evaluated single-agent and combination therapy in small cell cervical cancer (SSCC) cells. Patients administrated with PTX, IRI and TOPO experienced an ORR under 20%, therefore, proving the reduced effectiveness of these agents when administered alone (Frumovitz *et al.* 2017). An FDA-approved, three-drug combination consisting of TOPO, PTX and Bevacizumab/BVZ (TPB) produced a higher response rate of 47% and was therefore more favorable in treating SSCC (Frumovitz *et al.* 2017). A recent study further demonstrated that BVZ combined with chemotherapy and a platinum-PTX doublet proved advantageous in increasing the overall survival (OS) of cervical cancer patients (Moon *et al.* 2018). Table 1 illustrates the response rate from several studies in cervical cancer patients when treated with frequently used single agents (Green and Lainakis 2006; Pectasides *et al.* 2008; Gadducci *et al.* 2010; Kamura and Ushijima 2013; Yu and Garcia 2015; Tsuda *et al.* 2016; Moon *et al.* 2018).

Table 1. Response rates of cervical cancer patients following single-agent chemotherapy with common platinum-based drugs

Agent	**Response Rate (%)**
Cisplatin	17-40%
Carboplatin	15-28%
Paclitaxel	15-31%
Topotecan	13-19%
Irinotecan	16-21%
Ifosfamide	11-33%
Bevacizumab	10-11%

CDDP was chosen for this study on account of being the primary most active chemotherapeutic agent that demonstrates high levels of cytotoxicity in cervical carcinomas when administered as a single agent, compared to other single-use anticancer agents (Pectasides *et al.* 2008; Kamura and Ushijima 2013; Moon *et al.* 2018). CDDP exhibits favorable ORR that range from 17 to 40% with an average OS between 4 to 8 months in cervical cancer patients (Pectasides *et al.* 2008; Tsuda *et al.* 2016). Clinical evidence suggests that the standard administrative dose for CDDP is 50 mg/m^2 every 21 days to ensure effective anti-tumor activity, cytotoxicity, and practicality (Kamura and Ushijima 2013; Tsuda *et al.* 2016). Despite its high efficacy as a single-use agent, CDDP exhibits an increased ORR when combined with other agents, especially taxanes (Green and Lainakis 2006). Table 2 summarizes the efficacy of CDDP-combined agents from several studies in cervical cancer patients as depicted by their ORR (Green and Lainakis 2006; Pectasides *et al.* 2008; Gadducci *et al.* 2010; Kamura and Ushijima 2013; Yu and Garcia 2015; Tsuda *et al.* 2016; Moon *et al.* 2018).

Table 2. Response rates of cervical cancer patients following combination therapy with Cisplatin and other common platinum-based drugs

Drug Combination	**Response Rate (%)**
Cisplatin + Paclitaxel	45-47%
Cisplatin + Topotecan	27-28%
Cisplatin + Irinotecan	59-78%
Cisplatin + Ifosfamide	38-50%
Cisplatin + Paclitaxel + Bevacizumab	45-50%

In spite of the increased ORR of CDDP when combined with other agents, combination therapy with this drug does not improve OS and often leads to increased toxicity (Yu and Garcia 2015). Therefore, the high ORR after CDDP administration alone makes it a more feasible and preferred drug for evaluating its sensitivity in cervical cancer cell.

1.2.2. RNA Interference Therapy

In recent years, chemotherapy has been used in combination with RNA interference (RNAi) to combat many forms of cancer, especially those that exhibit multi-drug resistance (MDR) (Babu *et al.* 2017). This approach identifies novel chemoresistance or apoptosis regulators that can be down-regulated by gene-specific siRNA to prevent tumor progression and drug resistance and, ultimately, promote increased sensitivity towards chemotherapeutics (Guo *et al.* 2013; Mahmoodi Chalbatani *et al.* 2019).

Ganesh *et al*. (2013) investigated the therapeutic benefit of combining CDDP treatment with siRNA targeting anti-apoptotic genes, *Survivin* or *Bcl-2,* in CDDP-resistant human Non-small Cell Lung Cancer (NSCLC) cells. Their findings highlighted improved growth inhibition in the combination treatment, especially when both siRNAs were administered together with CDDP, compared to single-agent treatment (Ganesh *et al.* 2013). Similarly, CDDP sensitivity in resistant NSCLC was enhanced through siRNA-mediated down-regulation of Mitotic Arrest

Deficient-2 (Mad2), a crucial tumor protein involved in mitosis and chromosomal segregation (Nascimento *et al.* 2017). Furthermore, silencing *Notch-1*, through RNAi, in castration-resistant prostate cancer cells led to increased docetaxel sensitivity through downstream regulation of Bax and Bcl-2 apoptotic proteins (Ye *et al.* 2012). Likewise, siRNA mediated knockdown of Taxol Resistance Gene 1 (TXR 1) led to restoration of Taxol chemosensitivity in MCF-7 breast cancer cells through cell cycle arrest (Bai *et al.* 2012).

A study by Jiang and Milner (2002) utilized siRNA technology to silence expression of HR-HPV 16 E6 and E7 viral oncogenes. Silencing E7 enhanced apoptosis induction while knockdown of E6 led to increased p53 gene expression, which activated p21 and promoted decreased cell proliferation (Jiang and Milner 2002). Similarly, Koivusalo et al. (2005) silenced HR-HPV 18 E6 and E7 gene expression and investigated the sensitivity of different chemotherapeutics, including CDDP, in HeLa cervical cancer cells. Their findings highlighted that, following knockdown of these viral oncoproteins, HeLa cells exhibited increased drug sensitivity through elevated p53 levels and apoptotic cell death induction (Koivusalo *et al.* 2005).

Therefore, gene therapy in combination with chemotherapy enhances sensitivity of existing chemotherapeutics and potentially reduces the chances of acquired chemoresistance, thus, the use of this approach demonstrates great potential for success in treating cervical cancer (Díaz-González *et al.* 2015).

1.3. Cisplatin

Cisplatin (CDDP), also known as cisplatinum or *cis*-diammine-dichloro-platinum (II), is a white or yellow-orange metallic compound with square-planar geometry that is stable under normal temperatures and pressures (Dasari and Tchounwou 2014). The chemical structure of this inorganic drug consists of two chloride (Cl) groups and two amine (NH_3) ligands coordinated around a platinum (Pt) core (Dasari and Tchounwou 2014), as shown in Figure 1.

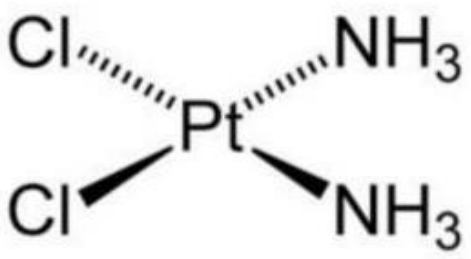

Figure 1. Chemical structure of Cisplatin.

The square-planar platinum complex consists of two chloride and two amine groups arranged in cis-orientation (Dasari and Tchounwou 2014).

1.3.1. Mechanism of Action

CDDP is administered intravenously into blood plasma and diffuses into cells through membrane proteins, such as Copper Transporter Receptor 1 (CTR1) (Johnstone *et al.* 2015). Once inside the cell, which possess a lower chloride ion concentration compared to blood plasma, CDDP undergoes aquation to form a potent, highly reactive, electrophilic compound. Activated CDDP migrates into the nucleus where it forms crosslinks with the major groove of DNA, particularly at the exposed nucleophilic N7 site of Guanine (Basu and Krishnamurthy 2010; Chavez *et al.* 2011; Dasari and Tchounwou 2014; Johnstone *et al.* 2015; Koraneekit *et al.* 2018). DNA damage from the covalent adduct triggers cell cycle arrest at Growth Phase 2 (G2). This ultimately signals the DNA repair machinery to remove a ~30 nucleotide long strand containing the platinated site and replace the damaged portion with a newly synthesized strand. If the damaged region cannot be repaired, DNA synthesis is inhibited, DNA transcription is suppressed, and the cell cycle is altered (Siddik 2003; Dasari and Tchounwou 2014). Ultimately, p53-mediated pro-apoptotic genes are up-regulated, which activate caspases that initiate programmed cell death (Siddik 2003; Basu and Krishnamurthy 2010; Johnstone *et al.* 2015). Figure 2 summarizes the mechanism of action of CDDP. Studies have indicated a linear correlation between the amount of platinum-drug bound to DNA and the extent of cytotoxicity induced (Siddik 2003). Despite its ability to interact with DNA, this mechanism of anti-tumor activity accounts for only a small fraction of CDDP activity (Basu and Krishnamurthy 2010).

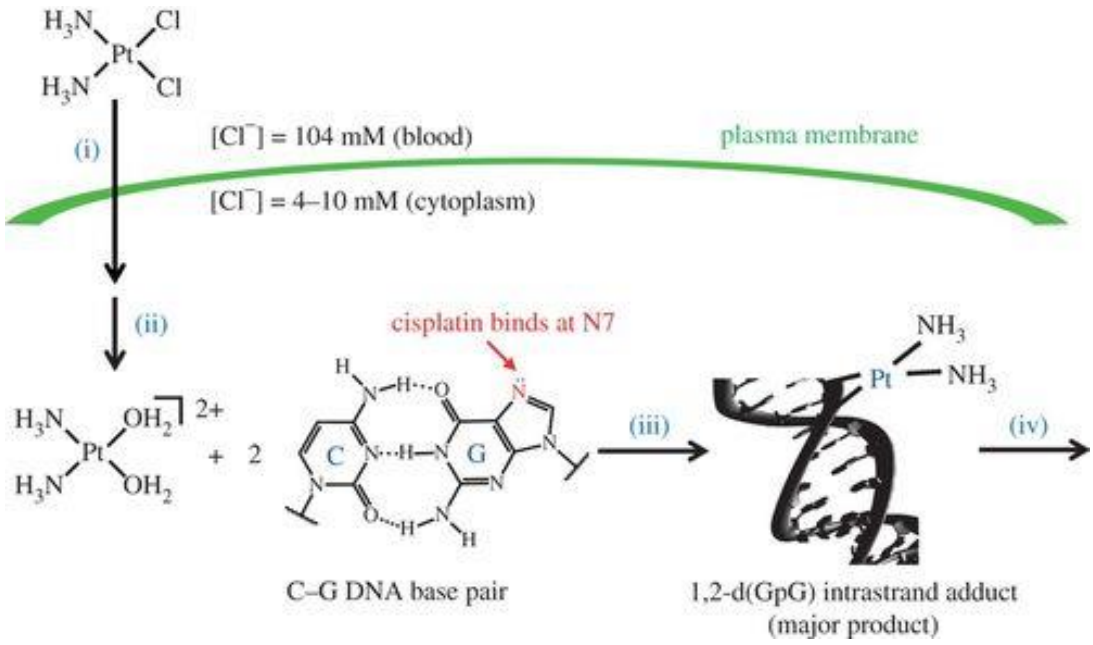

Figure 2. Mechanism of action of CDDP.

(i) Uptake of CDDP into cells via diffusion. **(ii)** Activation of CDDP through aquation. **(iii)** Intra-strand intercalation of CDDP into DNA. **(iv)** DNA repair or apoptosis signaling pathway (Johnstone et al. 2015).

1.4. Cisplatin and Cervical Cancer

CDDP was one of the first FDA-approved platinum-based anticancer compounds that was initially shown to inhibit cell division in *Escherichia coli* (*E. coli*) bacteria, and it displays promising activity in cervical cancer cells (Minagawa *et al.* 1999; Siddik 2003; Dasari and Tchounwou 2014; Leisching *et al.* 2015). This metallic drug is also used extensively to treat advanced stages of lung cancer, breast cancer, brain cancer, bladder cancer and several other malignancies (Basu and Krishnamurthy 2010; Ishida *et al.* 2010; Duan *et al.* 2017; Swanepoel *et al.* 2019). Success of CDDP is attributed to its cis-configuration, which plays a significant role in promoting anti-tumor activity in cancer cells (Basu and Krishnamurthy 2010). Single agent chemotherapy using CDDP demonstrates the highest ORR of 20-30% compared to the other common agents, such as TOPO and PTX, as mentioned previously (Tsuda *et al.* 2016), hence, it is recommended as the standard first line of treatment, with concurrent radiation therapy, for cervical cancer at stage IIB or more advanced (Jung *et al.* 2012; Makovec 2019).

In cervical cancer cells, success of CDDP at the molecular level is dependent on HPV infection, where CDDP targets E6 and E7 viral oncoproteins in HR-HPV-positive cells (Jung *et al.* 2012). Several publications report on CDDP-induced down-regulation of E6 and E7, which prevents E6-mediated degradation of p53 tumor suppressor protein in HR-HPV-18-positive HeLa cells (Wesierska-Gadek *et al.* 2002) and restores function of this protein in HR-HPV-16-positive SiHa cells (Huang *et al.* 2004). A study investigating E6/E7 silencing on CDDP sensitivity documented increased sensitivity of HeLa cells towards CDDP through p53 restoration, hypo-phosphorylation of pRB, and, as a result, elevated apoptosis in HR-HPV-positive cervical cancer cells (Putral *et al.* 2005; Jung *et al.* 2012).

1.4.1. Cisplatin Resistance in Cervical Cancer

Chemoresistance to anticancer drugs remains a big concern as it often results in modified drug efficacy. Cancer cells change and adapt to their surrounding environments and therefore, develop evasive resistance mechanisms in response to drug exposure (Jo *et al.* 2018). Chemoresistance occurs in two forms: acquired resistance, where the chemotherapeutic drug becomes ineffective over time, and intrinsic resistance, where the drug is ineffective during the onset of chemotherapy (Swanepoel *et al.* 2019).

When compared to other chemotherapeutic drugs administered to cervical cancer patients (Table 1), CDDP demonstrates a more favorable ORR and OS of ~40% and ~4 months, respectively, and is therefore the preferred drug for treatment of this malignancy. However, these statistics are still inadequate to fully support CDDP as being the most effective single agent. Consistent with most active single agents, cells tend to acquire resistance through various mechanisms. The low response rates observed for CDDP therefore suggest that chemoresistance may play a contributing role in the incomplete effectiveness of this platinum-based drug. Despite CDDP being widely used in cervical cancer treatment, cells tend to acquire resistance to the drug, thus reducing its chemotherapeutic value (Leisching *et al.* 2015).

Several molecular mechanisms underlying CDDP resistance have been documented in cervical cancer. Reduced accumulation of this drug within cells appears to be the leading cause of acquired resistance, where cervical cancer cells either decrease CDDP-uptake, increase CDDP-efflux, or inactivate CDDP through thiol-containing proteins (Zhu *et al.* 2016; Chen and Chang 2019). Support of these mechanisms is evident in studies on resistant HeLa cells, which revealed significant reduction in CDDP uptake by more than 50% and a subsequent reduction in the number of DNA-CDDP crosslinks formed (Chao 1994). Additionally, CTR1, which facilitates diffusion of CDDP into specific cervical cancer cells, was down-regulated in resistant HeLa cells and thus decreased its uptake (Zisowsky *et al.* 2007). Multi-drug resistant proteins (MRP), particularly MRP1 (Roy and Chakraborty Mukherjee 2014) of the Adenosine Triphosphate (ATP)-Binding Cassette (ABC)-transporter family and copper transporters, ATP7A and ATP7B (Zisowsky *et al.* 2007), have been associated with increased CDDP efflux from resistant cervical cancer cells (Zhu *et al.* 2016; Chen and Chang 2019). Furthermore, documented evidence suggests that several resistant cervical cancer cells stimulate synthesis of Glutathione (GSH), a thiol-containing protein with a high affinity for the reactive form of CDDP. This prevents formation of drug-DNA adducts and thus prevents DNA-damage mediated induction of apoptosis, which ultimately promotes acquired resistance towards CDDP (Galluzzi *et al.* 2012).

Cervical cancer cells also acquire resistance to CDDP by promoting repair of drug-DNA adducts via nucleotide excision repair (NER) and DNA mismatch repair (MMR) (Zhu *et al.* 2016). CDDP-resistant HeLa cells up-regulate Excision Repair Cross-Complementation Group 1 (ERCC1) proteins, which promote DNA repair via NER and thus negatively correlate with CDDP responsiveness in these cells (Chao 1994). In addition, disruption of DNA MMR and its associated proteins, MutS Homolog 2 (MSH2) and Post-meiotic segregation 2 (PMS2), were linked to increased drug-resistance in cervical cancer cells (Zhu *et al.* 2016). Furthermore, epigenetic modifications of DNA through methylation have been suggested to

alter expression of genes involved in CDDP sensitivity, thus leading to acquired resistance (Shen *et al.* 2012).

One of the main mechanisms promoting chemoresistance in tumor cells is the evasion of drug-induced apoptosis signals (Mollaei *et al.* 2017), which is seen in CDDP-resistant cervical cancer cells that disrupt proteins and signaling pathways involved in programmed cell death (Zhu *et al.* 2016). Studies investigating CDDP-resistant HeLa cells reported elevated levels of the anti-apoptotic proteins, Bcl-2 and Bad (Brozovic *et al.* 2004) and reduced Caspases 3, 8 and 9 activity in more resistant SiHa cells (Venkatraman *et al.* 2005).

HPV and its associated E6 oncogenic protein have also been implicated in disrupting chemotherapy-induced apoptotic signals. E6-mediated degradation of p53 desensitizes cervical cancer cells to CDDP due to cellular responses to DNA damage and oncogenic stress signals being disrupted (Jung *et al.* 2012; Mahapatra *et al.* 2021). Additional studies have demonstrated the ability of E6 to also degrade Bax, a pro-apoptotic protein that facilitates apoptosis induction (Thomas and Banks 1999). Furthermore, the presence of HPV in cervical cancer patients was shown to interfere with normal expression of anti-apoptotic and pro-apoptotic proteins of the Bcl-2 family, where the number of viral gene copies correlated with the overexpressed level of Bcl-2 anti-apoptotic proteins (Liang *et al.* 1995). A study by Padilla *et al.* (2002) showed that CaSki cervical cancer cells, which possess several HR-HPV-16 gene copies, exhibited more chemoresistance compared to SiHa cell lines, which possess less copies. This evidence suggested that the presence of HR-HPV strains in cervical cancer cells is likely to disrupt the chemotherapeutic potential of CDDP (Padilla *et al.* 2002).

Among the various mechanisms that are involved in CDDP acquired resistance, this study will investigate the role of Bcl-2 and p53-signalling pathways due to their association with the novel RBBP6 biomarker in HeLa and CaSki cervical cancer cells.

1.4.1.1. Bcl-2 and Cisplatin Resistance

The anti-apoptotic function of Bcl-2 controls cell death via the intrinsic pathway primarily through regulation of mitochondrial outer membrane permeability (MOMP), which promotes irreversible release of intermembrane space proteins that stimulate caspase activation and apoptosis induction (Kalkavan and Green 2018). Intracellular stress signals, such as chemotherapy, modulate the Bcl-2 family of proteins. Activator Bcl-2 Homology 3 (BH3)-only proteins are signaled to directly bind to and activate BAX and BAK pore-forming proteins, which promote MOMP. Pro-apoptotic proteins, such as Cytochrome c (Cyt c), that are released from the mitochondrial intermembrane space bind to Apoptotic Protease Activating Factor-1 (APAF-1) to promote apoptosome formation. The apoptosome activates initiator Caspase 9 which ultimately activates executioner Caspase 3 and 7 to carry out apoptosis (Shamas-Din *et al.* 2013; Kale *et al.* 2018). The anti-apoptotic protein, Bcl-2, inhibits activator BH3-only proteins and executioner caspases, thus preventing pore formation and mitochondrial membrane permeabilization needed for apoptosis induction (Shamas-Din *et al.* 2013). Some studies suggest that Bcl-2 regulates calcium (Ca^{2+}) homeostasis within the mitochondria by interacting with the Inositol 1,4,5-trisphosphate (IP3)-Ca^{+2} gated channels on the Endoplasmic Reticulum (ER) membrane and preventing the necessary Ca^{2+} influx into the mitochondria for cell death induction (Lewis *et al.* 2014; Zhou and Wang 2015; Tuohetimulati *et al.* 2018; Xu *et al.* 2018a). However, little is understood regarding this mechanism of Bcl-2 mediated apoptosis prevention (Pinton and Rizzuto 2006).

In addition to regulating apoptosis by controlling MOMP to apoptotic factors and cytokines (Zhu *et al.* 2016), Bcl-2 proteins play a major role in enabling malignant cells to resist anti-tumor effects of chemotherapeutic agents (Reed 2018). Studies have demonstrated that cancer cells with significant resistance to chemotherapeutic agents exhibit high levels of Bcl-2 (Miyashita and Reed 1992; Leisching *et al.* 2015; Zhou and Wang 2015; Maji *et al.* 2018) A study by Brozovic *et al*. (2004) and Leisching *et al.* (2015) documented a significant up-regulation of Bcl-2 in CDDP-resistant HeLa cervical cancer cells compared to CDDP-sensitive

healthy cells. They further highlighted elevated caspase 3 and 7 activity and subsequent apoptosis induction when *Bcl-2* gene expression was silenced in CDDP-treated HeLa and CaSki cells (Brozovic *et al.* 2004; Leisching *et al.* 2015). Similar expression patterns have been reported in drug-resistant tumors such as prostate cancer and breast cancer (Maji *et al.* 2018), however, contrasting findings were observed in CDDP-resistant small human lung cells, where Bcl-2 was down-regulated (Kumar Biswas *et al.* 2004). A study by Xu *et al*. (2018) verified that Bcl-2 over-expression in CDDP-resistant ovarian cells inhibited ER-mediated apoptosis induction, via the mitochondrial pathway, by reducing Ca^{2+} release from the ER into the mitochondria. Evidence of this mechanism of acquired resistance to apoptotic stimuli in cervical cancer cells was also reported in other studies (Zhou and Wang 2015). Therefore, published evidence validates Bcl-2 as a potential marker for CDDP resistance in tumor cells (Xu *et al.* 2018a).

1.4.1.2. p53 and Cisplatin Resistance

The tumor suppressor function of p53 activates p21 to regulate the cell cycle at G1/M checkpoints and induce premature cell cycle arrest and signal DNA repair factors or promote programmed cell death (PCD) in cases where DNA repair mechanisms fail (Siddik 2003). CDDP-based treatment is more successful in cervical cancer patients who possess wild-type (WT) p53 compared to those with mutant p53, where p53-postitve cells possess a higher ORR to CDDP compared to those that lack this protein (Zhu *et al.* 2016). Therefore, inactivation of p53 has been implicated in the development of resistance to chemotherapeutic drugs in many tumor types.

The anti-tumor importance of p53 was validated when knock down of p53 in CDDP-resistant and sensitive cell lines resulted in a decreased rate of apoptosis induction (Zhu *et al.* 2016; Zheng 2017). Therefore, acquired resistance towards CDDP is due to cervical cancer cells possessing minimal functional p53 activity, which is needed to stimulate apoptotic responses through activation of downstream signaling proteins (Minagawa *et al.* 1999). Additionally, in HPV-positive, CDDP-resistant cervical cancer cells, E6 viral oncoproteins degrade p53 to

evade p53-mediated cellular responses to DNA damage and stress signals (Padilla *et al.* 2002; Jung *et al.* 2012). Furthermore, when p53 is mutated, primarily in exons 4 to 9, it is unable to bind to damaged DNA and activate downstream proteins such as pro-apoptotic Bax. The resulting decrease in the Bax:Bcl-2 ratio, is considered a major factor influencing the resistant phenotype (Siddik 2003; Zhu *et al.* 2016). This leads to continued cell proliferation of resistant tumor cells in the presence of this platinum drug due to acquired tolerance to DNA damage and apoptosis evasion (Zhu *et al.* 2016). Evidence of CDDP-resistance in cervical cancer cells was also linked to overexpression of the β2-adrenergic receptor (β2-AR) pathway, which prevents p53 acetylation and downstream transcriptional inactivation through Silent Information Regulator 1 (Sirt1) up-regulation (Chen *et al.* 2017; Zheng 2017).

Studies have reported the presence of minimal p53 activity in HeLa cells and have suggested that they are more likely to acquire resistance towards CDDP and other chemotherapeutic drugs via p53-dependent and independent pathways (Minagawa *et al.* 1999). Therefore, the way in which p53 influences drug resistance and sensitivity in cervical cancer cells depends on the type of cell line, the cytotoxicity of the drug and its mode of action as well as the genetic mutations present in the p53 gene (Hientz *et al.* 2017).

1.5. Retinoblastoma Binding Protein 6

The Retinoblastoma Binding Protein 6 (RBBP6), also known as PACT (p53-Associated Cellular protein Testis-derived), P2P-R (Proliferation Potential Protein-Related) or RBQ-1 (RB-binding Q-protein) is a regulatory protein that also plays a significant role in regulating apoptosis (Xiao *et al.* 2018a). This nuclear protein is encoded for by the *rbbp6* gene located on chromosome 16 and it possesses multiple domains (Motadi *et al.* 2011; Mthembu 2013; Xiao *et al.* 2018a). As shown in Figure 3, the coding region of this gene is composed of 18 exons, from which four different isoforms are generated through alterative splicing (isoform 2 and 4) and alternative poly-adenylation (isoform 3) (Mbita *et al.* 2011; Xiao *et al.* 2018a). Isoforms 1 and 2 are multidomain proteins consisting of a Domain With No Name (DWNN) domain, Zinc-finger domain, Really Interesting New Gene (RING) domain, Proline (PRO) and

Serine (SER)-rich domains and Rb and p53-binding domains (Mbita *et al.* 2019). They differ in that isoform 2 lacks exon 16, while isoform 1 comprises of all 18 exons. Isoform 3 consists of only the first 3 exons, which encode the DWNN domain, while isoform 4 lacks the Rb-binding domain (Dlamini *et al.* 2019; Mbita *et al.* 2019). The DWNN domain, Zinc-finger domain and RING domain are evolutionarily conserved in all eukaryotic organisms (Moela 2018; Motadi *et al.* 2018).

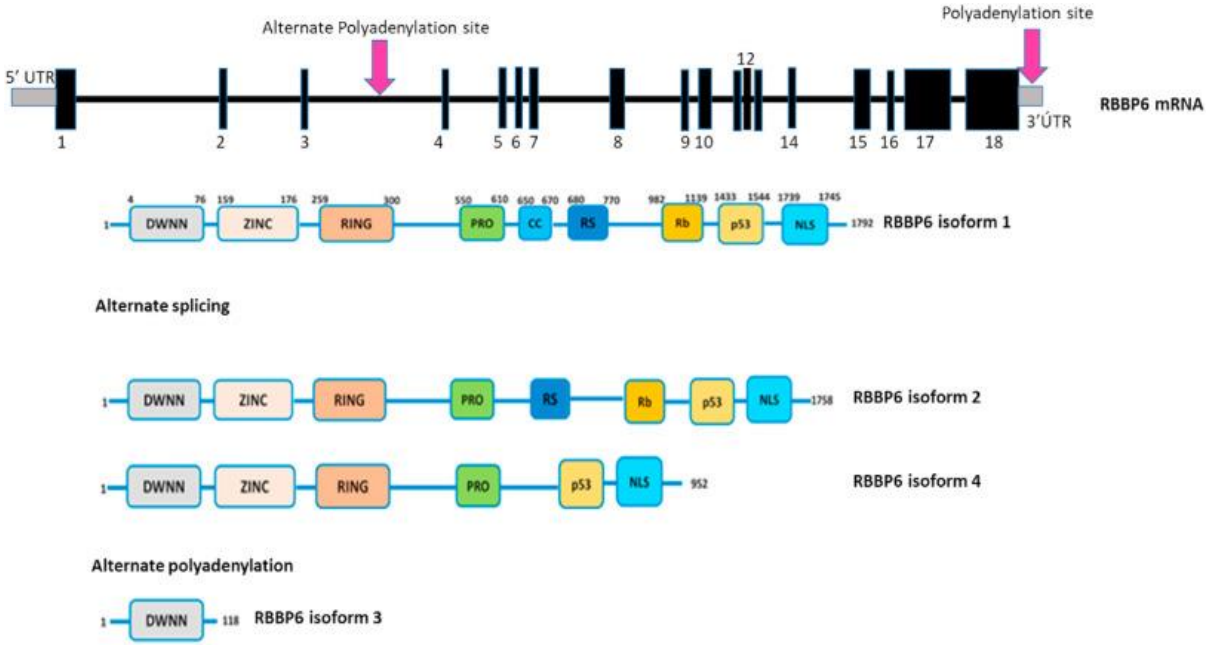

Figure 3. Exon and domain structure of RBBP6 isoforms.

Isoforms 1 and 2 possess: DWNN domain (N-terminal), Zinc-finger domain (exons 4-7), RING domain (exons 8-10), Proline-rich domain (exons 10-15), Serine-rich domain (exon 17), Rb-binding domain (exon 17), p53-binidng domain (exon 18) and a Nuclear Localization Signal (NLS). Isoform 4 lacks Rb-binding domain (exon 17). Isoform 3 only consists of DWNN domain (N-terminal). Isoforms 2 and 4 are generated from alternative splicing and isoform 3 from alternative poly-adenylation sites (Mbita et al. 2021).

1.5.1. RBBP6 and Cell Proliferation

Despite limited information being available on their function, evidence suggests that each RBBP6 isoform is differentially expressed in different cell types and has functional diversity, depending on the cells expressing them (Mbita *et al.* 2011; Motadi *et al.* 2018; Uf *et al.* 2018; Mbita *et al.* 2019). Isoforms 1 and 3 are well researched in the context of tumorigenesis, however, little is known about isoforms 2 and 4 (Mbita *et al.* 2011).

Studies suggest that RBBP6 isoform 1 promotes tumor progression through regulation of p53 and pRB, while isoform 3 is anti-cancerous and promotes cell cycle arrest and subsequent DNA repair to inhibit tumor growth (Mbita *et al.* 2019). Moreover, RBBP6 isoform 3 is present at elevated levels during cancer progression compared to isoform 1, which further validates their contrasting functions in carcinogenesis (Mbita *et al.* 2021). These findings were substantiated by Makgoo *et al.* (2019), who proposed that isoform 1 in breast cancer promotes cell proliferation and survival through its ubiquitin-ligase activity and therefore, becomes down regulated during apoptosis. They further implicated isoform 3 in premature cell cycle arrest at the G2/M point, therefore significant reduction of this isoform would occur to promote abnormal cell proliferation (Makgoo *et al.* 2019).

In spite of the conflicting findings regarding RBBP6 expression in human cancers, at both mRNA and protein level, growing evidence suggests that *RBBP6* is up-regulated in tumors (Mbita *et al.* 2019). RBBP6 protein expression levels are dependent on how advanced the cancer has progressed, with more advanced stages exhibiting higher levels of RBBP6 compared to less advanced stages (Motadi *et al.* 2018). Through its p53 and pRB-binding domains, RBBP6 functions as a negative regulator of tumor suppressor proteins, p53 and pRB (Motadi *et al.* 2011; Di Giammartino *et al.* 2014; Motadi *et al.* 2018). At overexpressed levels in tumor cells, this protein marks p53 and pRB for ubiquitin-mediated degradation through E3 ubiquitin ligase activity of its RING domain (Mthembu 2013; Xiao *et al.* 2018a). Additionally, RBBP6 facilitates the inhibitory interaction between p53 and Mouse Double Minute 2 (MDM2), to promote p53 degradation, which limits its DNA-binding abilities and as a result, prevents

programmed cell death (Di Giammartino *et al.* 2014). When RBBP6 expression is blocked, transcription of pro-apoptotic genes is stimulated and p53-responsive cell death pathways were activated (Porichi *et al.* 2009). Recent studies suggest that RBBP6 also binds to and degrades the transcription factor, Y-Box-binding protein 1 (YB-1), which is essential for cellular reproduction and apoptosis (Uf *et al.* 2018; Mbita *et al.* 2021). Thus, RBBP6 has been implicated in several cellular processes such as cell cycle regulation, RNA processing (Dlamini *et al.* 2019) and programmed cell death (Uf *et al.* 2018; Xiao *et al.* 2018a).

1.5.2. RBBP6 and Chemotherapy

A correlation between elevated RBBP6 levels and limited apoptosis induction and cell cycle deregulation following chemotherapy has been observed in several studies, which suggests acquired chemoresistance in different forms of cancer such as breast, lung, and cervical cancer (Motadi *et al.* 2011; Moela *et al.* 2014; Moela and Motadi 2016; Dlamini *et al.* 2019). Published reports confirm the resultant inhibition of cell proliferation and increased cell death, brought about by a combination of *RBBP6* gene silencing and CPT or Staurosporine (STS) treatment in breast cancer cells, indicating the importance of RBBP6 in promoting tumor spread (Moela *et al.* 2014). A similar study by Motadi *et al.* (2018), reported increased sensitivity of breast cancer cells to the anti-cancer agent, γ-aminobutyric acid (GABA), which induced apoptosis and cell cycle arrest in the absence of RBBP6. The presence of functional RBBP6, on the other hand, prevented apoptosis induction by activating the PKA/cAMP signaling pathway that inhibits phosphorylation-mediated activation of pro-apoptotic factors and, as a result, desensitized MCF-7 cells to GABA (Motadi *et al.* 2018).

A study by Xiao *et al*. (2018) linked RBBP6 in the development of radio-resistance in colorectal cancer, whereby its overexpression facilitated tumorigenesis. Down-regulation of this protein in radio-resistant cells increased sensitivity and subsequently reduced cell viability in response to radiotherapy (Xiao *et al.* 2018a). Silencing RBBP6 caused attenuation of the p53-MDM2 inhibitory interaction in radio-resistant cells, thus releasing p53 to stimulate p21-facilitated CyclinB1-CDK1 inhibition and cell cycle arrest in G2/M phase. Expression of pro-apoptotic

proteins, Bax and caspase 3, were up-regulated while anti-apoptotic protein, Bcl-2, was inhibited, resulting in p53-mediated cell death induction in radio-resistant cells in the absence of functional RBBP6 (Xiao *et al.* 2018a).

These studies highlight the importance of basal p53 levels on the extent of drug-induced apoptosis in resistant and sensitive cells and demonstrates the interactive relationship between RBBP6, p53 and Bcl-2 (Motadi *et al.* 2018). The frequent up-regulation of RBBP6 in most cancers highlights its potential as a novel therapeutic target (Mbita *et al.* 2021). Therefore, findings from this study will provide new knowledge on the role of RBBP6 in regulating p53 and Bcl-2 to sensitize cervical cancer cells to CDDP chemotherapy.

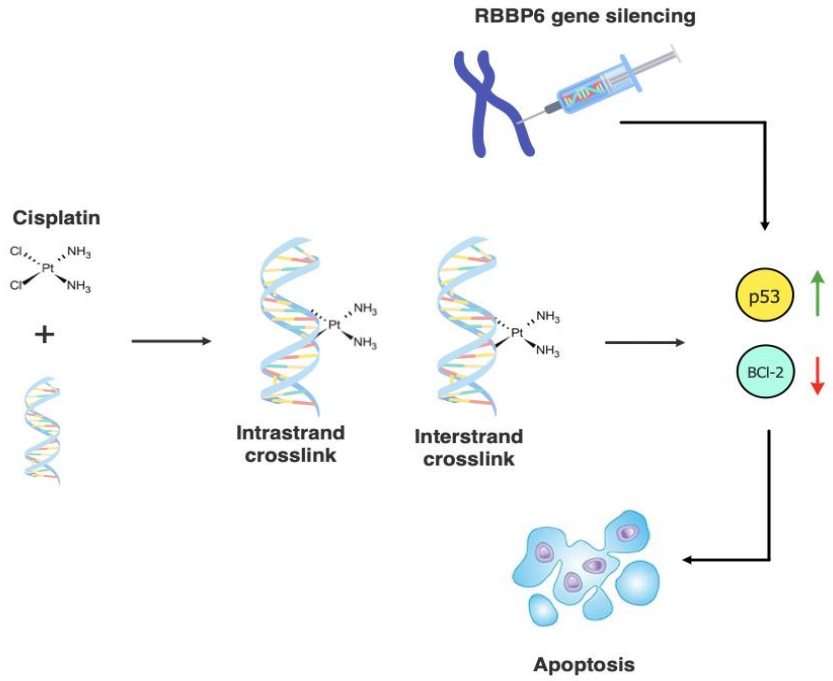

Figure 4. Illustration of the possible association between RBBP6 gene silencing and Cisplatin in inducing apoptosis.

CHAPTER 2: AIM AND OBJECTIVES

2.1. Aim

Studies report up-regulated RBBP6 protein in cancerous cells that undergo indefinite proliferation, however, the exact mechanism by which RBBP6 mediates uncontrolled growth is not well documented. Accumulating data reports that RBBP6 promotes transcription of anti-apoptotic protein, Bcl-2, while degrading tumor suppressor protein, p53, to programmed cell death. The CDDP anticancer agent disrupts E6 and E7 viral protein function of HPV-positive cervical cancer cells to up-regulate p53 and reduce Bcl-2 levels and promote growth inhibition and apoptosis. However, no studies have explored the possible relationship between the RBBP6 in Bcl-2 and p53-mediated apoptosis response of cervical cancer cells treated with CDDP. With CDDP being readily accessible to patients, understanding its relationship with RBBP6 can help improve its efficacy through personalized administration based on the expression profile of RBBP6 in cervical cancer cases that show resistance to treatment. Therefore, in this study we aim to probe the effects of *RBBP6* knockdown on the sensitivity of HR-HPV positive cervical cancer cells towards CDDP through Bcl-2 and p53-dependent pathways.

2.2. Objectives

- To silence *RBBP6* in HeLa, CaSki and Vero cells using RNA interference technology.
- To measure *p53* and *Bcl-2* mRNA expression in HeLa, CaSki and Vero cells following *RBBP6*-knockdown and CDDP treatment for different exposure intervals.
- To detect and measure cell death in HeLa, CaSki and Vero cells in response to combined siRBBP6 and CDDP treatment.
- To visualize changes in cell growth of HeLa, CaSki and Vero cells in response to combined siRBBP6 and CDDP treatment.

CHAPTER 3: MATERIALS AND METHODS

3.1. MATERIALS

3.1.1. Cell lines

Two cervical cancer cell lines and a non-tumorigenic cell line were used in this study to isolate mRNA and to monitor cell growth and apoptosis induction following treatment. The Henrietta Lacks (HeLa) cell line is an immortal, HPV 18-infected cervical cancer cell line derived from the adenocarcinoma cells of the cervix. The CaSki cell line is an HPV 16-infected cervical cancer cell line derived from the squamous carcinoma cells of the cervix. The Vero cell line is a normal, non-cancerous cell line derived from the kidney of an African green monkey. All cell lines were purchased from the National Institute of Biomedical Innovation, Health, and Nutrition (NIBIHN) (Japan).

3.1.2. RNAi Oligonucleotides

Silencing of *RBBP6* was achieved using Ambion™'s gene-specific Silencer® pre-designed siRNA (Life Technologies™, USA) with sequences shown in Table 1. The short interfering RNA was introduced into adherent cells using the lipid-based Lipofectamine® 3000 transfection reagent (Invitrogen™, USA) and Gibco®'s Opti-MEM™ reduced serum medium (Life Technologies™, USA). The siRNA was specific for both human and monkey DNA and was, therefore, compatible with HeLa, CaSki and Vero cell lines.

Table 3. *RBBP6*-specific siRNA sequence (Ambion™)

	Sense Strand	**Antisense Strand**
Sequence	5'- GCGAUGGCAACUACAAAAGtt -3'	5'- CUUUUGUAGUUGCCAUCGCtg -3'

3.1.3. Primers

Target genes of interest in this study were amplified and quantified using gene-specific primers. IDT Prime Time® qPCR pre-designed primers targeting *RBBP6* and *p53* were purchased from Whitehead Scientific (Pty) Ltd. (SA) and primers targeting *GAPDH* and *Bcl-2* were synthesized by and purchased from Inqaba® Biotechnical Industries (Pty) Ltd. (SA). All genes are conserved across humans and primates, so the primers were specific for both species' DNA, making them compatible with HeLa, CaSki and Vero cell lines. The primers do not target all isoforms of each gene. Sequences for each primer are shown in Table 2. Each primer offered sequence uniqueness with an ideal GC-content between 35-65%. Their melting temperature (T_m) fell within the range of 60-64°C with their optimum primer annealing temperature (T_a) being < 5°C below the T_m.

Table 4. Primer sequences for target genes (IDT Prime Time®/Inqaba®)

Primer	Forward Primer Sequence	Reverse Primer Sequence
RBBP6	5'-CAGCGACGACTAAAAGAAGAG-3'	5'-GAGCGGCTGAATGATCGAGA-3'
p53	5'-GACGCTAGGATCTGACTGC-3'	5'-GACACGCTTCCCTGGATTG-3'
GAPDH	5'-CAGCCGCATCTTCTTTTGCG-3'	5'-TGGAATTTGCCATGGGTGGA-3'
Bcl-2	5'-AGCCAGGAGAAATCAAACAGAC-3'	5'-GATGACTGAGTACCTGAACCG-3'

3.1.4. Cisplatin (CDDP)

The anticancer drug of interest in this study is CDDP which, as previously mentioned, is a platinum-based drug that is active against advanced forms of cancer. CDDP inhibits HeLa and CaSki cervical cancer cells due to its dependence on HPV infection, and it exhibits cytotoxicity by preventing DNA synthesis, altering cell cycle regulation, and inducing apoptosis through p53 and Bcl-2 signalling pathways in a dose-dependent manner. The European Pharmacopoeia (EP) reference standard was purchased from Sigma Aldrich® (USA).

3.2. METHODS

3.2.1. Cell Culture and Maintenance

HeLa and CaSki cervical cancer cells and Vero non-tumorigenic cells were maintained in Dulbecco's Modified Eagle's Medium (DMEM) (Gibco™, USA). This high-glucose medium was supplemented with 10% Fetal Bovine Serum (FBS), 1% Penicillin/Streptomycin antibiotic and 1% fungizone (Gibco™, USA). The cells were grown in a 37°C humidified Forma™ Steri-Cycle™ i160 incubator (Thermo Fisher Scientific Inc., USA) supplied with 5% carbon dioxide (CO_2). Cells near confluency were washed twice with 1X Phosphate Buffered Saline (PBS) (HyClone™, USA), trypsinized and re-nourished with fresh medium. All cell types were sub-cultured at least once a week and excess cultures were cryo-preserved. For long term storage, cells were resuspended in a freezing medium containing DMEM supplemented with 20% FBS and 10% Dimethyl sulfoxide (DMSO) (Sigma-Aldrich®, USA). Cultures were placed in a Mr. Frosty™ (Thermo Fisher Scientific, USA) freezing container with Isopropyl alcohol (IPOH) and frozen overnight at -80ºC to freeze cells at a cooling rate of -1°C/min. Following this, the cultures were transferred to liquid nitrogen storage.

3.2.2. Cell Viability Assay

Principle

The Methyl-Thiazolyl-Tetrazolium (MTT) colorimetric assay relies on cellular enzymatic activity to determine cell viability and, therefore, identify the drug concentration that inhibits 50% of cell growth (IC_{50}). MTT is a yellow colored compound that is endocytosed by cells and converted to a water-insoluble, violet formazan product by mitochondrial dehydrogenases and other enzymes present in metabolically active and viable cells. DMSO dissolves the formazan crystals, forming a colored solution whose absorbance can be measured at certain wavelengths by spectrophotometry. The amount of formazan produced, represented by the absorbance value, correlates to the percentage of viable cells present and, therefore, gives an indication of drug cytotoxicity. Cells that are not viable or dead lose the ability to reduce

MTT to formazan and, as a result, have lower absorbance values. The drug concentration that allows 50% of the cell population to remain viable after treatment, relative to the untreated control, is the IC_{50}.

Technique

Monolayer HeLa and CaSki cells at ~70-80% confluency were trypsinized and seeded into 96-well plates at 1×10^5 cells/well, then incubated overnight at 37ºC in a humidified incubator supplied with 5% CO_2. The attached cells were treated with various concentrations of CDDP (50, 25, 12.5 6.25 and 3,125 µg/mL), prepared by serially diluting a 1 mg/mL stock solution in distilled water (dH_2O). Treated cells were incubated in a 37ºC humidified chamber for 48 hr., in the presence of CO_2. MTT solution, prepared at 5 mg/mL in 1X PBS, was added to each well and incubated for 4 hr. in a 37ºC humidified chamber to allow MTT to be metabolized. Following incubation, the formazan crystals were resuspended in DMSO, and the absorbance of the resulting formazan solution was measured at 570 nm in a SpectraMax® Paradigm® multi-Mode microplate reader (Thermo Fisher Scientific Inc, USA). Percentage cell viability was then calculated from the absorbance values using Microsoft Excel 365 (Appendix A). The experiments were performed in triplicates.

3.2.3. RNA Interference

Principle

RNA interference is a form of post-transcriptional gene silencing that has been employed in various studies to suppress gene expression in eukaryotic organisms by degrading gene-specific mRNA using double-stranded siRNA sequences. The principle of this technique depends on complementarity of siRNAs to the target RNA where perfect base-pairing promotes RNA degradation, while imperfect base-pairing prevents RNA translation.

siRNAs are double stranded molecules, approximately 21-28 bases long, and made up of coding and non-coding sequences that bind perfectly to and degrade targeted RNA sequences. During RNA interference, siRNA is processed and cleaved by an RNase called

Dicer, which enzymatically digests long double stranded RNA sequences into smaller strands that each contain a 5' phosphate and a 3' overhangs of two nucleotide bases. Mature siRNA is recognized by a multi-protein complex called RNA-Induced Silencing Complex (RISC), where they are separated into two single strands: guide and passenger siRNA. While passenger siRNA gets degraded, the antisense strand functions as a guide to align the RISC complex onto the target mRNA, which becomes catalytically cleaved by a RISC-associated Argonaute enzyme (Ago2) and, therefore, transiently silenced.

Owing to their negative charge and large size, delivery of siRNA molecules into cells requires a vector. The "gold standard" approach utilizes a lipid-based transfection agent to achieve efficient DNA or RNA delivery into cells. The cationic lipid molecule, which is made up of a phospholipid bilayer, positively charged head group and one or two hydrocarbon tails, forms electrostatic interactions with the negatively charged phosphate backbone of siRNA via the inner polar head. This interaction facilitates their uptake into cells as the positively charged liposome mediates endocytosis through the negatively charged plasma membrane. Following transfection, siRNA-mediated gene knockdown persists for approximately five to seven days but, successful suppression can be evaluated two days post-transfection for reliable results.

Technique

HeLa, CaSki and Vero monolayer cells at ~70-80% confluency were trypsinized and seeded into 6-well plates at 3×10^5 cells/well, then incubated overnight at 37ºC in a humidified incubator. The attached cells were washed with 1XPBS and replaced with antibiotic-free media prior to transfection. Lipofectamine™ 3000 (Invitrogen™, USA) and Ambion®'s Silencer® pre-designed siRNA (Life Technologies™, USA) targeting *RBBP6* (100 pmol) were first diluted separately in Gibco®'s Opti-MEM™ reduced serum medium (Life Technologies™, USA), then combined in a 1:1 ratio. The mixture was incubated at room temperature for 15-20 minutes to allow formation of siRNA-lipid complexes after which, cells were transfected and incubated in a 37ºC humidified chamber with 5% CO_2 supply for 24 hr. to transiently silence *RBBP6*. Post transfection, cells were exposed to CDDP at its IC_{50} for an additional 24 and 48

hr. period and then harvested for subsequent analysis. The experiments were performed in duplicates.

3.2.4. RNA Extraction and Quantification

Principle

RNA is a vital molecule that translates genetic information carried by DNA into proteins that are vital to living organisms. Of the total RNA produced, 80-90% are ribosomal RNA (rRNA), 2.5-5% are messenger RNA (mRNA) and the remainder are transfer RNA (tRNA). RNA molecules exhibit a short half-life once isolated from cells and they are highly prone to degradation by RNases present in the surrounding environment. Therefore, they are very unstable molecules and extreme care is needed when extracting them from cells. RNA, particularly mRNA, is the starting material for various molecular biology experiments such as conventional Polymerase Chain Reaction (PCR) or real-time quantitative PCR (RT-qPCR), hence, isolation of high-quality RNA is crucial in performing these techniques.

RNA is isolated using TRIzol® Reagent, which is a monophasic solution used for obtaining pure cellular RNA of high integrity at favorable yields. It is composed of RNase inhibitory agents, phenol and guanidinium isothiocyanate (GITC), that function in dissolving biological material and dissociating nucleoprotein complexes while maintaining RNA stability. Addition of chloroform (Chl) to homogenized cells promotes phase separation, where proteins are extracted to the lower organic phase, DNA to the intermediate phase and RNA to the upper aqueous phase. Therefore, TRIzol® permits purification of RNA, DNA, and proteins from a single sample. Pure RNA that is free from DNA and protein contamination can then be precipitated from the aqueous phase using IPOH.

Extracted RNA is quantified by spectrophotometry using the NanoDrop® microvolume sample retention system, which measures small volumes of nucleic acid with high accuracy. This technology utilizes a combination of natural surface tension, optic fiber technology and a short path length in a liquid column to measure a wide range of nucleic acid concentrations. Owing

to its reduced sample consumption, ease of use and overall efficiency when quantifying nucleic acids, this system has become widely used.

Technique

Total RNA was extracted from CDDP-treated HeLa, CaSki and Vero cells post transfection using TRIzol® Reagent (Life Technologies™, USA), following the manufacturer's protocol. Monolayer cells were washed with cold 1XPBS and resuspended in TRIzol® Reagent for 5 min. Cell debris was pelleted by centrifugation at 5 000 rpm for 5 min in a Hermle® Z167-M microcentrifuge (Stellar Scientific Inc., USA) after which, Ribonuclease (RNase)-free Chl was mixed into the remaining supernatant in a fresh tube. The mixture was vortexed for 15 seconds, then centrifuged at 12 000 rpm for 15 minutes at 4ºC in a Prism™ R refrigerated microcentrifuge (Labnet International Inc., USA). The resultant upper aqueous layer containing RNA was mixed with IPOH for 10 min after which, the RNA pellet was precipitated by centrifugation at 12 000 rpm for 10 min at 4ºC. The pellet was washed with 70% ethanol (EtOH) before final centrifugation at 12 000 rpm for 5 min at 4ºC. The RNA pellet was air-dried for 10 min at room temperature then resuspended in UltraPure™ Deoxyribonuclease (DNase)/RNase-free distilled water (Invitrogen™, USA). RNA was quantified using a NanoDrop® ND-1000 Spectrophotometer (Thermo Fisher Scientific Inc., USA) where A260/A280 nm absorbance ratios greater than 1.8 were indicative of pure RNA extracts. The 18s and 20s rRNA bands were visualized on a 2% ethidium bromide (EtBr)-stained agarose gel to confirm RNA purity and integrity. Experiments were performed in duplicates.

3.2.5. Reverse Transcription

Principle

To quantify genes at mRNA level by real time qPCR, total cellular RNA is first converted to complementary DNA (cDNA) by reverse transcription. With the starting template for reverse transcription being mature and processed mRNA molecules, the length of DNA to be amplified is reduced and thus, loss of coding regions of target genes is prevented. Reverse transcription

makes use of RNA-dependent DNA polymerase or Reverse Transcriptase enzymes (RTases) to direct synthesis of the first strand of cDNA from primers that anneal to the 3'-end of mRNA. Free deoxy-nucleotide triphosphates (dNTPs), nuclease-free water and a reaction buffer are added to these components in a master mix to assist in cDNA synthesis. The double stranded cDNA product serves as a template for subsequent qPCR reactions, where multiple copies of target genes can be produced for expressional analysis.

Technique

Total cellular RNA from CDDP-treated HeLa, CaSki and Vero cells post transfection was reverse transcribed into cDNA using the PrimeScript™ RT Master Mix kit (Takara Bio Inc., Japan) according to the manufacturer's guidelines. A 20 µL reaction mixture containing 5X PrimeScript™ RT Master Mix [composed of PrimeScript™ RTase, RNase Inhibitor, Oligo dT Primer, Random 6 mers, dNTP Mixture, and Magnesium ($Mg2^{+}$)-containing reaction buffer], RNase-free dH_2O and the RNA template was prepared. Reverse transcription was performed in a T100™ Thermal Cycler (Bio-Rad Laboratories Inc., USA) under the following conditions: reverse transcription at 37ºC for 15 min followed by 5 sec heat inactivation of reverse transcriptase at 85ºC. Synthesized cDNA was quantified using the NanoDrop® ND-1000 Spectrophotometer (Thermo Fisher Scientific Inc., USA) where A260/A230 nm absorbance ratios greater than 2 were indicative of pure cDNA. The experiments were performed in duplicates.

3.2.6. Real time qPCR

Principle

RT-qPCR is a quantitative technique for measuring expressional changes of gene-specific cDNA at regular intervals during thermocycling. Detection of these changes is achieved through fluorescence-sensitive cameras within the thermocycler. Like conventional PCR, real time qPCR makes use of thermostable *Thermus aquaticus* (*Taq)* DNA Polymerase, gene-specific primers, dNTPs, and a reaction buffer to amplify specific cDNA sequences. However,

unlike conventional PCR, qPCR includes an intercalating SYBR™ Green dye in the reaction mixture. SYBR™ Green is an affordable but precise dye with a high binding affinity for the minor groove of double stranded DNA. When SYBR™ Green is incorporated into newly synthesized DNA molecules, fluorescence emission by this dye increases. Thus, the intensity of fluorescent signals generated informs on the number of amplicons synthesized in real time.

Within the thermal cycler, double stranded DNA undergoes multiple cycles of denaturation, primer annealing and extension. Denaturation of cDNA, to form single stranded molecules, occurs at high temperatures of 94-98°C. Next, gene-specific primers and DNA polymerase anneal to the target gene at temperatures between 45-65°C. Here, complementary nucleotides incorporate into the newly synthesized strand at a slow rate. Finally, the temperature is raised to 65-75°C, where *Taq* polymerase functions optimally to extend the primers and produce more amplicons at a faster rate. As double-stranded DNA is being synthesized, SYBR™ Green intercalates into the minor groove and fluorescence is detected at specific excitation and emission wavelengths.

Technique

Gene expression analysis of CDDP-treated HeLa, CaSki and Vero cells post transfection was performed in a 10 µL reaction mixture containing Luminaris™ Color HiGreen qPCR master mix [composed of SYBR Green, Magnesium Chloride ($MgCl_2$), Taq polymerase, and dNTPs], forward and reverse primers specific to *RBBP6*, *p53* or *Bcl-2*, cDNA template (1000 µg/mL) and nuclease-free dH_2O. The *GAPDH* housekeeping gene was used as a reference to evaluate quality of cDNA amplification. Temperature gradients for target gene primers were performed to identify their optimum T_a (Appendix B1). Standard curves (Appendix B2) and melt peaks (Appendix B3) were then generated by performing a 1:10 serial dilution before measuring the relative expression changes of *RBBP6*, *p53* and *Bcl-2* against *GAPDH*. RT-qPCR was performed in a CFX96™ Real Time System C1000™ Thermal Cycler (Bio-Rad Laboratories Inc., USA) under the following conditions: initial denaturation at 95ºC for 10 min followed by 45 cycles of denaturation at 95ºC for 15 sec, primer annealing at 60ºC for 30 sec

and extension at 72ºC for 30 sec. Melt curve analysis was performed under the following conditions: 95ºC for 30 sec followed by cooling to 65ºC for 5 sec before the temperature was raised to 95ºC again at a rate of 0.5º/sec with continuous fluorescence generation. The experiments were performed in duplicates.

3.2.7. Flow Cytometry

Principle

Annexin V-FITC/PI staining and subsequent flow cytometry analysis is a widely adopted approach for detecting the number of cells undergoing cell death via apoptosis or necrosis. The principle of this technique involves the binding of Annexin V-FITC, a Fluorescein Isothiocyanate-conjugated cellular protein, to Phosphatidylserine (PS), a phospholipid that is associated with the apoptotic pathway. In normal cells, PS is expressed on the inner face of the membrane. During the early stages of apoptosis, it is translocated to the outer surface of the plasma membrane, where Annexin V-FITC can bind to exposed PS more readily and detect it. Propidium Iodide (PI) is a DNA-binding dye that leaks through damaged, permeabilized plasma membranes of cells undergoing late apoptosis or necrosis. These stains therefore act as a probe for apoptosis and necrosis detection using flow cytometry. Viable cells are both Annexin V-FITC and PI negative since the plasma membrane is intact and PS remains internalized. Cells undergoing early apoptosis are Annexin V-FITC positive and PI negative and cells that are in late apoptosis or already dead are both Annexin V-FITC and PI positive. No differentiation can be made between cells undergoing late apoptosis or necrosis however, the different stages of apoptosis can be tracked by analyzing the different signal intensities generated by each stain.

Technique

Apoptosis induction was measured in CDDP-treated HeLa, CaSki and Vero cells post transfection using the BD Pharmingen™ Annexin V-FITC Apoptosis Detection Kit I (BD Biosciences, USA), following the manufacturer's protocol. Cells were seeded in 6-well plates

and transfected with siRBBP6 for 24 hr. before treating them with apoptosis-inducing CDDP for an additional 24 and 48 hr. Detached cells were first collected, then attached cells were trypsinized, resuspended in growth media, and transferred into 15 mL tubes. The cells were pelleted at 1500 rpm for 5 min in an Eppendorf™ 5702 centrifuge. The pellet was washed with cold 1XPBS before resuspending it in 100 µL 1X Binding Buffer at a concentration of 1 x 10^6 cells/mL. In 1.5 mL tubes, the cell suspensions were stained with 5 µL Annexin V-FITC and 5 µL PI then incubated in the dark at room temperature for 15 min. Finally, 400 µL 1X Binding Buffer was added and apoptosis was detected by flow cytometry within an hour in the CytoFLEX™ Flow Cytometer (Beckman Coulter Life Sciences). The data generated was analyzed in Kaluza Analysis software (Beckman Coulter Life Sciences). Only a single repeat was performed.

3.2.8. xCELLigence

Principle

The xCELLigence System™ Real-Time Cell Analyzer (RTCA) is a non-invasive, sensitive, and accurate label-free technology that detects and measures changes in cellular growth in real time. In addition to compound-induced cytotoxicity or apoptosis, changes in cell number, viable morphology and proliferation are detected by deviations in the electrical impedance signals that are generated by gold microelectrodes embedded at the bottom of each well on RTCA E-plates. When adherent cells attach to the electrodes, flow of current between the electrodes is obstructed and the electrical impedance value, represented as a Cell Index (CI) value, increases. As cells continue to proliferate and ultimately reach confluency, the CI value reaches a constant plateau. Therefore, an increase in CI is indicative of viable and proliferating cells while a decline in CI is characteristic of cell death.

Technique

Cell growth and morphological changes were monitored in CDDP-treated HeLa, CaSki and Vero cells post transfection using the xCELLigence System™ RTCA DP (ACEA Biosciences

Inc., USA). Prior to seeding cells, background interference was accounted for through subjecting antibiotic-free media in 16-well E-plates to a current induced by the instrument. Cells were seeded into the 16-well E-plates at 1.5×10^4 cells/well and incubated for 24 hr. at 37ºC in the xCELLigence System™ instrument to monitor cell proliferation prior to further treatments. Once logarithmic phase was reached, cells were transfected with siRBBP6 before exposing them to CDDP for an additional 24 and 48 hr. CI values were recorded at 15 min interval sweeps for the duration of the experiment, under the following conditions: [1st step: 1 sweep, 1 min interval, 00:00:39 total time; 2nd step: 100 sweeps, 15 min interval, 22:52:07 total time; 3rd step: 100 sweeps, 15 min interval, 47:38:30 total time; 4th step: 100 sweeps, 15 min interval, 72:12:25 total time]. The experiments were performed in duplicates.

3.2.9. Statistical Analysis

Statistical significance of the differences observed for each series of experiments was determined using the paired Student's t-test. Each experiment was done using two technical and biological replicates. The results were expressed as the mean ± standard error of the mean (SEM) and presented as either $p \leq 0.05$ *(*)*, $p \leq 0.01$ *(**)*, or $p \leq 0.001$ *(***)*, where $p \leq 0.05$ suggests that the differences between two groups are statistically significant and not due to chance.

CHAPTER 4: RESULTS

4.1. The effects of *RBBP6* knockdown on *p53* and *Bcl-2* gene expression

Prior to investigating the relationship between RBBP6 and CDDP sensitivity in HeLa, CaSki and Vero cells, successful silencing of *RBBP6* was verified using RT-qPCR. The relative ratio of *RBBP6* reduced significantly to 0.22 ± 0.02 SEM ($p < 0.05$) in HeLa cells, indicating an approximate 78% reduction in expression post transfection (Figure 5A). The relative expression ratio of *Bcl-2* in *RBBP6*-knockdown HeLa cells reduced significantly to 0.54 ± 0.17 SEM ($p < 0.05$), indicating an approximate 46% decrease in expression post transfection (Figure 5B). Although the relative ratio of *p53* increased to 1.29 ± 0.28 SEM, the increase in expression was not statistically significant ($p > 0.05$) relative to the untreated control (Figure 5C).

In CaSki cells, *RBBP6* expression reduced significantly by approximately 70% to a relative ratio of 0.31 ± 0.06 SEM ($p < 0.05$) (Figure 6A). CaSki cells exhibited a reduction in *Bcl-2* relative expression to a ratio of 0.26 ± 0.05 SEM ($p < 0.05$), indicating a 74% decrease in gene expression post transfection (Figure 6B). Although the relative expression ratio of *p53* decreased to 0.60 ± 0.10 SEM, the reduction in expression was not statistically significant ($p > 0.05$) relative to the untreated control (Figure 6C).

In Vero cells, *RBBP6* was successfully knocked down by approximately 77% (Figure 7A) to a relative ratio of 0.23 ± 0.03 SEM ($p < 0.05$). Despite the reduction observed post transfection, the changes in *Bcl-2* expression were not statistically significant relative to the untreated control (Figure 7B). *p53*, despite being absent in the untreated control, demonstrated an approximate 70% increase in expression after *RBBP6* was silenced (Figure 7C).

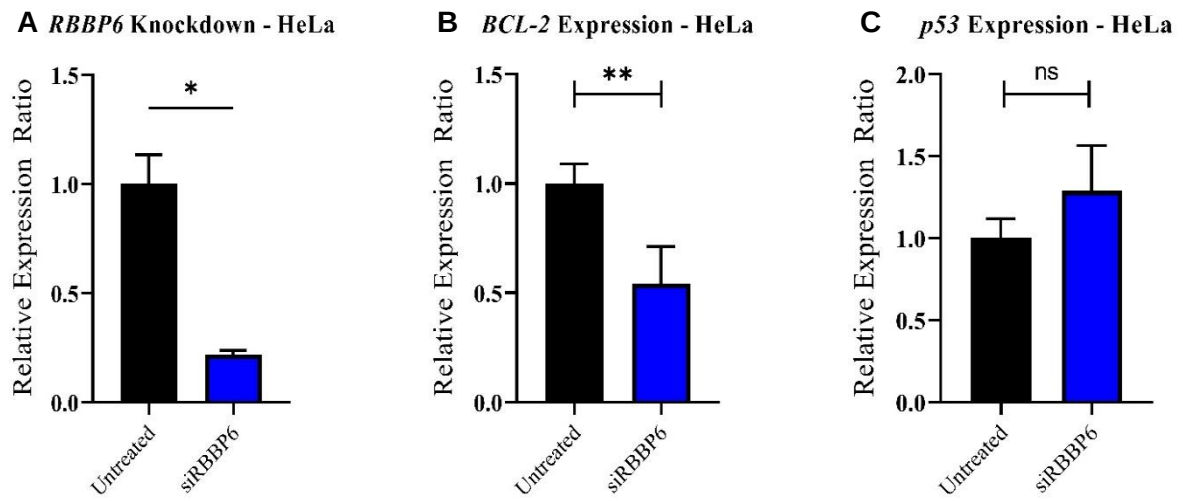

Figure 5. mRNA expression analysis in HeLa cells after transfection with 100 pmol siRNA targeting *RBBP6*.

(A) Confirmation of *RBBP6* knockdown in HeLa cells. Effect of *RBBP6* silencing on **(B)** *Bcl-2* and **(C)** *p53* gene expression in HeLa cells. Experiments were performed in duplicates. *(*)* $p < 0.05$, *(**)* $p < 0.01$, *(ns)* $p > 0.05$.

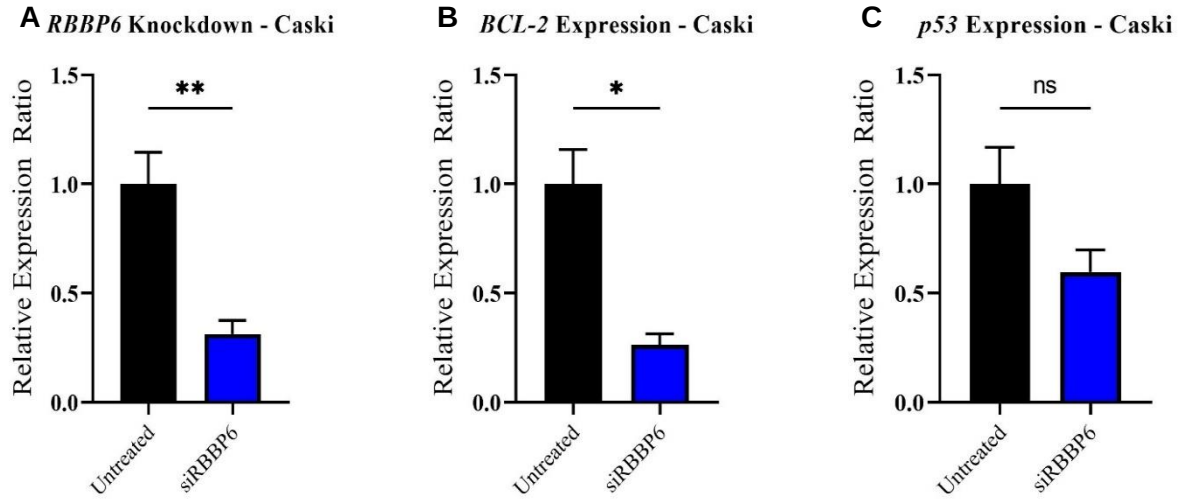

Figure 6. mRNA expression analysis in CaSki cells after transfection with 100 pmol siRNA targeting *RBBP6*.

(A) Confirmation of *RBBP6* knockdown in CaSki cells. Effect of *RBBP6* silencing on **(B)** *Bcl-2* and **(C)** *p53* gene expression in CaSki cells. Experiments were performed in duplicates. *(*)* $p < 0.05$, *(**)* $p < 0.01$, *(ns)* $p > 0.05$.

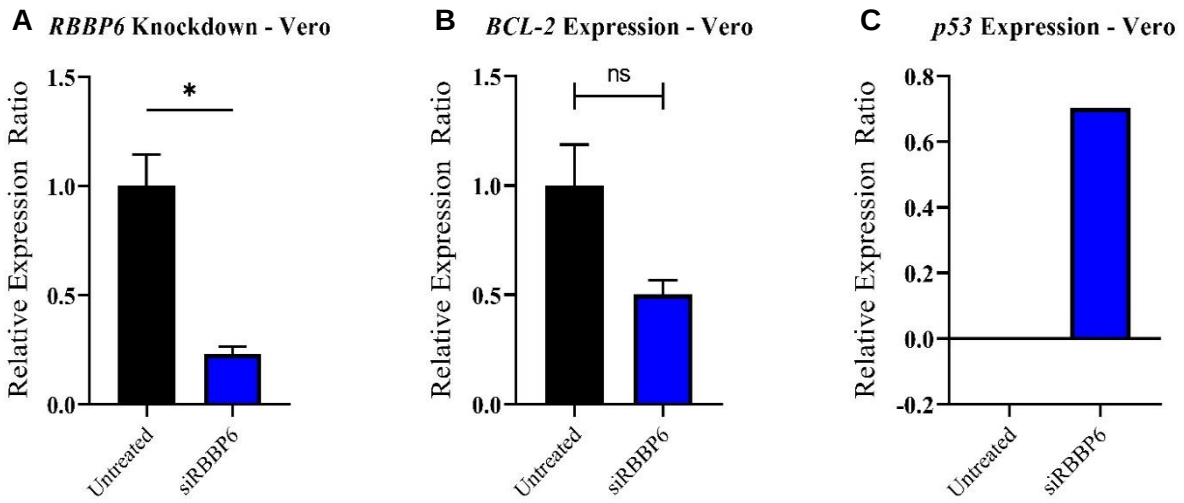

Figure 7. mRNA expression analysis in Vero kidney cells after transfection with 100 pmol siRNA targeting *RBBP6*.

(A) Confirmation of *RBBP6* knockdown in Vero cells. Effect of *RBBP6* silencing on **(B)** *Bcl-2* and **(C)** *p53* gene expression in Vero cells. Experiments were performed in duplicates. *(*)* $p < 0.05$, *(ns)* $p > 0.05$.

4.2. Determination of CDDP treatment dose using cell viability assay

Prior to investigating the effects of CDDP in HeLa and CaSki cells, the IC_{50} of this drug was determined using an MTT assay. Cell viability was expressed as a percentage relative to an untreated control (100% viable). In Hela cells, CDDP at 50 µg/mL and 25 µg/mL reduced cell viability significantly to ~30% ± 4.1% ($p < 0.05$) and ~45% ± 2.1% ($p < 0.05$), respectively. All concentrations below 25 µg/mL (12.5, 6.25 and 3.125 µg/mL) had no significant cytotoxic effect ($p > 0.05$) in these cells relative to the untreated control, as observed by the unexpected increase in percentage viability at these concentrations (Figure 8).

Similarly, in CaSki cells, CDDP at 50, 25 and 12.5 µg/mL reduced cell viability significantly to ~36% ± 3.9% ($p < 0.05$), ~49% ± 12.4% ($p < 0.05$) and ~79% ± 7.0% ($p < 0.05$). Concentrations at 6.25 and 3.125 µg/mL did not induce any significant cytotoxic effects ($p > 0.05$) in CaSki cells as observed by the non-significant change in percentage cell viability relative to the untreated control (Figure 9). CDDP at 25 µg/mL induced close to 50% cell death in both HeLa and CaSki cells and was indicative of being the working inhibitory concentration of CDDP in this study.

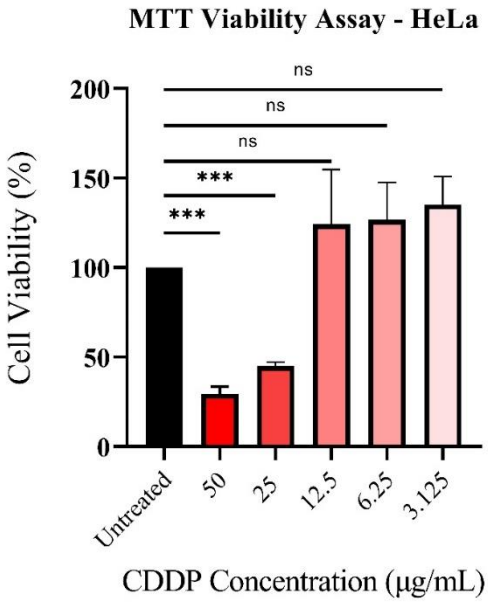

Figure 8. MTT viability assay of HeLa cells in response to CDDP.

Cells were treated with CDDP at 50, 25, 12.5, 6.25 and 3.125 µg/mL and compared against an untreated control. Experiments were performed in triplicates. *(***)* $p < 0.001$, *(ns)* $p > 0.05$.

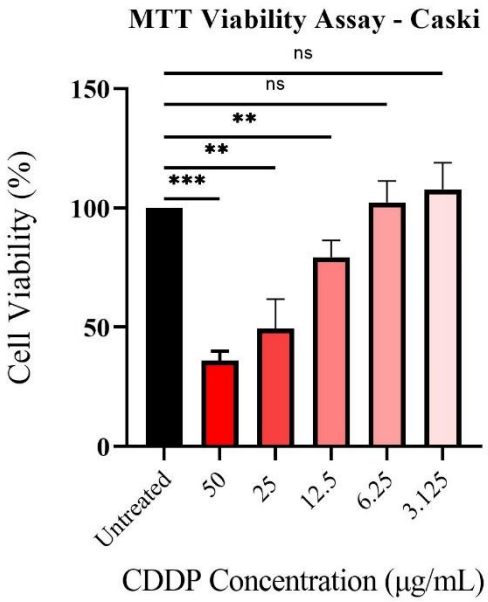

Figure 9. MTT viability assay of CaSki cells in response to CDDP.

Cells were treated with CDDP at 50, 25, 12.5, 6.25 and 3.125 µg/mL and compared against an untreated control. Experiments were performed in triplicates. *(**)* $p < 0.01$, *(***)* $p < 0.001$, *(ns)* $p > 0.05$.

4.3. *RBBP6, Bcl-2* and *p53* gene expression in response to CDDP treatment

The effect of CDDP treatment on *RBBP6, Bcl-2* and *p53* mRNA expression in HeLa, CaSki and Vero cells was examined after 24 and 48 hr. exposure periods. The relative expression ratio of *RBBP6* did not change significantly ($p > 0.05$) after 24 hr. of CDDP exposure in HeLa cells (Figure 10A). Interestingly, 48 hr. of exposure promoted a significant increase in the relative expression ratio of *RBBP6* to 1.38 ± 0.06 SEM ($p < 0.05$), indicating an approximate 38% increase in expression (Figure 10A). Despite an observed decrease in the expression of *Bcl-2* after 24 and 48 hr. of CDDP treatment, the differences were non-significant ($p > 0.05$) relative to the untreated control (Figure 10B). As expected, significant changes in *p53* expression level were observed after CDDP treatment, where it increased by ~3-fold (3.12 ± 0.26 SEM, $p < 0.05$) and ~ 8-fold (8.15 ± 0.88 SEM, $p < 0.05$) after 24 and 48 hr., respectively (Figure 10C).

Interestingly, the relative expression ratio of *RBBP6* in CaSki cells increased by ~4-fold (4.12 ± 0.41 SEM, $p < 0.05$) and ~2-fold (2.27 ± 0.12 SEM, $p < 0.05$) after 24 and 48 hr. CDDP exposure, respectively (Figure 11A). After 24 hr. CDDP exposure, the relative expression ratio of *Bcl-2* reduced to 0.09 ± 0.02 SEM ($p < 0.05$), indicating a 91% decrease in expression (Figure 11B). Similarly, after 48 hr. exposure *Bcl-2* expression reduced by approximately 73% to a relative ratio of 0.27 ± 0.07 ($p < 0.05$) (Figure 11B). As expected, *p53* expression increased significantly by 63% (1.63 ± 0.15 SEM, $p < 0.05$) after 24 hr. and by 2-fold (2.00 ± 0.19 SEM, $p < 0.05$) after 48 hr. CDDP exposure (Figure 11C).

In Vero cells, CDDP reduced the expression level of *RBBP6* significantly to 0.21 ± 0.04 SEM ($p < 0.05$) and 0.07 ± 0.01 SEM ($p < 0.05$) after 24 and 48 hr. of exposure, respectively (Figure 12A). Following CDDP treatment, *Bcl-2* exhibited less than ~4% ($p < 0.05$) expression after both exposure intervals (Figure 12B). No *p53* expression was observed (data not shown), suggesting complete absence of this tumor suppressor gene in CDDP treated cells. CDDP therefore promoted *RBBP6* expression in HeLa cells, while inhibiting it in Vero cells.

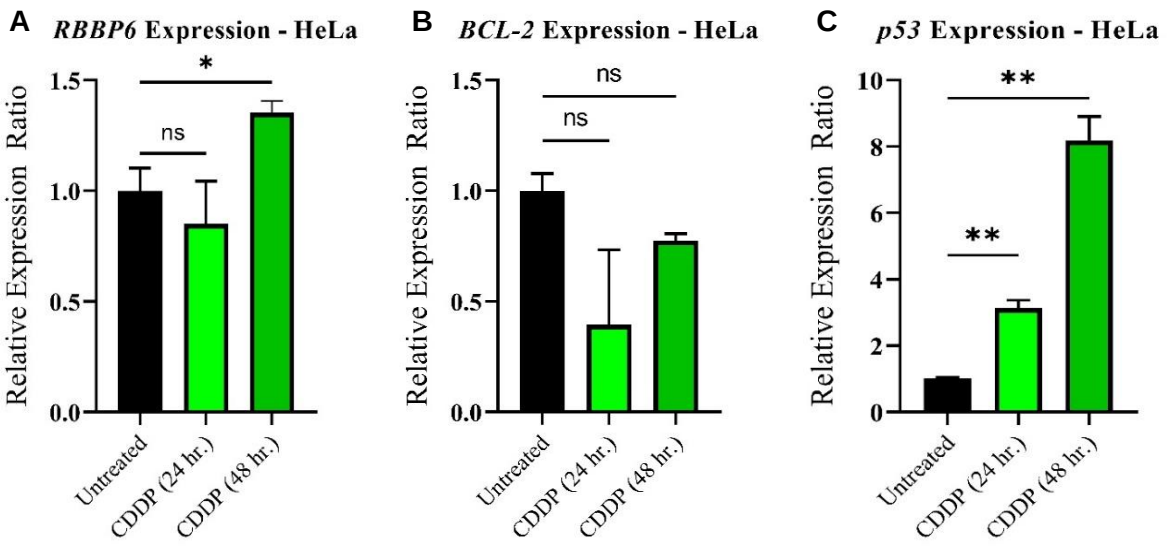

Figure 8. mRNA expression analysis in HeLa cervical cancer cells after exposure to 25 µg/mL CDDP for 24 and 48 hr. periods.

Effect of CDDP treatment on **(A)** *RBBP6*, **(B)** *Bcl-2* and **(C)** *p53* gene expression in HeLa cells. Experiments were performed in duplicates. *(*)* $p < 0.05$, *(**)* $p < 0.01$, *(ns)* $p > 0.05$.

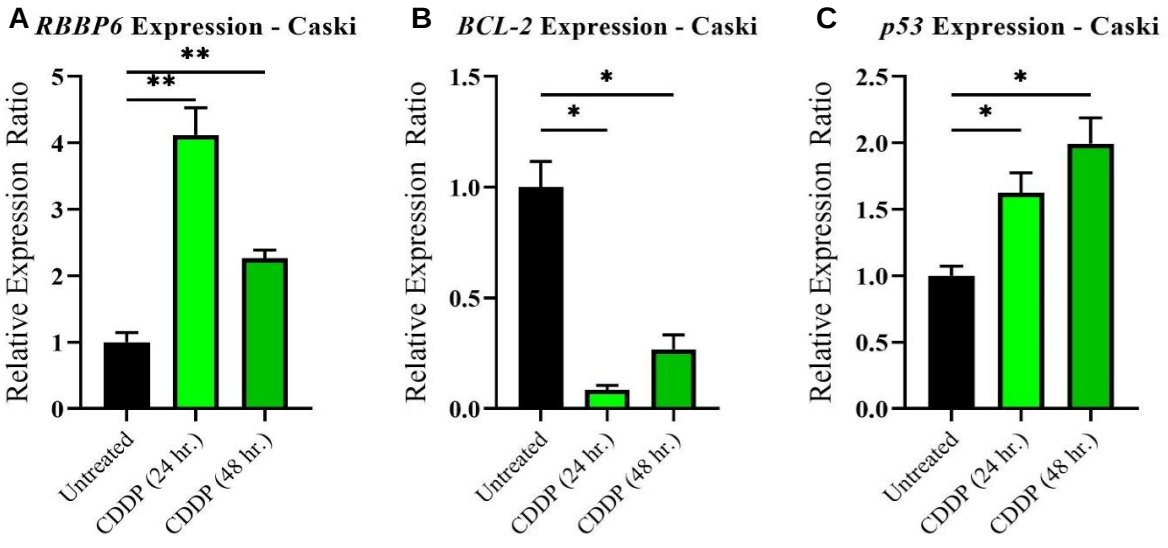

Figure 9. mRNA expression analysis in CaSki cervical cancer cells after exposure to 25 µg/mL CDDP for 24 and 48 hr. periods.

Effect of CDDP treatment on **(A)** *RBBP6*, **(B)** *Bcl-2* and **(C)** *p53* gene expression in CaSki cells. Experiments were performed in duplicates. *(*)* $p < 0.05$, *(**)* $p < 0.01$.

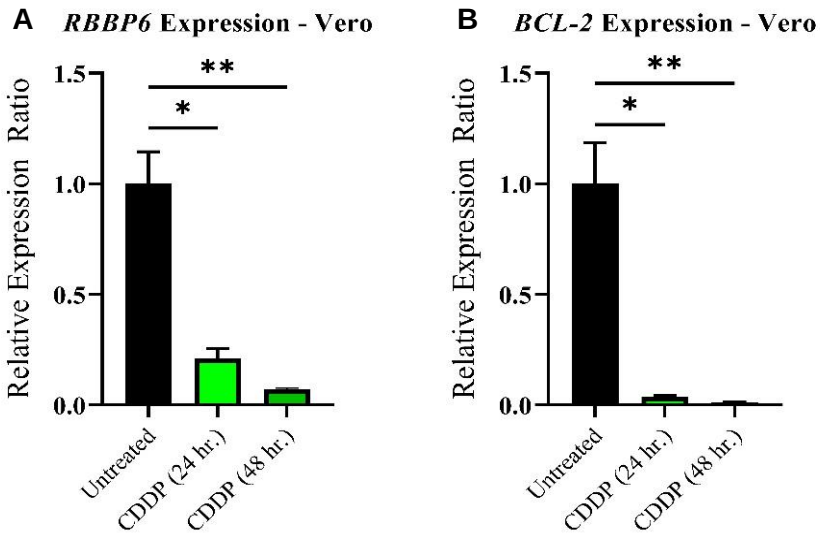

Figure 10. mRNA expression analysis in Vero kidney cells after exposure to 25 µg/mL CDDP for 24 and 48 hr. periods.

Effect of CDDP treatment on **(A)** *RBBP6* and **(B)** *Bcl-2* gene expression in Vero cells. Experiments were performed in duplicates. *(*)* $p < 0.05$, *(**)* $p < 0.01$.

4.4. Gene expression in response to combined *RBBP6* knockdown and CDDP treatment

Having observed the effects of *RBBP6* knockdown and CDDP treatment separately on gene expression, we were interested in investigating the combined effect of *RBBP6* knockdown and CDDP treatment on *RBBP6, Bcl-2* and *p53* expression in HeLa and Vero cells after 24 and 48 hr. exposure periods. In HeLa cells, *RBBP6* expression significantly increased by 87% increase in relative expression ratio (1.87 ± 0.17 SEM, $p < 0.05$) after 24 hr. of CDDP exposure post transfection (Figure 13A). However, no expression of *RBBP6* was detected after 48 hr. of CDDP exposure post transfection (Figure 13A). A similar pattern was observed with *Bcl-2*, where 24 hr. of CDDP exposure had no significant effect ($p > 0.05$) on expression levels but, 48 hr. of exposure completely hindered the expression of this (Figure 13B). After 24 hr. of CDDP exposure post transfection, *p53* expression significantly increased by approximately 6-fold (5.97 ± 0.38 SEM, $p < 0.05$). However, after 48 hr. of exposure, no significant difference ($p > 0.05$) in *p53* expression was observed relative to the untreated control (Figure 13C).

Following CDDP exposure for 24 hr. post-transfection, the relative expression ratio of *RBBP6* in CaSki cells increased by approximately 2-fold ($p < 0.05$), to 1.98 ± 0.05 SEM (Figure 14A). However, after 48 hr. CDDP exposure, *RBBP6* exhibited a non-significant decrease in relative expression ratio to 0.48 ± 0.26 SEM ($p > 0.05$) when compared to the untreated control (Figure 14A). After 24 hr. CDDP exposure post transfection, *Bcl-2* reduced by ~94% (0.06 ± 0.001 SEM, $p < 0.05$) and after 48 hr. exposure, *Bcl-2* gene expression was reduced completely (Figure 14B). After 24 hr. CDDP exposure post transfection, *p53* demonstrated a non-significant increase in expression, however, 48 hr. CDDP exposure increased *p53* by 67% ($p < 0.05$) to a relative expression ratio of 1.67 ± 0.10 SEM (Figure 14C).

In Vero cells, CDDP treatment of transfected cells reduced *RBBP6* expression to less than ~10% ($p < 0.05$) after both exposure intervals (Figure 15A), while *Bcl-2* expression reduced almost completely ($p < 0.05$) after co-treatment (Figure 15B). *p53* was completely repressed as was observed by lack of amplification of this gene in co-treated samples (data not shown).

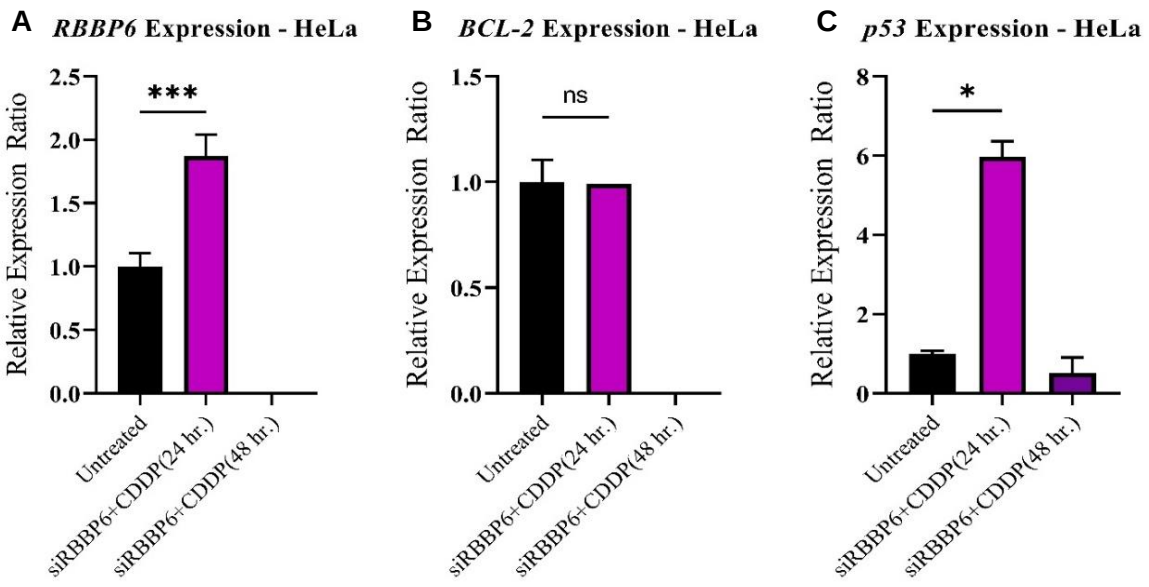

Figure 113. mRNA expression analysis in HeLa cervical cancer cells following co-treatment with siRBBP6 and CDDP for 24 and 48 hr. periods.

Effect of CDDP treatment post transfection on **(A)** *RBBP6*, **(B)** *Bcl-2* and **(C)** *p53* gene expression in HeLa cells. Experiments were performed in duplicates. *(*)* $p < 0.05$, *(***)* $p < 0.001$, *(ns)* $p > 0.05$.

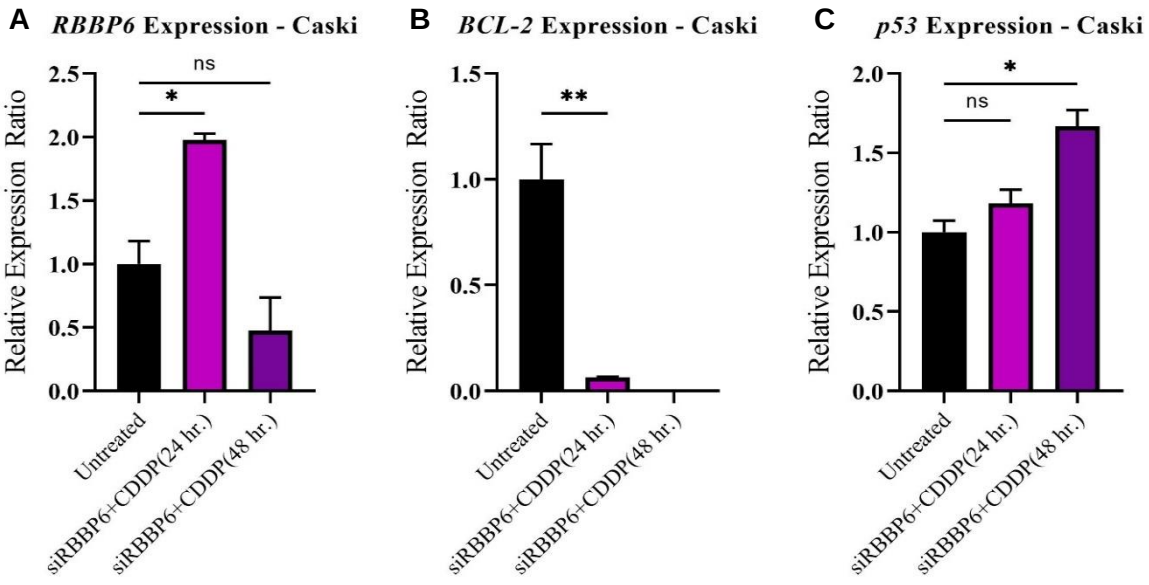

Figure 14. mRNA expression analysis in CaSki cervical cancer cells following co-treatment with siRBBP6 and CDDP for 24 and 48 hr. periods.

Effect of CDDP treatment post transfection on **(A)** *RBBP6*, **(B)** *Bcl-2* and **(C)** *p53* gene expression in CaSki cells. Experiments were performed in duplicates. *(*)* $p < 0.05$, *(**)* $p < 0.01$, *(ns)* $p > 0.05$.

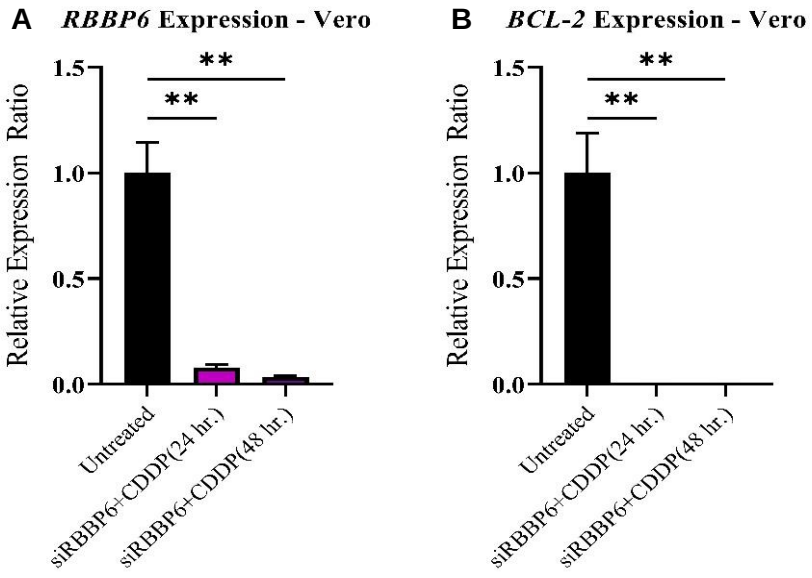

Figure 12. mRNA expression analysis in Vero kidney cells following co-treatment with siRBBP6 and CDDP for 24 and 48 hr.

Effect of CDDP treatment post transfection on **(A)** *RBBP6* and **(B)** *Bcl-2* gene expression in Vero cells. Experiments were performed in duplicates. *(**)* $p < 0.01$.

4.5. Apoptosis detection assay

Apoptosis induction was analyzed by flow cytometry in cells following transfection and/or CDDP treatment for 24 and 48 hr. exposure periods. The cells are gated into 4 different categories based on differential Annexin V-FITC and PI staining: viable cells (Annexin V-FITC and PI negative), early apoptotic cells (Annexin V-FITC positive, PI negative), late apoptotic cells (Annexin V-FITC positive, PI positive) and necrotic cells (Annexin V-FITC negative, PI positive). HeLa, CaSki and Vero cells undergoing early and late apoptosis following transfection and/or CDDP exposure were identified relative to an untreated control (Figure 16A, Figure 17A and Figure 18A).

Knocking down *RBBP6* in HeLa cells induced apoptosis and necrosis in 25.7% and 10.1% of the cell population, respectively, and 64.2% remained viable post transfection (Table 5 and Figure 16B). Following exposure to CDDP for 24 hr., 62.3% of the population remained viable while 32.4% and 5.3% underwent apoptosis and necrosis, respectively (Table 5 and Figure 16C). After 48 hr. of CDDP exposure, the percentage of apoptotic cells increased to 77%, while 13.6% underwent necrosis (Table 5 and Figure 16D). Combined with *RBBP6* gene silencing, CDDP exposure after 24 hr. induced 23% apoptosis and 11.8% necrosis, while 65.3% remained viable (Table 5 and Figure 16E). CDDP treatment for 48 hr. post transfection induced 59.4% apoptosis and 40.3% necrosis (Table 5 and Figure 16F).

In CaSki cells, RBBP6 gene silencing induced 17.9% apoptosis while 81.9% of the cell population remained viable (Table 6 and Figure 17B). Following CDDP exposure for 24 hr., 33.6% of cells remained viable while 66.4% underwent apoptosis (Table 6 and Figure 17C). Increasing CDDP exposure to 48 hr. induced 57.3% apoptosis with 42.7% of the population remaining viable (Table 6 and Figure 17D). Of the cell population treated with CDDP for 24 hr. post transfection, 37.1% underwent apoptosis (Table 6 and Figure 17E) and prolonged exposure to CDDP for 48 hr. following *RBBP6* silencing induced 70.5% apoptosis (Table 6 and Figure 17F). *RBBP6* knockdown and/or CDDP exposure for 24 and 48 hr. periods did not induce any necrosis in CaSki cells (Table 6 and Figures 17A-F).

In Vero cells, knockdown of *RBBP6* and/or treatment with CDDP for 24 and 48 hr. exposure periods induced less than or equal to 5% apoptosis and necrosis across all treatments and more than 95% of the cell population remained viable (Table 7 and Figure 18A-F).

Table 5. Flow cytometry analysis of cell death in HeLa cells following co-treatment with siRBBP6 and Cisplatin for 24 and 48 hr. periods

	Untreated	**siRBBP6**	**CDDP 24H**	**CDDP 48H**	**siRBBP6+CDDP 24H**	**siRBBP6+CDDP 48H**
Viable cells (%)	93.2	64.2	62.3	9.4	65.3	0.3
Apoptotic (Early/Late) cells (%)	6.4	25.7	32.4	77.0	23.0	59.4
Necrotic cells (%)	0.3	10.1	5.3	13.6	11.8	40.3

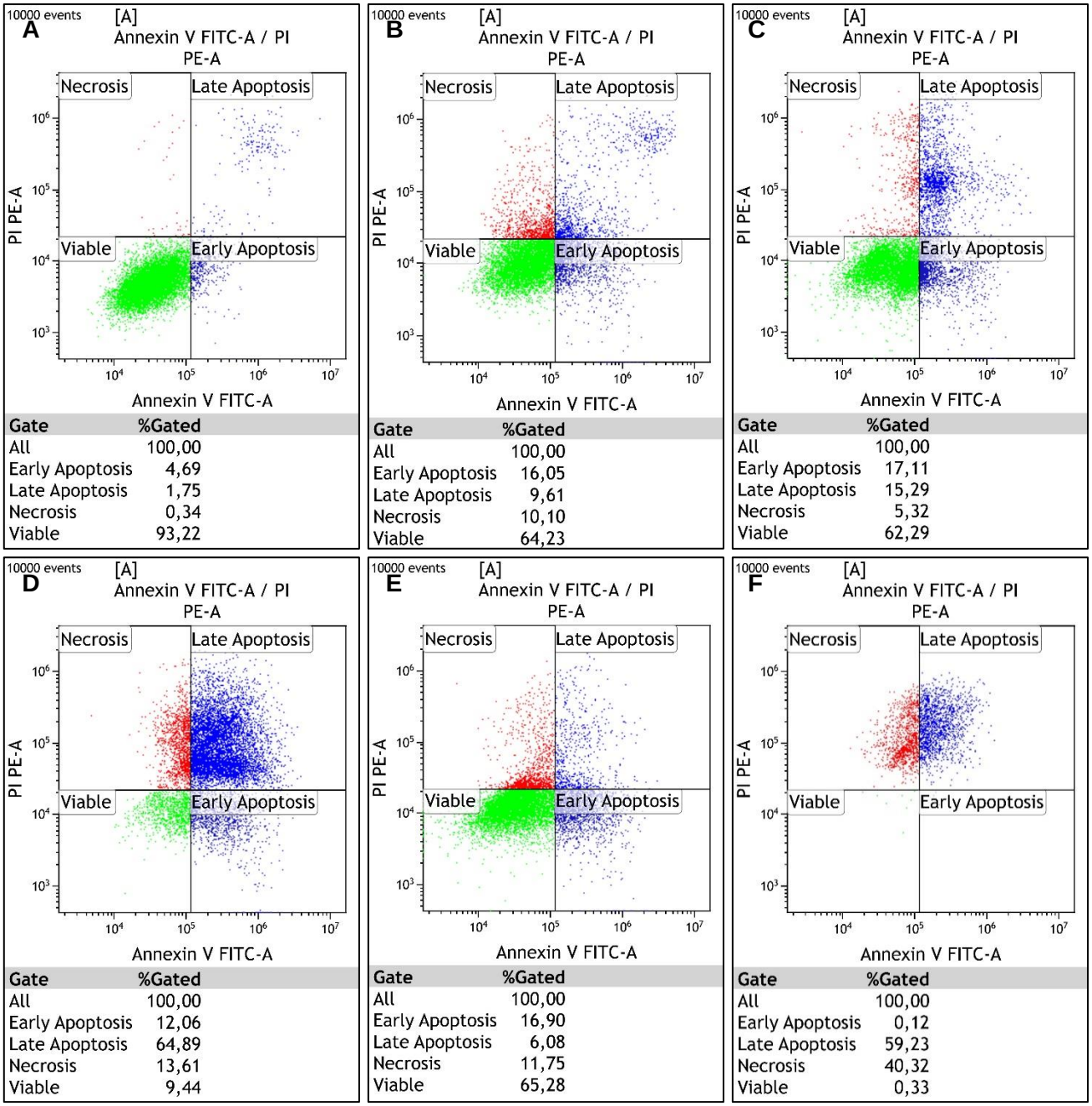

Figure 13. Flow cytometry analysis of apoptosis induction in HeLa cervical cells using Annexin V-FITC and PI following co-treatment with siRBBP6 and CDDP for 24 and 48 hr. periods.

Viable cells (green), early and late apoptotic cells (blue) and necrotic cells (red) were detected in **(A)** untreated cells, cells treated with **(B)** siRBBP6, **(C)** CDDP for 24 hr., **(D)** CDDP for 48 hr. **(E)** siRBBP6 and CDDP for 24 hr. and **(F)** siRBBP6 and CDDP for 48 hr.

Table 6. Flow cytometry analysis of cell death in CaSki cells following co-treatment with siRBBP6 and Cisplatin for 24 and 48 hr. periods

	Untreated	**siRBBP6**	**CDDP 24H**	**CDDP 48H**	**siRBBP6+CDDP 24H**	**siRBBP6+CDDP 48H**
Viable cells (%)	95.7	81.9	33.6	42.7	62.8	29.2
Apoptotic (Early/Late) cells (%)	4.2	17.9	66.4	57.3	37.1	70.5
Necrotic cells (%)	0.1	0.1	0.0	0.0	0.1	0.3

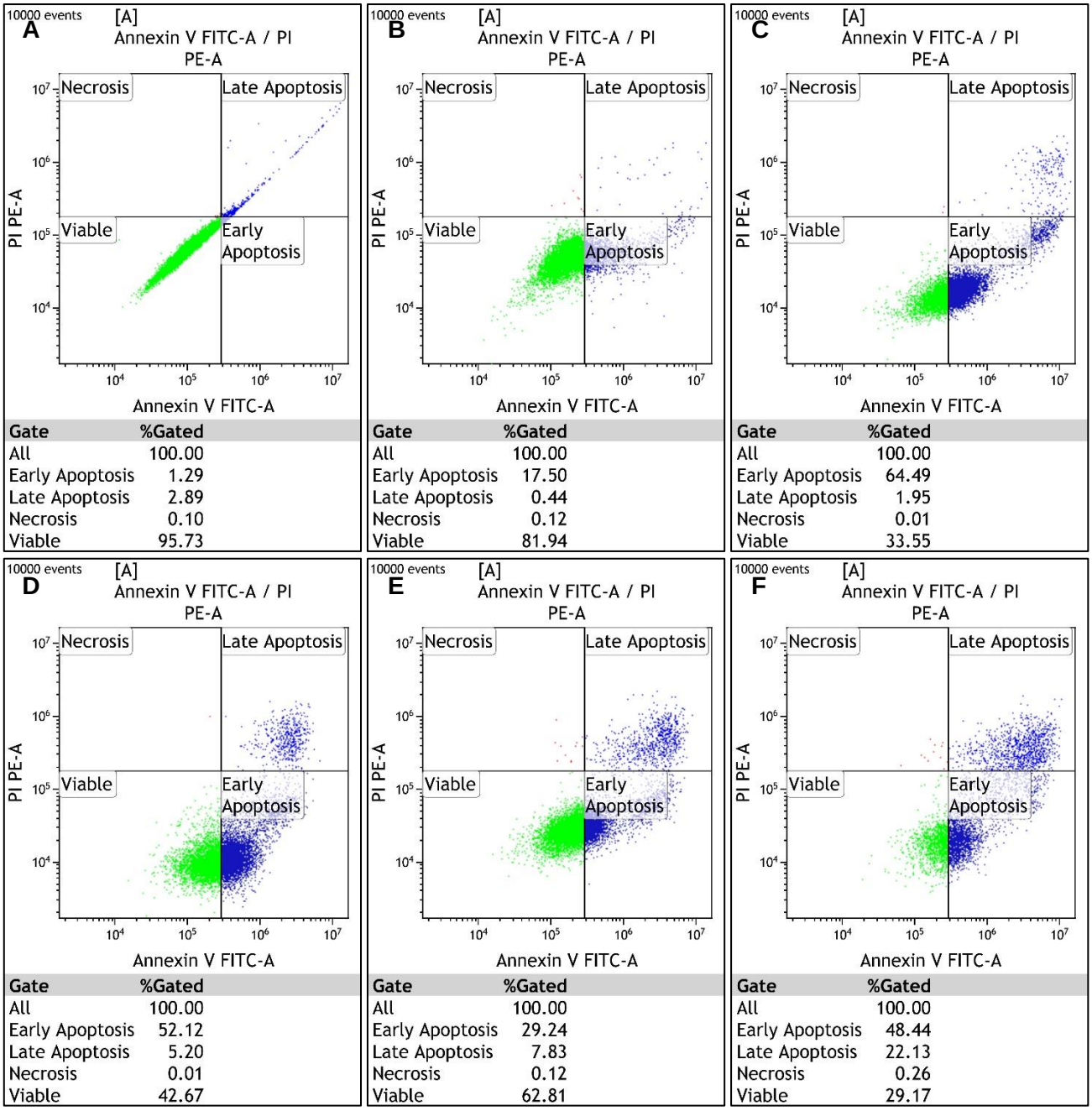

Figure 14. Flow cytometry analysis of apoptosis induction in CaSki cervical cells using Annexin V-FITC and PI following co-treatment with siRBBP6 and CDDP for 24 and 48 hr. periods.

Viable cells (green), early and late apoptotic cells (blue) and necrotic cells (red) were detected in **(A)** untreated cells, cells treated with **(B)** siRBBP6, **(C)** CDDP for 24 hr., **(D)** CDDP for 48 hr. **(E)** siRBBP6 and CDDP for 24 hr. and **(F)** siRBBP6 and CDDP for 48 hr.

Table 7. Flow cytometry analysis of cell death in Vero cells following co-treatment with siRBBP6 and Cisplatin for 24 and 48 hr. periods

	Untreated	**siRBBP6**	**CDDP 24H**	**CDDP 48H**	**siRBBP6+CDDP 24H**	**siRBBP6+CDDP 48H**
Viable cells (%)	95.5	99.0	94.1	96.8	96.3	98.4
Apoptotic (Early/Late) cells (%)	3.5	0.1	5.0	1.7	1.6	0.2
Necrotic cells (%)	1.0	0.9	0.9	1.5	2.1	1.4

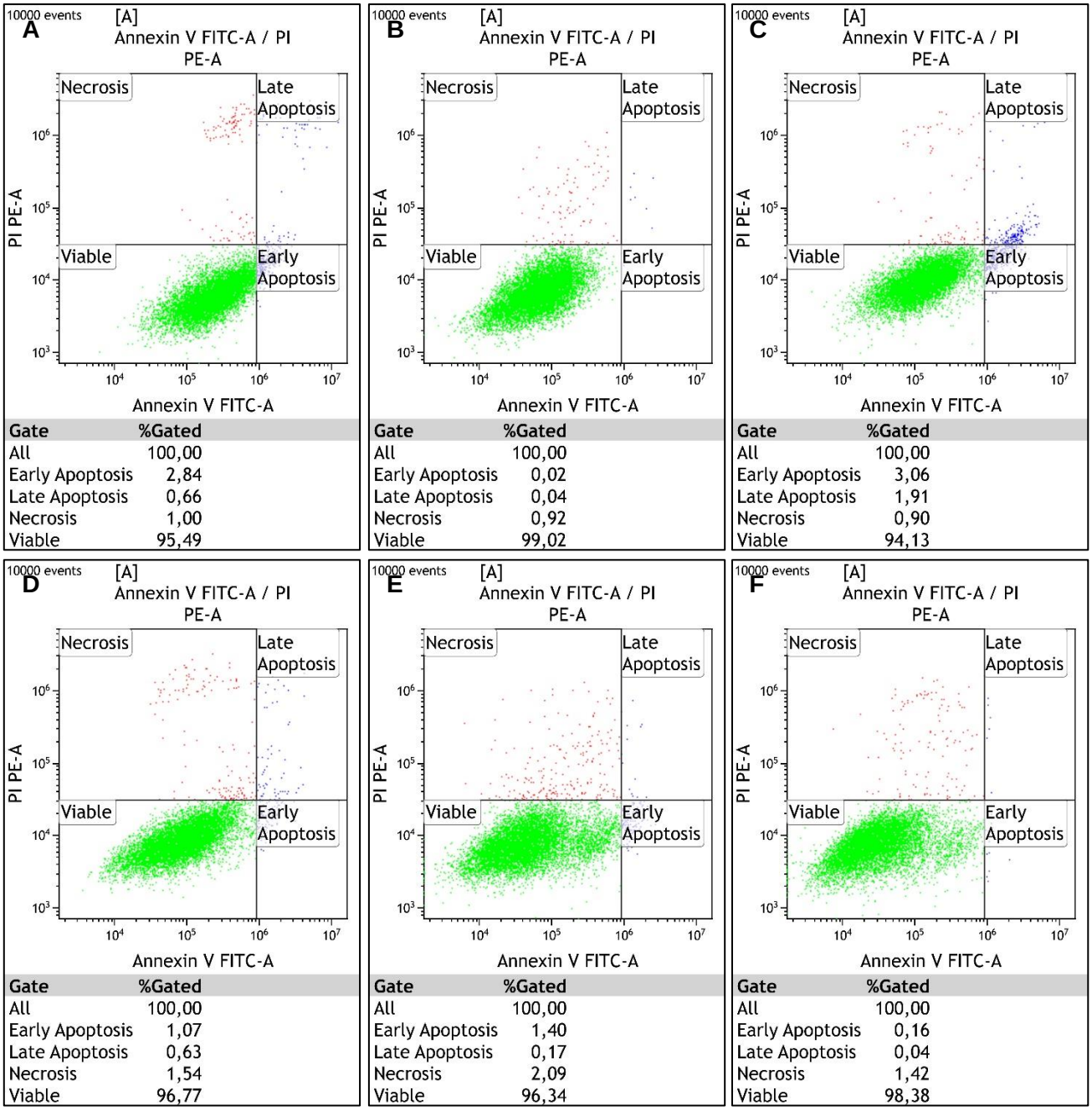

Figure 15. Flow cytometry analysis of apoptosis induction in Vero kidney cells using Annexin V-FITC and PI following co-treatment with siRBBP6 and CDDP for 24 and 48 hr. periods.

Viable cells (green), early and late apoptotic cells (blue) and necrotic cells (red) were detected in **(A)** untreated cells, cells treated with **(B)** siRBBP6, **(C)** CDDP for 24 hr., **(D)** CDDP for 48 hr. **(E)** siRBBP6 and CDDP for 24 hr. and **(F)** siRBBP6 and CDDP for 48 hr.

4.6. Real time cell growth analysis

Cell proliferation following transfection and/or CDDP treatment was monitored in HeLa, CaSki and Vero cells over a period of 72 hr. using the xCELLigence RTCA system. Cell growth was measured through real time detection of changes in electrical impedance and cell index (CI). In Hela cells, the growth inhibiting effect of *RBBP6* knockdown was validated through a steady decline in CI from the 48th hour following transfection with siRBBP6 (Figure 19, green growth curve). Treatment of HeLa cells with CDDP at 25 µg/mL resulted in higher cell growth inhibition compared to CDDP at 12.5 µg/mL. In fact, the cells treated with the lower dose (12.5 µg/mL) of CDDP remained in a plateaued state over the exposure period (Figure 19, turquoise blue growth curve), whereas cells treated with 25 µg/mL CDDP dose show growth reduction for approximately 42 hours before they start to recover (Figure 19, blue growth curve). Interestingly, the combination of siRBBP6 and CDDP (25 µg/mL) reduced HeLa cell growth significantly beyond the point of CDDP exposure alone at the same concentration (Figure 19, pink growth curve), however, growth inhibition was delayed compared to CDDP treatment alone. A similar delay was observed with the combination of siRBBP6 and CDDP (12.5 µg/mL) and although cell growth was suppressed significantly (Figure 19, dark green growth curve), a lower CDDP concentration was less effective.

In CaSki cells, *RBBP6* silencing alone had minimal growth inhibiting effects as observed by the constant, unchanged CI post transfection (Figure 20, green growth curve), relative to the untreated control (Figure 20, red growth curve). Interestingly, exposure to CDDP at 12.5 µg/mL (Figure 20, turquoise blue growth curve) and 25 µg/mL (Figure 20, blue growth curve) promoted cell growth following treatment, with the higher dose resulting in more proliferation compared to the lower dose. Eventually, CDDP-treated CaSki cells showed a steady, but delayed decline in CI around the 48th hr. Combined treatment with siRBBP6 and CDDP (25 µg/mL) reduced cell growth immediately compared to CDDP treatment alone at the same concentration (Figure 20, pink growth curve), however, growth inhibition was minimal. A similar pattern was observed with combination treatment of siRBBP6 and CDDP (12.5 µg/mL), where

immediate but limited growth inhibition occurred compared to CDDP-treated cells (Figure 20, dark green growth curve). Combination treatment at 25 µg/mL had stronger growth inhibiting effects compared to CDDP at a lower dose of 12.5 µg/mL in CaSki cells.

In Vero cells (Figure 21), a similar pattern of growth inhibition was observed when cells were exposed to different CDDP concentrations, however, this drug appeared to be highly cytotoxic compared to cancer cells as seen by the significant reduction in cell growth after treatment. On the contrary, the combination of siRBBP6 and CDDP (25 and 12.5 µg/mL) had minimal effect on Vero cell growth inhibition compared to HeLa and CaSki cells as seen by the similar growth pattern at both drug concentrations (Figure 21). Overall, combined-treatment proved to be less cytotoxic in HeLa cells and more cytotoxic in CaSki cells compared to CDDP-treatment alone.

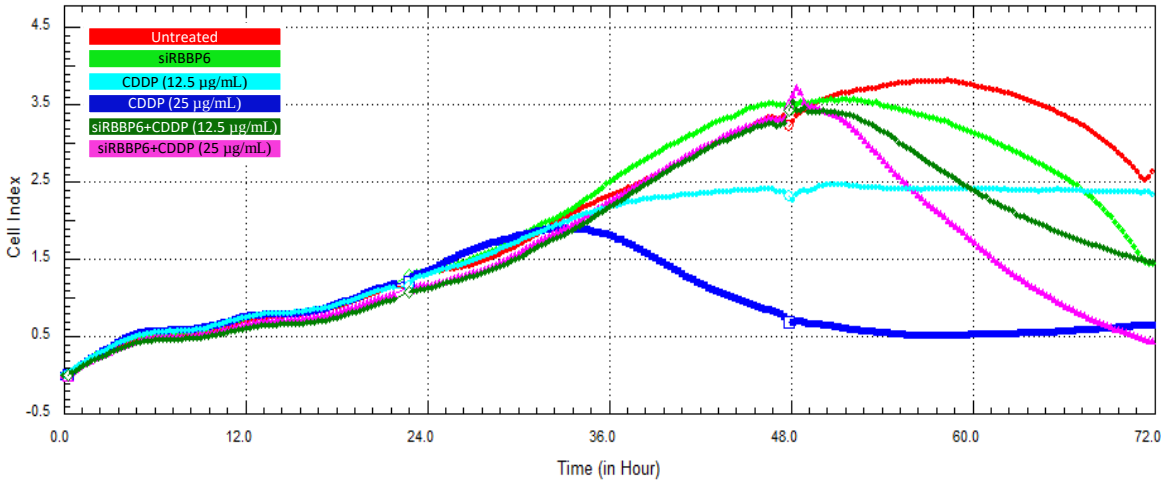

Figure 16. xCELLigence real time cell growth analysis of HeLa cells following *RBBP6*-knockdown and co-treatment with CDDP over 72 hr. period.

Proliferation of untreated cells (red), cells treated with siRBBP6 (green), 12.5 µg/mL CDDP (turquoise blue), 25 µg/mL CDDP (blue), cells co-treated with siRBBP6 + 12.5 µg/mL CDDP (dark green) and siRBBP6 + 25 µg/mL CDDP (pink) was monitored in real time over a period of 72 hr. Experiments were performed in duplicates.

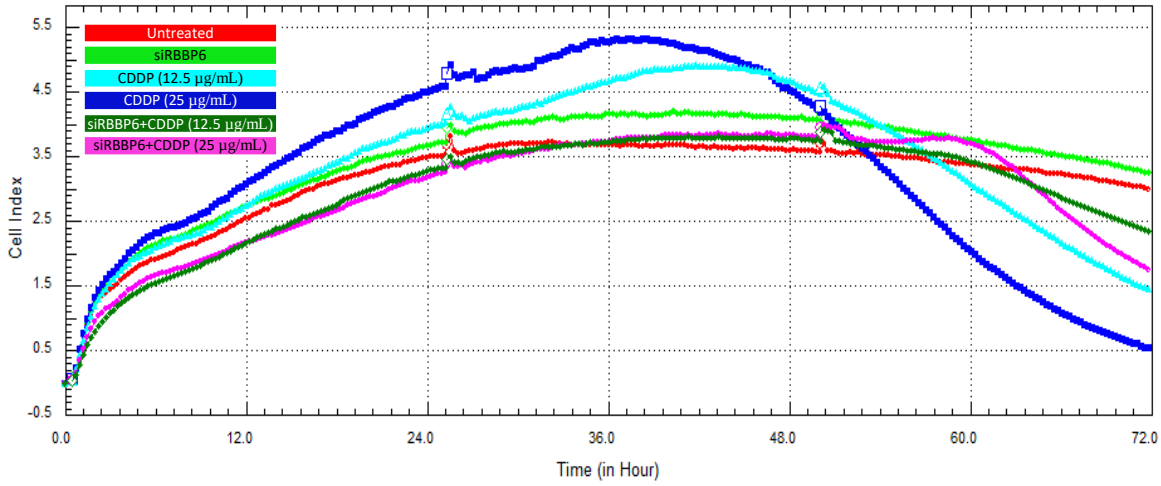

Figure 17. xCELLigence real time cell growth analysis of CaSki cells following *RBBP6*-knockdown and co-treatment with CDDP over 72 hr. period.

Proliferation of untreated cells (red), cells treated with siRBBP6 (green), 12.5 µg/mL CDDP (turquoise blue), 25 µg/mL CDDP (blue), cells co-treated with siRBBP6 + 12.5 µg/mL CDDP (dark green) and siRBBP6 + 25 µg/mL CDDP (pink) was monitored in real time over a period of 72 hr. Experiments were performed in duplicates.

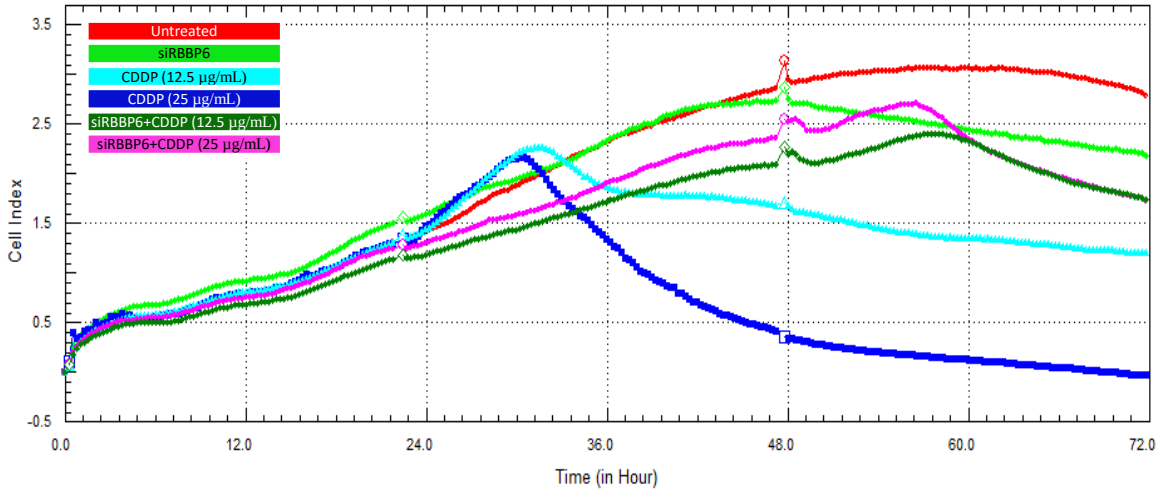

Figure 18. xCELLigence real time cell growth analysis of Vero cells following *RBBP6*-knockdown and co-treatment with CDDP over 72 hr. period.

Proliferation of untreated cells (red), cells treated with siRBBP6 (green), 12.5 µg/mL CDDP (turquoise blue), 25 µg/mL CDDP (blue), cells co-treated with siRBBP6 + 12.5 µg/mL CDDP (dark green) and siRBBP6 + 25 µg/mL CDDP (pink) was monitored in real time over a period of 72 hr. Experiments were performed in duplicates.

CHAPTER 5: DISCUSSION

Advanced cervical carcinomas are usually aggressive with poor prognosis, and patients on CDDP chemotherapy present with significantly improved survival. However, due to interindividual variability in genes coding for proteins that are involved in DNA repair and cell proliferation, some patients present with acquired resistance to CDDP chemotherapy, mainly through WT-p53 repression and Bcl-2 up-regulation. There is, therefore, a need for new therapeutic interventions that can help improve prognosis, either as single agents or in combination with current regimens. Cancer biomarkers offer an advancement to the currently existing anticancer treatment methods (Crafton and Salani 2016). Current research in the field of personalized medicine is focusing on biomarkers discovery that have a potential of developing tailor-made cancer therapy for individual patients, which will make cancer management more efficient while minimizing adverse side effects. The reason why there is attention on personalized medicine is mainly due to the considerable variations in treatment outcomes between individual cancer patients undergoing chemotherapy. There is enough evidence showing that targeting newly identified tumor markers in personalized medicine improves treatment outcome with chemotherapy (Bertsimas and Zhuo 2020).

RBBP6 is a proliferation-associated protein that is highly expressed during embryonic development and in rapidly dividing testis-derived cells. Owing to its ability to bind tumor suppressors, p53 and pRB, RBBP6 expression is associated with pathogenesis, specifically malignancies, where it is widely implicated in apoptosis and cell proliferation (Mbita *et al.* 2011; Motadi *et al.* 2018). Through the evolutionary conserved DWNN domain, RBBP6 is believed to regulate these proteins, among others, via the proteasomal pathway (Pugh *et al.* 2006) in several forms of cancer (Xiao *et al.* 2018a), thus making it a potential biomarker and target in personalized anticancer therapy. The *RBBP6* gene is alternatively spliced to generate four isoforms that are differentially expressed at different tumor stages, with more advanced cancers exhibiting higher levels of RBBP6 compared to less advanced stages (Motadi *et al.* 2018; Dlamini *et al.* 2019). Other studies have shown that RBBP6 promotes uncontrolled cell

growth and is associated with apoptosis during carcinogenesis (Moela *et al.* 2014; Makgoo *et al.* 2019). Also, more information is emerging regarding the role of RBBP6 in cancer treatment, specifically its potential to sensitize cancer cells to radiation and chemotherapeutic agents such as CPT, STS and GABA, as mentioned earlier (Motadi *et al.* 2018; Xiao *et al.* 2018a).

In the present study, we show the potential role of RBBP6 expression on the sensitivity of HeLa (HR-HPV-18-positive) and CaSki (HR-HPV-16-positive) cervical cancer cells to CDDP chemotherapy. The data generated should be interpreted with caution due to a limited number of repeats performed for each experiment. While the observed results cannot be used to draw concrete conclusions at this stage, the findings revealed in this study should not be discounted and should form grounds for further investigation. We recommend using more replicates in future studies to further validate the findings of this study.

Our findings show that these cervical cancer cells undergo significant apoptosis induction coupled with WT-*p53* gene up-regulation when treated with CDDP. Similarly, *RBBP6* knockdown results in apoptosis induction and a significant down-regulation of the *Bcl-2* anti-apoptotic gene in these cells. Furthermore, prolonged exposure of *RBBP6*-knockdown cervical cancer cells to CDDP results in a marked induction of apoptosis and growth inhibition coupled with *p53* up-regulation and *Bcl-2* down-regulation, more especially in CaSki cells, suggesting that this HR-HPV-16-positive cell line becomes sensitized to CDDP in the absence of *RBBP6* expression. In contrast, HeLa cells underwent a significant apoptosis reduction with no changes in *Bcl-2* expression, coupled with a significantly delayed cell growth repression in response to combined treatment, suggesting that the presence of *RBBP6* is necessary for sensitizing HR-HPV-18 positive HeLa cells to CDDP. The differential response between the two cell lines can be attributed to their physiological differences as mentioned earlier, and the fact that CaSki was derived from a less aggressive tumor site compared to HeLa (Paulraj *et al.* 2015; Xiao *et al.* 2018b; Sanchez-Sandoval and Gomora 2019).

CDDP shows promising cytotoxicity in advanced cervical cancer patients when administered as a single agent or in adjuvant therapy, as observed by its higher ORR compared to other

platinum-based chemotherapeutics (Yu and Garcia 2015). The IC_{50} of CDDP was determined using an MTT assay to identify the concentration that inhibits 50% cell growth in HeLa (Figure 8) and CaSki (Figure 9) cells. In both cell lines, CDDP at 25 µg/mL induced close to 50% cell death compared to higher and lower concentrations, which proved to be too cytotoxic or not cytotoxic enough, respectively. Therefore, the working IC_{50} of CDDP for subsequent analysis in this study was 25 µg/mL. CDDP less than 12.5 µg/mL did not exhibit significant cytotoxicity in both cell lines. This observation contradicts previous studies that report IC_{50} of CDDP ranging from 12 to 18 µg/mL in HeLa cells (Kashif *et al.* 2015; Wang *et al.* 2016; Artanti *et al.* 2020) and 10 to 30 µg/mL in CaSki cells (Byun *et al.* 2013; Koraneekit *et al.* 2018). Assessing cytotoxicity of CDDP in HeLa and CaSki cells at more concentrations (data points) between 12.5 and 25 µg/mL may provide a more accurate representation of the IC_{50} however, inconsistencies in IC_{50} values, especially with CDDP, are characteristic of cancer cells and can be explained by cell physiology, cell density variations or natural changes in cellular chemoresistance (He *et al.* 2016).

Cancer cells that acquire resistance to CDDP prolong their proliferation through evasion of apoptosis, particularly through Bcl-2 and p53-mediated pathways (Zhu *et al.* 2016). Cervical cancer cells demonstrate elevated levels of Bcl-2 anti-apoptotic protein (Brozovic *et al.* 2004) as well as a reduced WT-p53 expression due to degradation by HPV E6AP (Jung *et al.* 2012), a signature that promotes increased resistance to chemotherapy. Nonetheless, these cells illustrated an enhanced response to CDDP as shown by the significant apoptosis induction, a marked up-regulation of WT-p53, as well as a reduced Bcl-2 expression.

Our findings show CDDP-treated HeLa and CaSki cells displaying significant spikes in *p53* mRNA parallel to a significant reduction in cell growth through consequential apoptosis induction. HeLa cells displayed a significant 3-fold surge in p53 expression (Figure 10C) coupled with 32% apoptosis induction after 24 hr. CDDP exposure (Figure 16C and Table 5), and after 48 hr. an 8-fold surge in *p53* mRNA (Figure 10C) coupled with 77% apoptosis (Figure 16D and Table 5) was observed. Therefore, *p53* mRNA expression correlated directly with the

percentage of apoptosis induced in HeLa cells, thus validating the proposed mechanism of CDDP-induced cell death in cervical cancer cells by Jung *et al.* (2012). These observations lead us to propose that CDDP promotes apoptosis via the p53-pathway and not the Bcl-2 pathway, as seen by the lack of significant changes in *Bcl-2* following CDDP exposure (Figure 10B). Nevertheless, p53 and Bcl-2 protein expression analysis would shed more light on these findings. In CaSki cells, no correlation was seen between *p53* mRNA expression and apoptosis induction. In the presence of a 50% gene up-regulation after 24 hr. (Figure 11C), 66% apoptosis was induced in these cells (Figure 17C and Table 6) while a 2-fold gene up-regulation after 48 hr. (Figure 11C) induced 57% apoptosis (Figure 17D and Table 6). However, *Bcl-2* mRNA exhibited significant reductions at both exposure periods (Figure 11B), leading us to believe that apoptosis may be triggered via the Bcl-2 and p53 pathways. Once again, protein analysis of these apoptotic markers could substantiate our claims.

Interestingly, while HeLa cells underwent elevated levels of CDDP-induced apoptosis after 48 hr. (Figure 16D and Table 5), with significant reduction in cell growth (Figure 19, blue growth curve) compared to 24 hr., an unexpected 38% surge in *RBBP6* expression was observed (Figure 10A). *RBBP6* expression was up-regulated more significantly in CaSki cells, especially after 24 hr. CDDP exposure (Figure 11A), when *Bcl-2* was significantly down-regulated (Figure 11B) and a higher percentage of apoptosis was seen (Figure 17C and Table 6) compared to 48 hr. treatment. While unusual, these observations are consistent with findings by Dlamini *et al*. (2019), where elevated RBBP6 isoform 3 levels coupled with diminished Bcl-2 anti-apoptotic proteins induced cell death via the apoptotic pathway rather than the necrotic pathway. These findings suggest a possible interaction between CDDP and RBBP6 in the presence of HR-HPV infection, as well as early insights into the possibility of RBBP6 acting in alliance during CDDP-induced apoptosis via the WT-p53 and Bcl-2 expression signature. Though we cannot say this for certain unless protein expression analysis is performed, particularly on RBBP6 isoform 3 which has been implicated in apoptosis and cell growth inhibition.

.Overall, HeLa cells presented more pronounced CDDP-induced responses compared to CaSki cells, in terms of *p53* up-regulation, cell growth inhibition and cell death induction. These observations are explained by Funaoka *et al.* (1996), who reported that HeLa cells exhibit better sensitivity towards CDDP treatment compared to CaSki cells (Funaoka *et al.* 1996). HeLa cells exhibited an 8-fold spike in *p53* expression following prolonged CDDP treatment (Figure 10C), while CaSki cells only up-regulated *p53* by 2-fold (Figure 11C). In addition, HeLa cells exhibited CDDP-induced cell growth inhibition 8 hr. after administration (Figure 19, blue growth curve), whereas CaSki cells took double the time to reduce growth after experiencing a surge in proliferation following drug treatment (Figure 20, blue growth curve). Furthermore, a lower percentage of total cell death was induced in CaSki cells treated with CDDP for 48 hr. (Figure 17D and Table 6) compared to HeLa cells, which underwent higher percentages of apoptosis and necrosis (Figure 16D and Table 5). In fact, CaSki cells displayed a 9% reduction in apoptosis between 24 hr. (Figure 17C and Table 6) and 48 hr. (Figure 17D and Table 6) following CDDP treatment. This observation further supports the findings of Funaoka *et al.* (1996) who report on the limited sensitivity of CaSki cells towards CDDP. This leads us to speculate that the reduced apoptotic population observed after 48 hr. could be the result of naturally acquired chemoresistance towards CDDP, which would also explain the increase in *Bcl-2* after 48 hr. (Figure 11B) coupled with elevated *RBBP6* expression (Figure 11A). Furthermore, a phenomenon called apoptosis-reversal, which has been associated with increased drug resistance and invasion (Wang *et al.* 2014), could explain the decreased apoptotic population observed after prolonged CDDP treatment. Here, dying cells naturally reverse apoptosis by undoing the effects of DNA damage or Caspase 3, thus, promoting survival (Xu *et al.* 2018b). However, additional repeats could shed more light on our speculations. Their differing responses hint at the prospect of RBBP6 playing opposing roles in sensitizing HeLa and CaSki cells towards CDDP, possibly due to their differing cellular physiologies.

RBBP6 expression was knocked down successfully, by more than 70%, in HeLa (Figure 5A) and CaSki (Figure 6A) human cervical cancer cells using RNAi technology. This was followed by the evaluation of *Bcl-2* and *p53* gene expression in *RBBP6*-knockdown cells. Studies show that *RBBP6* promotes *Bcl-2* mRNA transcription in cancer cells, which consequently promotes continuous proliferation and evasion of apoptotic signals (Xiao *et al.* 2018a). Furthermore, a review by Haronikova *et al.* (2019) highlighted how *p53* mRNA can differentiate p53-mediated responses to signaling pathways. They describe an important interaction between *p53* mRNA and MDM2, which regulates synthesis of p53 and controls ubiquitin-mediated degradation of this tumor suppressor protein (Haronikova *et al.* 2019). MDM2 is phosphorylated at Ser395 in response to DNA damage, enabling it to bind to *p53* mRNA and assemble ATM (Ataxia Telangiectasia Mutated) kinase and the 5S RNP (RNA-Protein) complex to synthesize phosphorylated p53 proteins that cannot bind MDM2, thus promoting p53 translation (Haronikova *et al.* 2019). It is evident that mRNA plays a role as targets in signaling pathways and for this reason, focus was made on changes in mRNA expression for *Bcl-2* and *p53*. Also, it will be interesting for future studies to look into the changes in Bcl-2 and p53 proteins and how it correlates with findings at the mRNA level.

As expected, *Bcl-2* mRNA expression reduced significantly in both cell lines (Figures 5B and 6B), which is consistent with findings by Xiao et al. (2018a) and confirms that *Bcl-2* expression is regulated by RBBP6. WT-*p53* mRNA expression level in HeLa cells increased in response to *RBBP6* gene knockdown (Figure 5C), and although the increase was not statistically significant, this observation is coherent with previous studies where p53 expression was up-regulated in response to *RBBP6* knockdown (Li *et al.* 2007; Moela *et al.* 2014; Xiao *et al.* 2018a). But, once again, p53 protein expression analysis could further confirm these observations. Contrasting findings were observed in CaSki cells, where WT-*p53* displayed a non-significant decrease in mRNA expression post transfection (Figure 6C). A drawback of the RNA interference analysis performed in this study is the absence of a negative control which entails transfecting cells with a “scramble” siRNA sequence that has no target, and

which differs from the test siRNA sequence. However, a very similar study by Mosweu et al. (2020) investigated the effects of the same negative siRNA sequence in HeLa and CaSki cells and reported that there was no significant difference in *RBBP6* expression between the untreated and scramble siRNA-treated cells, as one would expect. That notwithstanding, a repetition of this experiment would have been appropriate to demonstrate reproducibility and confirm their observations.

WT-p53 is strongly believed to be regulated by RBBP6 since it contains its binding domain, however the exact mechanism is not yet clear. Previous studies suggest that RBBP6 promotes ubiquitin-mediated degradation of the WT-p53 tumor suppressor protein using E3-ligase activity within its DWNN domain (Midgley and Lane 1997; Chibi *et al.* 2008; Motadi *et al.* 2018). These studies speculate that, by either degrading p53 or promoting its inhibitory interaction with MDM2 (Di Giammartino *et al.* 2014), RBBP6 reduces the expression of p53 in cancer cells, thus promoting cell proliferation. Therefore, a more significant up-regulation of *p53* mRNA, needed for protein translation, was expected following *RBBP6* silencing. The non-significant changes in *p53* expression following *RBBP6* silencing may be attributed to the presence of diminished but functional RBBP6 at sufficient levels to negatively regulate *p53* expression in HeLa and CaSki cells. As a result, majority of *RBBP6*-knockdown HeLa and CaSki cell populations remained viable, with only a small percentage undergoing apoptosis and cell growth inhibition in the presence of down-regulated *Bcl-2* and possibly other pathways independent of *p53*.

Vero cells, sourced from African green monkey kidney epithelial cells, were used as the control in this study due to limited availability of a preferred normal human cell line, such as MRC-5 derived from lung tissue or HCK1T derived from cervical keratinocytes. However, the use of Vero cells has been widely adopted in several other cervical cancer studies for comparative purposes (Daduang et al. 2015; Promraksa et al. 2015) since they are derived from normal kidney cells and not immortal cells and can retain the attributes of normal cells (Mullan and Marsh 2020).

RBBP6 expression was reduced significantly by ~77% in Vero cells (Figure 7A). As expected, a non-significant reduction in *Bcl-2* was observed post-transfection (Figure 7B), however, a significant increase in *p53* mRNA expression was observed (Figure 7C), which is most likely due to the cells' DNA repair machinery responding to the temporary stress inflicted by transfection with foreign nucleotide material. This is further supported by the lack of apoptosis induction where almost 99% of the Vero cell population remained viable post-transfection (Figure 18B and Table 7), thus indicating that the up-regulation of *p53* was temporary with no consequential p53-mediated apoptosis induction. Furthermore, real time cell growth analysis revealed a ~2.2 decrease in CI (Figure 21, green growth curve), which is minor compared to the untreated control, further suggesting that the knockdown of *RBBP6* had no major impact on the growth of Vero cells.

siRBBP6 and/or CDDP treatment was expected to have minimal or no significant effect on the control Vero cells, and as observed, at least 94% of the cell population remained viable following both treatments (Figures 18C-F and Table 7). Real time cellular analysis further supported the minimal changes expected in Vero cells following both treatments (Figure 21, turquoise blue, pink and dark green growth curves). While significant growth inhibition was seen in response to 25 µg/mL CDDP alone (Figure 21, dark blue growth curve), CDDP proved to be too cytotoxic at this concentration for the lower cell density used and exposure to 12.5 µg/mL gave rise to a more favourable outcome (Figure 21, turquoise growth curve). Surprisingly, mRNA expression analysis revealed significant down-regulation of the anti-apoptotic gene, *Bcl-2,* in response to CDDP treatment (Figure 12B) and combined treatment (Figure 15B). This observation could suggest that *Bcl-2* down-regulation may not be involved in the survival of Vero cells towards CDDP in the presence or absence of RBBP6, and a different biochemical pathway could play a role. A more probable explanation for the lack of correlation observed between mRNA expression analysis and apoptosis induction or cell growth inhibition is the phenomenon described by Niepel *et al*. (2017). They report on different

cell lines exhibiting significant transcriptional changes in response to drug treatment without any effect on phenotypic responses (Niepel *et al.* 2017).

The effects of *RBBP6* knockdown on CDDP sensitivity in HeLa cervical cancer cells was evaluated by measuring the mRNA expression levels of WT-*p53* and *Bcl-2* post CDDP treatment. A surprising observation was made in co-treated HeLa (Figure 13A) where *RBBP6* exhibited a spike in mRNA expression after 24 hr. drug exposure despite the presence of siRBBP6. In fact, co-treated HeLa cells exhibited a surge in *RBBP6* that was 87% greater than in cells treated with CDDP alone for 24 hr. (Figure 10A). Considering the outcome of CDDP-treated cells discussed earlier (Figures 10A and 11A), we can speculate that the *RBBP6*-promoting effects of CDDP, may have counteracted the silencing effects of siRBBP6 in HeLa cells, which exhibited a delayed response to transfection. However, no logical explanations for this spike can be made at this stage and through further investigations, this interesting observation can be explored further. *RBBP6* repression in HeLa following 48 hr. CDDP exposure post transfection (Figure 13A) was a greater reduction compared to siRBBP6 treatment alone (Figure 5A), suggesting that prolonged exposure was required for the combination treatment to take effect, since maximum mRNA knockdown is often seen between 24-48 hr. after transfection. There was no change in *Bcl-2* expression after 24 hrs. (Figure 13B), possibly due to the presence of elevated *RBBP6* levels that sustained transcription of *Bcl-2*, however, the cells showed an up-regulation of WT-p53 (Figure 13C) that is consistent with CDDP-only treatment (Figure 10C). After 48 hr. of CDDP treatment post-transfection, *Bcl-2* was completely repressed (Figure 13B), which was also a greater down-regulation compared to siRBBP6 treatment alone (Figure 5B) and thus, further confirms the need for prolonged exposure. No change was seen in *p53* mRNA expression (Figure 13C).

At the mRNA level, these results suggest that *RBBP6* silencing promotes down-regulation of *Bcl-2* in CDDP-treated cells, thus leading us to anticipate enhanced apoptosis induction. However, the level of CDDP-induced apoptosis in *RBBP6*-knockdown HeLa cells was reduced (Figure 16E-F and Table 5), leading us to believe that *Bcl-2* down-regulation is not the only

mechanism responsible for the observed apoptotic cell death. In the complete absence of *RBBP6* and *Bcl-2* expression following combined treatment, WT-*p53* expression was expected to increase significantly to promote more p53-medited apoptosis compared to when CDDP was administered alone. However, the lack of WT-*p53* up-regulation in response to CDDP post transfection (Figure 13C) further suggests that *RBBP6* knockdown does not promote sensitization of HeLa cells to CDDP via the p53 pathway. Though, protein expression analysis is needed to support these statements.

This is illustrated by the apoptosis detection data where 24 hr. CDDP exposure post transfection led to only 23% of the cell population undergoing apoptosis (Figure 16E and Table 5) compared to 33% in CDDP-only treatment (Figure 16C and Table 5). A much higher increase in apoptosis induction was expected to correlate with the significant up-regulation of *p53* mRNA in these cells, however, the opposite took place where a 10% reduction in apoptosis was observed. Furthermore, cells exposed to siRBBP6 and CDDP for 48 hrs. underwent an 18% reduction in apoptosis, from 77% in CDDP-only treatment (Figure 16D and Table 5) to 59% in the combined treatment (Figure 16F and Table 5). With *RBBP6 and Bcl-2* expression completely inhibited after 48 hr. drug exposure, *p53* expression was expected to increase significantly to promote downstream apoptosis due to absence of its supposed negative regulator. The compromised apoptosis induction in combined treatment despite WT-*p53* up-regulation at 24 hr. exposure and *Bcl-2* repression at 48 hr. exposure suggests that RBBP6 may play a role in the sensitization of Hela cells to CDDP. This is also insinuated by real time monitoring of cell growth in the presence of siRBBP6 and CDDP treatment, which shows that knocking down *RBBP6* delays cell death induced by CDDP (Figure 19, pink growth curve). The large proportion of necrotic HeLa cells in response to siRBBP6 and CDDP co-treatment (Figure 16F) can be attributed to a phenomenon called necroptosis, a mode of cell death that involves binding of the TNF-α and Fas ligand to their respective cell surface receptors to activate a series of receptor interacting protein kinase (RIPK)-related signal

transduction events that promote the release of intracellular contents into the extracellular space (Dasgupta *et al.* 2016).

Comparable and contrasting observations were made with mRNA expression of WT-*p53* and *Bcl-2* post *RBBP6* silencing and CDDP treatment in CaSki cervical cancer cells. Similar to HeLa cells, co-treated CaSki cells exhibited an unexpected up-regulation of *RBBP6* at 24 hr. (Figure 14A), even though this was less significant in comparison to CDDP treatment alone (Figure 11A). At 48 hr., *RBBP6* exhibited a non-significant 48% reduction (Figure 14A). Prolonging exposure was not as effective in co-treated CaSki cells compared to HeLa cells, and despite expression being lower than CDDP treatment alone (Figure 11A), siRBBP6 alone yielded a more favorable reduction (Figure 6A). Again, we can speculate that CDDP may have delayed the effects of siRBBP6, causing *RBBP6* to express at sufficient levels to limit sensitivity of these cells towards the drug in co-treated CaSki cells. Despite the presence of up-regulated *RBBP6, Bcl-2* expression decreased significantly in knockdown cells after 24 hr. exposure, until it was completely repressed with prolonged drug treatment (Figure 14B). This observed pattern of expression was a noticeable improvement compared to CDDP treated cells (Figure 11B).

WT-*p53* exhibited a similar pattern of expressional changes that was consistent with CDDP-only treatment (Figure 11C), despite knockdown of its negative regulator in combination treatment (Figure 14C). A more pronounced up-regulation of *p53* was anticipated following CDDP treatment in the absence of *RBBP6*, however, its unchanged level of expression suggests that the p53-pathway may not be associated with sensitizing *RBBP6*-knockdown CaSki cells to CDDP.

At mRNA level, the up-regulation of *p53* and down-regulation of *Bcl-2* mediated by *RBBP6* silencing in CDDP-treated CaSki cells was predicted to correlate with accelerated apoptosis induction. However, CDDP exposure had minimal effects on *p53* expression in these cells, and a 24 hr. incubation post transfection triggered apoptosis in 37% of the cell population (Figure 17E and Table 6), which was a reduction compared to 67% in CDDP-only treated cells

(Figure 17C and Table 6). A possible explanation for the observed lack of both *p53* up-regulation and apoptosis improvement after 24 hr. exposure may be that the presence of the HR-HPV strain in these cells led to E6 oncoprotein competing for p53 protein degradation, thus devaluing the efforts of silencing *RBBP6* alone to preserve p53. It would, therefore, be interesting to observe CDDP sensitivity in the absence of both RBBP6 and E6 oncoprotein or in HPV-negative cell lines. Remarkably though, increasing drug exposure to 48 hr. post transfection induced cell death in 70% of CaSki cells (Figure 17F and Table 6), a 13% increase from 57% in CDDP-only cells (Figure 17D and Table 6). This further highlights the importance of prolonged CDDP exposure in *RBBP6*-knockdown CaSki cells to counteract possible interference by E6 to induce enhanced levels of apoptosis compared to CDDP alone, and further implicates *Bcl-2* down-regulation as the mechanism responsible for mediating CDDP sensitivity in these cells. This is confirmed by real time growth analysis of CaSki cells, which demonstrated delayed growth inhibition in response to CDDP treatment alone (Figure 20, blue growth curve) compared to co-treatment (Figure 20, pink growth curve). Our observations validate the relationship between RBBP6, and *Bcl-2* expression as previously reported by Xiao *et al.* (2018a) and suggests that targeting *RBBP6* for knockdown does not increase p53-mediated apoptosis through *p53* gene up-regulation in CDDP-treated CaSki cells, as formerly predicted. The observed delay in cell growth inhibition in CDDP-treated cells and the increase in apoptosis induction following prolonged co-treatment with siRBBP6 and CDDP suggests that the presence of *RBBP6* limits sensitization of CaSki cervical cancer cells to CDDP. However, protein expression analysis would shed more light on these speculations.

This is the first study to document the potential role of RBBP6 in the response of cervical cancer cells to CDDP. We hypothesized that in the presence of RBBP6, cancer cells would exhibit poor sensitivity towards this drug, which correlates with previous studies that reported increased sensitivity of HPV E6-knockdown HeLa cells towards CDDP through restoration of p53 and induction of apoptosis and senescence (Putral *et al.* 2005; Jung *et al.* 2012). We report that *RBBP6* expression promotes the sensitivity of HeLa cells to CDDP, despite being

associated with cell proliferation, similarly to HPV E6, but the presence of *RBBP6* desensitizes CaSki cells to CDDP. However, it is worth noting that RBBP6 is a multifunctional protein (Pugh *et al.* 2006), and, by definition, this is a type of protein that structurally consists of a single type of polypeptide chain but has multiple catalytic or binding functions (Kirschner and Bisswanger 1976). For example, in addition to the binding domains for p53 and pRB, RBBP6 consists of a RING finger domain that functions to conjugate ubiquitin moieties to substrate proteins, and the SR domain and zinc knuckle that occur in mRNA-associated splicing proteins (Pugh *et al.* 2006). It therefore goes without saying that RBBP6 may be capable of having different characteristics and functions depending on the HPV profile of the cancer, stage, and tumor localization.

This agrees with a study by Dlamini *et al.* (2019) who found that high levels of both RBBP6 and p53 were present in severe dysplasia and invasive cervical carcinoma sites that had accumulation of apoptosis, which implies that the presence of RBBP6 can promote apoptosis. In addition, this can be explained by tumor heterogeneity and clonal evolution, which is marked by the presence of more than one clone, which often gives rise to different expression patterns of genes involved in cell growth and apoptosis (Caswell and Swanton 2017). Indeed, some forms of carcinomas with elevated levels of RBBP6 can acquire resistance towards radiotherapy and certain chemotherapeutic agents; and knockdown of RBBP6 improves their sensitivity through apoptosis induction. For example, radio-resistant colorectal cells showed overexpressed levels of RBBP6, which was needed to accelerate tumorigenesis, and knockdown of this gene increased their sensitivity towards radiotherapy through attenuation of the p53-MDM2 inhibitory interaction, stimulation of pro-apoptotic protein, Bax and caspase 3, inhibition of Bcl-2, and subsequent induction of p53-mediated cell death (Xiao *et al.* 2018a). Similarly, in breast cancer cells with highly expressed RBBP6, apoptosis induction occurred in the presence of CPT and GABA, post transfection with siRBBP6 (Moela *et al.* 2014; Motadi *et al.* 2018).

CHAPTER 6: CONCLUSION AND FUTURE WORK

Outcomes of this study suggest a possible relationship between *RBBP6* knockdown and enhanced sensitivity of CaSki cells to CDDP-induced apoptosis correlated with *Bcl-2* down-regulation and *p53* up-regulation. In HeLa cells, however, knockdown of *RBBP6* shows signs of limiting apoptosis induction and delaying cell growth inhibition in response to CDDP, suggesting that these cells could be desensitized to the drug. The presence of RBBP6 in HeLa seems to promote CDDP sensitivity as was indicated by the significant apoptosis induction coupled with *Bcl-2* down-regulation when *RBBP6* was not silenced, though overexpressing *RBBP6* in these cells may shed more light on this speculation. Furthermore, the up-regulation of *RBBP6* in CDDP-treated cells provides very early insights into a possible interaction between RBBP6 and CDDP that is worth exploring. Overall, these findings illustrate the potential role of *RBBP6* in the sensitivity of cervical cancer cells to CDDP chemotherapy and the knowledge obtained here could possibly improve CDDP efficacy through personalized administration based on RBBP6 expression profiles among individual cervical cancer patients. Future studies can include a more robust investigation on additional HR-HPV positive (e.g. SiHa) and HPV-negative (e.g. C33A) cervical cancer cell lines to further investigate the effects of HPV infection on RBBP6 function in CDDP responses. Furthermore, measurement of Bcl-2 and p53 at protein level is essential and overexpressing *RBBP6* in a cervical cancer cell line that does not express the gene can fully substantiate the findings of this study and their implications. Finally, assessing the role of RBBP6 in cervical cancer cell responses to CDDP *in vivo,* using a cancer mouse model, can shed more light into the molecular mechanisms of CDDP acquired resistance.

CHAPTER 7: REFERENCES

Artanti, A. N., U. H. Pujiastuti, F. Prihapsara and R. Rakhmawati, 2020 Synergistic Cytotoxicity Effect by Combination of Methanol Extract of Parijoto Fruit (*Medinilla speciosa* Reinw. ex Bl*)* and Cisplatin against HeLa Cell Line. Indonesian Journal of Cancer Chemoprevention 11**:** 16-21.

Babu, A., A. Munshi and R. Ramesh, 2017 Combinatorial therapeutic approaches with RNAi and anticancer drugs using nanodrug delivery systems. Drug development and industrial pharmacy 43**:** 1391-1401.

Bai, Z., Z. Zhang, X. Qu, W. Han and X. Ma, 2012 Sensitization of breast cancer cells to taxol by inhibition of taxol resistance gene 1. Oncology letters 3**:** 135-140.

Basu, A., and S. Krishnamurthy, 2010 Cellular responses to Cisplatin-induced DNA damage. Journal of nucleic acids 2010**:** 201367.

Bertsimas, D., and Y. D. Zhuo, 2020 Novel Target Discovery of Existing Therapies: Path to Personalized Cancer Therapy. INFORMS Journal on Optimization 2**:** 1-13.

Bray, F., J. Ferlay, I. Soerjomataram, R. L. Siegel, L. A. Torre *et al.*, 2018 Global cancer statistics 2018: GLOBOCAN estimates of incidence and mortality worldwide for 36 cancers in 185 countries. CA: A Cancer Journal for Clinicians 68**:** 394-424.

Brisson, M., and M. Drolet, 2019 Global elimination of cervical cancer as a public health problem. The Lancet Oncology 20**:** 319-321.

Brozovic, A., G. Fritz, M. Christmann, J. Zisowsky, U. Jaehde *et al.*, 2004 Long-term activation of SAPK/JNK, p38 kinase and fas-L expression by cisplatin is attenuated in human carcinoma cells that acquired drug resistance. Int J Cancer 112**:** 974-985.

Burd, E. M., 2003 Human papillomavirus and cervical cancer. Clinical microbiology reviews 16**:** 1-17.

Byun, J., D. Jeong, D. Lee, J. Kim, S. Park *et al.*, 2013 Tetraarsenic oxide and cisplatin induce apoptotic synergism in cervical cancer. Oncology reports 29.

Carter, M., 2020 Women with HIV have sixfold increase in risk of cervical cancer, pp., AidsMap.

Caswell, D. R., and C. Swanton, 2017 The role of tumour heterogeneity and clonal cooperativity in metastasis, immune evasion and clinical outcome. BMC medicine 15**:** 133-133.

Chao, C. C., 1994 Decreased accumulation as a mechanism of resistance to cis-diamminedichloroplatinum(II) in cervix carcinoma HeLa cells: relation to DNA repair. Mol Pharmacol 45**:** 1137-1144.

Chavez, J. D., M. R. Hoopmann, C. R. Weisbrod, K. Takara and J. E. Bruce, 2011 Quantitative proteomic and interaction network analysis of cisplatin resistance in HeLa cells. PloS one 6**:** e19892-e19892.

Chen, H., W. Zhang, X. Cheng, L. Guo, S. Xie *et al.*, 2017 β2-AR activation induces chemoresistance by modulating p53 acetylation through upregulating Sirt1 in cervical cancer cells. Cancer science 108**:** 1310-1317.

Chen, S. H., and J. Y. Chang, 2019 New Insights into Mechanisms of Cisplatin Resistance: From Tumor Cell to Microenvironment. Int J Mol Sci 20.

Chibi, M., M. Meyer, A. Skepu, D. J. G. Rees, J. C. Moolman-Smook *et al.*, 2008 RBBP6 Interacts with Multifunctional Protein YB-1 through Its RING Finger Domain, Leading to Ubiquitination and Proteosomal Degradation of YB-1. Journal of Molecular Biology 384**:** 908-916.

Cibula, D., N. R. Abu-Rustum, P. Benedetti-Panici, C. Kohler, F. Raspagliesi *et al.*, 2011 New classification system of radical hysterectomy: emphasis on a three-dimensional anatomic template for parametrial resection. Gynecologic Oncology 122**:** 264-268.

Clifford, G. M., J. S. Smith, T. Aguado and S. Franceschi, 2003 Comparison of HPV type distribution in high-grade cervical lesions and cervical cancer: a meta-analysis. British journal of cancer 89**:** 101-105.

Crafton, S. M., and R. Salani, 2016 Beyond Chemotherapy: An Overview and Review of Targeted Therapy in Cervical Cancer. Clin Ther 38**:** 449-458.

Daduang, J., A. Palasap, S. Daduang, P. Boonsiri, P. Suwannalert *et al.*, 2015 Gallic Acid Enhancement of Gold Nanoparticle Anticancer Activity in Cervical Cancer Cells, pp. 169-174 in *Asian Pacific journal of cancer prevention : APJCP*.

Dasari, S., and P. B. Tchounwou, 2014 Cisplatin in cancer therapy: molecular mechanisms of action. European journal of pharmacology 740**:** 364-378.

Dasgupta, A., M. Nomura, R. Shuck and J. Yustein, 2016 Cancer's Achilles' Heel: Apoptosis and Necroptosis to the Rescue. International Journal of Molecular Sciences 18**:** 23.

Denny, L., 2010 Cervical cancer in South Africa: An overview of current status and prevention strategies. Continuing Medical Education 28.

Denny, L., and L. Kuhn, 2017 Cervical cancer prevention and early detection from a South African perspective. South African Health Review 2017**:** 189-195.

Di Giammartino, D. C., W. Li, K. Ogami, J. J. Yashinskie, M. Hoque *et al.*, 2014 RBBP6 isoforms regulate the human polyadenylation machinery and modulate expression of mRNAs with AU-rich 3' UTRs. Genes & development 28**:** 2248-2260.

Díaz-González, S. d. M., J. Deas, O. Benítez-Boijseauneau, C. Gómez-Cerón, V. H. Bermúdez-Morales *et al.*, 2015 Utility of microRNAs and siRNAs in cervical carcinogenesis. BioMed research international 2015**:** 374924-374924.

Dlamini, Z., T. Ledwaba, R. Hull, S. Naicker and Z. Mbita, 2019 RBBP6 Is Abundantly Expressed in Human Cervical Carcinoma and May Be Implicated in Its Malignant Progression. Biomarkers in cancer 11**:** 1179299X19829149-11179299X19829149.

Duan, G., Q. Tang, H. Yan, L. Xie, Y. Wang *et al.*, 2017 A Strategy to Delay the Development of Cisplatin Resistance by Maintaining a Certain Amount of Cisplatin-Sensitive Cells. Scientific Reports 7**:** 432.

Ferreira, M. P., A. E. Coghill, C. B. Chaves, A. Bergmann, L. C. Thuler *et al.*, 2017 Outcomes of cervical cancer among HIV-infected and HIV-uninfected women treated at the Brazilian National Institute of Cancer. Aids 31**:** 523-531.

Finocchario-Kessler, S., C. Wexler, M. Maloba, N. Mabachi, F. Ndikum-Moffor *et al.*, 2016 Cervical cancer prevention and treatment research in Africa: a systematic review from a public health perspective. BMC women's health 16**:** 29-29.

Frumovitz, M., M. F. Munsell, J. K. Burzawa, L. A. Byers, P. Ramalingam *et al.*, 2017 Combination therapy with topotecan, paclitaxel, and bevacizumab improves progression-free survival in recurrent small cell neuroendocrine carcinoma of the cervix. Gynecologic Oncology 144**:** 46-50.

Funaoka, K., M. Shindoh, T. Yamashita, K. Fujinaga, A. Amemiya *et al.*, 1996 High-risk HPV-positive human cancer cell lines show different sensitivity to cisplatin-induced apoptosis correlated with the p21 Waf1/Cip1 level. Cancer Letters 108**:** 15-23.

Gadducci, A., R. Tana, S. Cosio and L. Cionini, 2010 Treatment options in recurrent cervical cancer (Review). Oncol Lett 1**:** 3-11.

Galluzzi, L., L. Senovilla, I. Vitale, J. Michels, I. Martins *et al.*, 2012 Molecular mechanisms of cisplatin resistance. Oncogene 31**:** 1869-1883.

Ganesh, S., A. K. Iyer, J. Weiler, D. V. Morrissey and M. M. Amiji, 2013 Combination of siRNA-directed Gene Silencing With Cisplatin Reverses Drug Resistance in Human Non-small Cell Lung Cancer. Molecular therapy. Nucleic acids 2**:** e110-e110.

Green, J. A., and G. Lainakis, 2006 Cytotoxic chemotherapy for advanced or recurrent cervical cancer. Ann Oncol 17 Suppl 10**:** x230-232.

Guan, P., R. Howell-Jones, N. Li, L. Bruni, S. de Sanjosé *et al.*, 2012 Human papillomavirus types in 115,789 HPV-positive women: A meta-analysis from cervical infection to cancer. International Journal of Cancer 131**:** 2349-2359.

Guo, W., W. Chen, W. Yu, W. Huang and W. Deng, 2013 Small interfering RNA-based molecular therapy of cancers. Chinese journal of cancer 32**:** 488-493.

Haronikova, L., V. Olivares-Illana, L. Wang, K. Karakostis, S. Chen *et al.*, 2019 The p53 mRNA: an integral part of the cellular stress response. Nucleic Acids Res 47**:** 3257-3271.

He, Y., Q. Zhu, M. Chen, Q. Huang, W. Wang *et al.*, 2016 The changing 50% inhibitory concentration (IC50) of cisplatin: A pilot study on the artifacts of the MTT assay and the precise measurement of density-dependent chemoresistance in ovarian cancer. Oncotarget 7.

Hientz, K., A. Mohr, D. Bhakta-Guha and T. Efferth, 2017 The role of p53 in cancer drug resistance and targeted chemotherapy. Oncotarget 8**:** 8921-8946.

Huang, H., S. Y. Huang, T. T. Chen, J. C. Chen, C. L. Chiou *et al.*, 2004 Cisplatin restores p53 function and enhances the radiosensitivity in HPV16 E6 containing SiHa cells. J Cell Biochem 91**:** 756-765.

Ishida, S., F. McCormick, K. Smith-McCune and D. Hanahan, 2010 Enhancing tumor-specific uptake of the anticancer drug cisplatin with a copper chelator. Cancer cell 17**:** 574-583.

Jhingran, A., A. H. Russell, M. V. Seiden, L. R. Duska, A. Goodman *et al.*, 2020 84 - Cancers of the Cervix, Vulva, and Vagina, pp. 1468-1507.e1468 in *Abeloff's Clinical Oncology (Sixth Edition)*, edited by J. E. Niederhuber, J. O. Armitage, M. B. Kastan, J. H. Doroshow and J. E. Tepper. Content Repository Only!, Philadelphia.

Jiang, M., and J. Milner, 2002 Selective silencing of viral gene expression in HPV-positive human cervical carcinoma cells treated with siRNA, a primer of RNA interference. Oncogene 21**:** 6041-6048.

Jo, Y., N. Choi, K. Kim, H.-J. Koo, J. Choi *et al.*, 2018 Chemoresistance of Cancer Cells: Requirements of Tumor Microenvironment-mimicking In Vitro Models in Anti-Cancer Drug Development. Theranostics 8**:** 5259-5275.

Johnstone, T. C., K. Suntharalingam and S. J. Lippard, 2015 Third row transition metals for the treatment of cancer. Philosophical Transactions of the Royal Society A: Mathematical, Physical and Engineering Sciences 373**:** 20140185.

Jung, H. S., O. C. Erkin, M. J. Kwon, S. H. Kim, J. I. Jung *et al.*, 2012 The synergistic therapeutic effect of cisplatin with Human papillomavirus E6/E7 short interfering RNA on cervical cancer cell lines in vitro and in vivo. International Journal of Cancer 130**:** 1925-1936.

Kale, J., E. J. Osterlund and D. W. Andrews, 2018 BCL-2 family proteins: changing partners in the dance towards death. Cell Death & Differentiation 25**:** 65-80.

Kalkavan, H., and D. R. Green, 2018 MOMP, cell suicide as a BCL-2 family business. Cell Death & Differentiation 25**:** 46-55.

Kamura, T., and K. Ushijima, 2013 Chemotherapy for advanced or recurrent cervical cancer. Taiwanese Journal of Obstetrics and Gynecology 52**:** 161-164.

Kashif, M., S. Bano, S. Naqvi, S. Faizi, Lubna *et al.*, 2015 Cytotoxic and antioxidant properties of phenolic compounds from Tagetes patula flower. Pharmaceutical Biology 53**:** 672-681.

Kirschner, K., and H. Bisswanger, 1976 Multifunctional Proteins. Annual Review of Biochemistry 45**:** 143-166.

Koivusalo, R., E. Krausz, H. Helenius and S. Hietanen, 2005 Chemotherapy compounds in cervical cancer cells primed by reconstitution of p53 function after short interfering RNA-mediated degradation of human papillomavirus 18 E6 mRNA: opposite effect of siRNA in combination with different drugs. Mol Pharmacol 68**:** 372-382.

Kombe, A. J., B. Li, A. Zahid, H. M. Mengist, G.-A. Bounda *et al.*, 2021 Epidemiology and Burden of Human Papillomavirus and Related Diseases, Molecular Pathogenesis, and Vaccine Evaluation. Frontiers in Public Health 8.

Koraneekit, A., T. Limpaiboon, A. Sangka, P. Boonsiri, S. Daduang *et al.*, 2018 Synergistic effects of cisplatin-caffeic acid induces apoptosis in human cervical cancer cells via the mitochondrial pathways. Oncology letters 15**:** 7397-7402.

Kumar Biswas, S., J. Huang, S. Persaud and A. Basu, 2004 Down-regulation of Bcl-2 is associated with cisplatin resistance in human small cell lung cancer H69 cells. Mol Cancer Ther 3**:** 327-334.

Leisching, G., B. Loos, M. Botha and A.-M. Engelbrecht, 2015 Bcl-2 confers survival in cisplatin treated cervical cancer cells: circumventing cisplatin dose-dependent toxicity and resistance. Journal of translational medicine 13**:** 328-328.

Lewis, A., T. Hayashi, T.-P. Su and M. J. Betenbaugh, 2014 Bcl-2 family in inter-organelle modulation of calcium signaling; roles in bioenergetics and cell survival. Journal of bioenergetics and biomembranes 46**:** 1-15.

Li, L., B. Deng, G. Xing, Y. Teng, C. Tian *et al.*, 2007 PACT is a negative regulator of p53 and essential for cell growth and embryonic development. Proceedings of the National Academy of Sciences 104**:** 7951.

Liang, X. H., S. Mungal, A. Ayscue, J. D. Meissner, P. Wodnicki *et al.*, 1995 Bcl-2 protooncogene expression in cervical carcinoma cell lines containing inactive p53. J Cell Biochem 57**:** 509-521.

Lin, M., M. Ye, J. Zhou, Z. P. Wang and X. Zhu, 2019 Recent Advances on the Molecular Mechanism of Cervical Carcinogenesis Based on Systems Biology Technologies. Computational and Structural Biotechnology Journal 17**:** 241-250.

Lobo, R., D. Gershenson and G. Lentz, 2020 Malignant Diseases of the Cervix: Microinvasive and Invasive Carcinoma: Diagnosis and Management in *Comprehensive Gynecology*. Elsevier.

Lukac, A., N. Sulovic, S. Smiljic, A. N. Ilic and O. Saban, 2018 The Prevalence of the Most Important Risk Factors Associated with Cervical Cancer. Materia socio-medica 30**:** 131-135.

Mahapatra, E., S. Das, S. Biswas, A. Ghosh, D. Sengupta *et al.*, 2021 Insights of Cisplatin Resistance in Cervical Cancer: A Decision Making for Cellular Survival in *Cervical Cancer - A Global Public Health Treatise*, edited by R. Rajkumar.

Mahmoodi Chalbatani, G., H. Dana, E. Gharagouzloo, S. Grijalvo, R. Eritja *et al.*, 2019 Small interfering RNAs (siRNAs) in cancer therapy: a nano-based approach. International journal of nanomedicine 14**:** 3111-3128.

Maji, S., S. Panda, S. K. Samal, O. Shriwas, R. Rath *et al.*, 2018 Bcl-2 Antiapoptotic Family Proteins and Chemoresistance in Cancer. Adv Cancer Res 137**:** 37-75.

Makgoo, L., K. Laka and Z. Mbita, 2019 Downregulation of RBBP6 variant 1 during arsenic trioxide-mediated cell cycle arrest and curcumin-induced apoptosis in MCF-7 breast cancer cells, pp. FSO409 in *Future science OA*.

Makovec, T., 2019 Cisplatin and beyond: molecular mechanisms of action and drug resistance development in cancer chemotherapy. Radiology and oncology 53**:** 148-158.

Manikandan, S., S. Behera, N. M. Naidu, V. Angamuthu, O. F. B. Mohammed *et al.*, 2019 Knowledge and Awareness Toward Cervical Cancer Screening and Prevention Among the Professional College Female Students. Journal of pharmacy & bioallied sciences 11**:** S314-S320.

Mbita, Z., R. Hull, M. Mbele, T. Makhafola and Z. Dlamini, 2019 Expression Analysis of RbBP6 in human cancers: a Prospective biomarker. Anti-Cancer Drugs 30.

Mbita, Z., R. Hull, F. Mokoena, C.-H. Lai and Z. Dlamini, 2021 RBBP6 interactome: RBBP6 isoform 3/DWNN and Nek6 interaction is critical for cell cycle regulation and may play a role in carcinogenesis. Informatics in Medicine Unlocked 23**:** 100522.

Mbita, Z., M. Meyer, A. Skepu, M. Hosie, J. Rees *et al.*, 2011 De-regulation of the RBBP6 isoform 3/DWNN in human cancers. Molecular and cellular biochemistry 362**:** 249-262.

Mbulawa, Z. Z. A., D. Coetzee and A.-L. Williamson, 2015 Model systems of human papillomavirus-associated disease. BMC Infectious Diseases 15**:** 459.

Meijer, C. J., P. J. Snijders and A. J. van den Brule, 2000 Screening for cervical cancer: should we test for infection with high-risk HPV? CMAJ : Canadian Medical Association journal = journal de l'Association medicale canadienne 163**:** 535-538.

Midgley, C. A., and D. P. Lane, 1997 p53 protein stability in tumour cells is not determined by mutation but is dependent on Mdm2 binding. Oncogene 15**:** 1179-1189.

Minagawa, Y., J. Kigawa, H. Itamochi, Y. Kanamori, M. Shimada *et al.*, 1999 Cisplatin-resistant HeLa cells are resistant to apoptosis via p53-dependent and -independent Pathways. Japanese Journal of Cancer Research 90**:** 1373–1379.

Miyashita, T., and J. C. Reed, 1992 bcl-2 gene transfer increases relative resistance of S49.1 and WEHI7.2 lymphoid cells to cell death and DNA fragmentation induced by glucocorticoids and multiple chemotherapeutic drugs. Cancer Res 52**:** 5407-5411.

Moela, P., 2018 Functional studies of the RBBP6 (retinoblastoma binding protein 6) gene and its related genes in breast and cervical cancer: a promising diagnostic and management assay for cancer progression, pp. 250 in *Faculty of Science*. University of Witwatersrand, Gauteng, Johannesburg.

Moela, P., M. M. Choene and L. R. Motadi, 2014 Silencing RBBP6 (Retinoblastoma Binding Protein 6) sensitises breast cancer cells MCF7 to staurosporine and camptothecin-induced cell death. Immunobiology 219**:** 593-601.

Moela, P., and L. R. Motadi, 2016 RBBP6: a potential biomarker of apoptosis induction in human cervical cancer cell lines. OncoTargets and therapy 9**:** 4721-4735.

Mollaei, H., R. Safaralizadeh, E. Babaei, M. R. Abedini and R. Hoshyar, 2017 The anti-proliferative and apoptotic effects of crocin on chemosensitive and chemoresistant cervical cancer cells. Biomed Pharmacother 94**:** 307-316.

Moon, J. Y., I.-C. Song, Y. B. Ko and H. J. Lee, 2018 The combination of cisplatin and topotecan as a second-line treatment for patients with advanced/recurrent uterine cervix cancer. Medicine 97**:** e0340.

Motadi, L., K. Bhoola and Z. Dlamini, 2011 Expression and function of retinoblastoma binding protein 6 (RBBP6) in human lung cancer. Immunobiology 216**:** 1065-1073.

Motadi, L. R., M. M. Lekganyane and P. Moela, 2018 RBBP6 expressional effects on cell proliferation and apoptosis in breast cancer cell lines with distinct p53 statuses. Cancer management and research 10**:** 3357-3369.

Mthembu, N. N., 2013 Screening of Traditional Medicine for RBBP6 Anti-Cancer Therapy in Cervical Cancer, pp. in *Molecular and Cell Biology*. University of Witwatersrand, Johannesburg.

Mullan, A., and A. Marsh, 2020 Summary of Using Vero Cells in Biology Studies, pp.

Mwaka, A. D., C. G. Orach, E. M. Were, G. Lyratzopoulos, H. Wabinga *et al.*, 2016 Awareness of cervical cancer risk factors and symptoms: cross-sectional community survey in post-conflict northern

Uganda. Health expectations : an international journal of public participation in health care and health policy 19**:** 854-867.

Nascimento, A. V., A. Singh, H. Bousbaa, D. Ferreira, B. Sarmento *et al.*, 2017 Overcoming cisplatin resistance in non-small cell lung cancer with Mad2 silencing siRNA delivered systemically using EGFR-targeted chitosan nanoparticles. Acta biomaterialia 47**:** 71-80.

Niepel, M., M. Hafner, Q. Duan, Z. Wang, E. O. Paull *et al.*, 2017 Common and cell-type specific responses to anti-cancer drugs revealed by high throughput transcript profiling. Nature Communications 8**:** 1186.

Padilla, L. A., B. S. Leung and L. F. Carson, 2002 Evidence of an association between human papillomavirus and impaired chemotherapy-induced apoptosis in cervical cancer cells. Gynecol Oncol 85**:** 59-66.

Paulraj, F., F. Abas, N. H. Lajis, I. Othman, S. S. Hassan *et al.*, 2015 The Curcumin Analogue 1,5-Bis(2-hydroxyphenyl)-1,4-pentadiene-3-one Induces Apoptosis and Downregulates E6 and E7 Oncogene Expression in HPV16 and HPV18-Infected Cervical Cancer Cells. Molecules 20**:** 11830-11860.

Pectasides, D., K. Kamposioras, G. Papaxoinis and E. Pectasides, 2008 Chemotherapy for recurrent cervical cancer. Cancer Treatment Reviews 34**:** 603-613.

Peralta-Zaragoza, O., V. H. Bermúdez-Morales, C. Pérez-Plasencia, J. Salazar-León, C. Gómez-Cerón *et al.*, 2012 Targeted treatments for cervical cancer: a review. OncoTargets and therapy 5**:** 315-328.

Petry, K. U., 2014 HPV and cervical cancer. Scandinavian Journal of Clinical and Laboratory Investigation 244**:** 59-62; discussion 62.

Pinton, P., and R. Rizzuto, 2006 Bcl-2 and Ca2+ homeostasis in the endoplasmic reticulum. Cell Death & Differentiation 13**:** 1409-1418.

Porichi, O., M. E. Nikolaidou, A. Apostolaki, A. Tserkezoglou, N. Arnogiannaki *et al.*, 2009 BCL-2, BAX and P53 expression profiles in endometrial carcinoma as studied by real-time PCR and immunohistochemistry. Anticancer Res 29**:** 3977-3982.

Promraksa, B., J. Daduang, T. Khampitak, R. Tavichakorntrakool, A. Koraneekit *et al.*, 2015 Anticancer Potential of Cratoxylum formosum Subsp. Pruniflorum (Kurz.) Gogel Extracts Against Cervical Cancer Cell Lines, pp. 6117-6121 in *Asian Pacific journal of cancer prevention : APJCP*.

Pugh, D. J. R., E. Ab, A. Faro, P. T. Lutya, E. Hoffmann *et al.*, 2006 DWNN, a novel ubiquitin-like domain, implicates RBBP6 in mRNA processing and ubiquitin-like pathways. BMC Structural Biology 6**:** 1.

Putral, L. N., M. J. Bywater, W. Gu, N. A. Saunders, B. G. Gabrielli *et al.*, 2005 RNA interference against human papillomavirus oncogenes in cervical cancer cells results in increased sensitivity to cisplatin. Mol Pharmacol 68**:** 1311-1319.

Reed, J. C., 2018 Bcl-2 on the brink of breakthroughs in cancer treatment. Cell Death & Differentiation 25**:** 3-6.

Roy, M., and S. Chakraborty Mukherjee, 2014 Reversal of Resistance towards Cisplatin by Curcumin in Cervical Cancer Cells. Asian Pacific journal of cancer prevention : APJCP 15**:** 1403-1410.

Sabeena, S., P. Bhat, V. Kamath and G. Arunkumar, 2017 Possible non-sexual modes of transmission of human papilloma virus. Journal of Obstetrics and Gynaecology Research 43**:** 429-435.

Sanchez-Sandoval, A. L., and J. C. Gomora, 2019 Contribution of voltage-gated sodium channel β-subunits to cervical cancer cells metastatic behavior. Cancer cell international 19**:** 35-35.

Santacroce, L., M. Di Cosola, L. Bottalico, S. Topi, I. A. Charitos *et al.*, 2021 Focus on HPV Infection and the Molecular Mechanisms of Oral Carcinogenesis. Viruses 13**:** 559.

Šarenac, T., and M. Mikov, 2019 Cervical Cancer, Different Treatments and Importance of Bile Acids as Therapeutic Agents in This Disease. Frontiers in Pharmacology 10.

Schiffman, M., and D. Solomon, 2013 Cervical-cancer screening with Human Papillomavirus and cytologic cotesting. New England Journal of Medicine 369**:** 2324-2331.

Shamas-Din, A., J. Kale, B. Leber and D. W. Andrews, 2013 Mechanisms of action of Bcl-2 family proteins. Cold Spring Harbor perspectives in biology 5**:** a008714.

Shen, D.-W., L. M. Pouliot, M. D. Hall and M. M. Gottesman, 2012 Cisplatin resistance: a cellular self-defense mechanism resulting from multiple epigenetic and genetic changes. Pharmacological reviews 64**:** 706-721.

Shrestha, A. D., D. Neupane, P. Vedsted and P. Kallestrup, 2018 Cervical Cancer Prevalence, Incidence and Mortality in Low and Middle Income Countries: A Systematic Review. Asian Pacific Journal of Cancer Prevention 19**:** 319-324.

Siddik, Z. H., 2003 Cisplatin: mode of cytotoxic action and molecular basis of resistance. Oncogene 22**:** 7265-7279.

Singh, E., 2019 National Cancer Registry - NICD, pp.

Singh, E., M. Sengayi, M. Urban, C. Babb, P. Kellett *et al.*, 2014 The South African National Cancer Registry: an update. The Lancet Oncology 15**:** e363.

Stelzle, D., L. F. Tanaka, K. K. Lee, A. Ibrahim Khalil, I. Baussano *et al.*, 2021 Estimates of the global burden of cervical cancer associated with HIV. The Lancet Global Health 9**:** e161-e169.

Sung, H., J. Ferlay, R. L. Siegel, M. Laversanne, I. Soerjomataram *et al.*, 2021 Global Cancer Statistics 2020: GLOBOCAN Estimates of Incidence and Mortality Worldwide for 36 Cancers in 185 Countries. CA: A Cancer Journal for Clinicians 71**:** 209-249.

Swanepoel, B., G. M. Nitulescu, O. T. Olaru, L. Venables and M. van de Venter, 2019 Anti-Cancer Activity of a 5-Aminopyrazole Derivative Lead Compound (BC-7) and Potential Synergistic Cytotoxicity with Cisplatin against Human Cervical Cancer Cells. International Journal of Molecular Sciences 20**:** 5559.

Thomas, M., and L. Banks, 1999 Human papillomavirus (HPV) E6 interactions with Bak are conserved amongst E6 proteins from high and low risk HPV types. J Gen Virol 80 (Pt 6)**:** 1513-1517.

Tsuda, N., H. Watari and K. Ushijima, 2016 Chemotherapy and molecular targeting therapy for recurrent cervical cancer. Chinese journal of cancer research = Chung-kuo yen cheng yen chiu 28**:** 241-253.

Tuohetimulati, G., M. Zhu, J. Chen and M. Niyazi, 2018 Expressions and clinical significance of Bcl-2, Bcl-xL and c-IAP1 protein in cervical cancer, pp.

Uf, C., M. Ntwasa and E. Nweke, 2018 The Retinoblastoma Binding Protein 6 Family is Essential for Embryonic Development and Carcinogenesis.

Vaccarella, S., M. Laversanne, J. Ferlay and F. Bray, 2017 Cervical cancer in Africa, Latin America and the Caribbean and Asia: Regional inequalities and changing trends. International Journal of Cancer 141**:** 1997-2001.

Venkatraman, M., R. J. Anto, A. Nair, M. Varghese and D. Karunagaran, 2005 Biological and chemical inhibitors of NF-kappaB sensitize SiHa cells to cisplatin-induced apoptosis. Mol Carcinog 44**:** 51-59.

Wang, H., X. Liu, J. X. Sun, J. H. Liu, N. Liu *et al.*, 2016 Inhibition of the cervical cancer growth by cidan and cisplatin combination through induction of apoptosis. 9**:** 13872-13877.

Wang, S.-J., Z. Cheng, C. Peng, H. Zhang, Y.-P. Jiang *et al.*, 2013 Plants and cervical cancer: An overview. Expert opinion on investigational drugs 22.

Wang, S. S., X. Xie, C. S. Wong, Y. Choi and M. C. Fung, 2014 HepG2 cells recovered from apoptosis show altered drug responses and invasiveness. Hepatobiliary Pancreat Dis Int 13**:** 293-300.

Wesierska-Gadek, J., D. Schloffer, V. Kotala and M. Horky, 2002 Escape of p53 protein from E6-mediated degradation in HeLa cells after cisplatin therapy. Int J Cancer 101**:** 128-136.

Wilailak, S., M. Kengsakul and S. Kehoe, 2021 Worldwide initiatives to eliminate cervical cancer. International Journal of Gynecology & Obstetrics 155**:** 102-106.

Wipperman, J., T. Neil and T. Williams, 2018 Cervical Cancer: Evaluation and Management. Am Fam Physician 97**:** 449-454.

Xiao, C., Y. Wang, M. Zheng, J. Chen, G. Song *et al.*, 2018a RBBP6 increases radioresistance and serves as a therapeutic target for preoperative radiotherapy in colorectal cancer. Cancer science 109**:** 1075-1087.

Xiao, J.-B., X.-L. Li, L. Liu, G. Wang, S.-N. Hao *et al.*, 2018b The association of semaphorin 5A with lymph node metastasis and adverse prognosis in cervical cancer. Cancer cell international 18**:** 87.

Xu, L., Q. Xie, L. Qi, C. Wang, N. Xu *et al.*, 2018a Bcl-2 overexpression reduces cisplatin cytotoxicity by decreasing ER-mitochondrial Ca2+ signaling in SKOV3 cells. Oncology reports 39**:** 985-992.

Xu, Y., C. So, H. M. Lam, M. C. Fung and S. Y. Tsang, 2018b Apoptosis Reversal Promotes Cancer Stem Cell-Like Cell Formation. Neoplasia 20**:** 295-303.

Ye, Q.-F., Y.-C. Zhang, X.-Q. Peng, Z. Long, Y.-Z. Ming *et al.*, 2012 Silencing Notch-1 induces apoptosis and increases the chemosensitivity of prostate cancer cells to docetaxel through Bcl-2 and Bax. Oncology letters 3**:** 879-884.

Yu, S., and A. A. Garcia, 2015 Advancements in Recurrent and Metastatic Cervical Cancer. The American Journal of Hematology/Oncology 11**:** 26-31.

Zheng, H.-C., 2017 The molecular mechanisms of chemoresistance in cancers. Oncotarget 8**:** 59950-59964.

Zhou, X. L., and M. Wang, 2015 Expression levels of survivin, Bcl-2, and KAI1 proteins in cervical cancer and their correlation with metastasis. Genetics and molecular research: GMR 14**:** 17059-17067.

Zhu, H., H. Luo, W. Zhang, Z. Shen, X. Hu *et al.*, 2016 Molecular mechanisms of cisplatin resistance in cervical cancer. Drug design, development and therapy 10**:** 1885-1895.

Zisowsky, J., S. Koegel, S. Leyers, K. Devarakonda, M. U. Kassack *et al.*, 2007 Relevance of drug uptake and efflux for cisplatin sensitivity of tumor cells. Biochem Pharmacol 73**:** 298-307.

APPENDICES

Appendix A: Percentage cell viability calculations

Absorbance and percentage cell viability for **(A)** HeLa and **(B)** CaSki cells treated with Cisplatin at varying concentrations prepared by a 2-fold serial dilution.

A

HeLa + Cisplatin							
Concentration (µg/mL)	**Untreated**	**50**	**25**	**12.5**	**6.25**	**3.125**	**Blank**
Absorbance 1	1,013	0,376	0,505	1,56	1,493	1,528	0,045
Viability 1 (%)	100	34,1942149	47,5206612	156,508264	149,586777	153,202479	
Absorbance 2	1,329	0,396	0,611	1,587	1,439	1,656	0,046
Viability 2 (%)	100	27,2798129	44,0374123	120,109119	108,573655	125,48714	
Absorbance 3	1,279	0,379	0,585	1,226	1,549	1,614	0,046
Viability 3 (%)	100	27,0072993	43,7145174	95,701541	121,89781	127,169505	
Average Absorbance	1,207	0,38366667	0,567	1,45766667	1,49366667	1,59933333	0,04566667
Average Viability (%)	100,00	29,49	45,09	124,11	126,69	135,29	
Standard Deviation	0	4,07297954	2,11045073	30,5997965	20,9216319	15,5385872	

B

CasKi + Cisplatin							
Concentration (µg/mL)	**Untreated**	**50**	**25**	**12.5**	**6.25**	**3.125**	**Blank**
Absorbance 1	2,583	1,02	1,31	2,084	2,778	2,852	0,046
Viability 1 (%)	100	38,3918013	49,8226251	80,3310997	107,686244	110,603074	
Absorbance 2	2,821	0,9226	1,071	2,045	2,595	2,699	0,047
Viability 2 (%)	100	31,5645278	36,9142033	72,0259553	91,85292	95,6020187	
Absorbance 3	2,564	1,008	1,597	2,208	2,748	2,999	0,046
Viability 3 (%)	100	38,2049245	61,5965052	85,8617951	107,307387	117,275616	
Average Absorbance	2,656	0,98353333	1,326	2,11233333	2,707	2,85	0,04633333
Average Viability (%)	100	36,0537512	49,4444445	79,4062834	102,282183	107,826903	
Standard Deviation	0	3,88890424	12,345496	6,96412805	9,03399335	11,1002949	

Formula:

$$\%\ Cell\ Viability = \left[\frac{(Treated\ Absorbance\ -\ Blank\ Absorbance)}{(Untreated\ Absorbance\ -\ Blank\ Absorbance)}\right] \times 100$$

Appendix B: RT-qPCR optimizations

Appendix B1: Temperature gradients

Amplification curves for **(A)** *RBBP6* **(B)** *p53* and **(C)** *Bcl-2* primers at temperature gradient range of 55.0 – 60.0 ºC

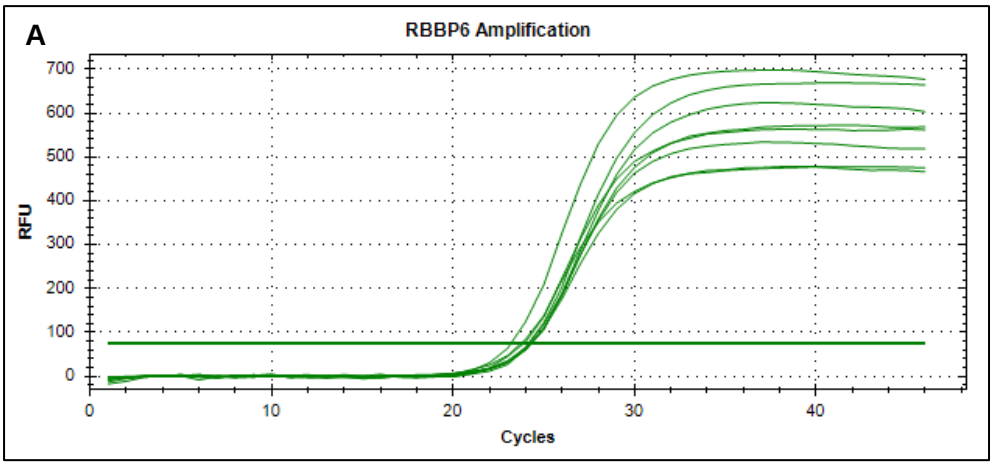

RBBP6	
Ta	**Cq**
60.0ºC	23.70
59.7ºC	23.85
59.2ºC	23.16
58.2ºC	24.24
57.0ºC	24.16
56.0ºC	24.30
55.3ºC	24.12
55.0ºC	24.25

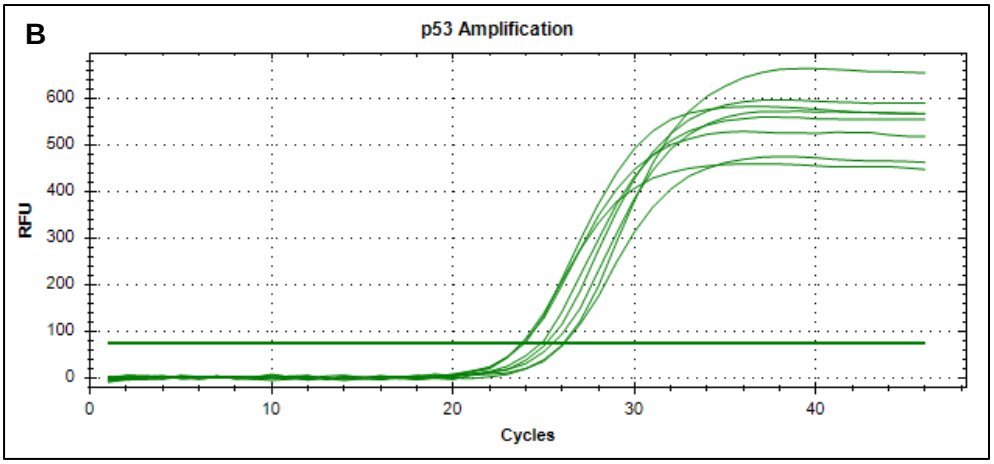

p53	
Ta	**Cq**
60.0ºC	23.74
59.7ºC	23.81
59.2ºC	23.94
58.2ºC	24.84
57.0ºC	25.13
56.0ºC	25.48
55.3ºC	26.08
55.0ºC	26.12

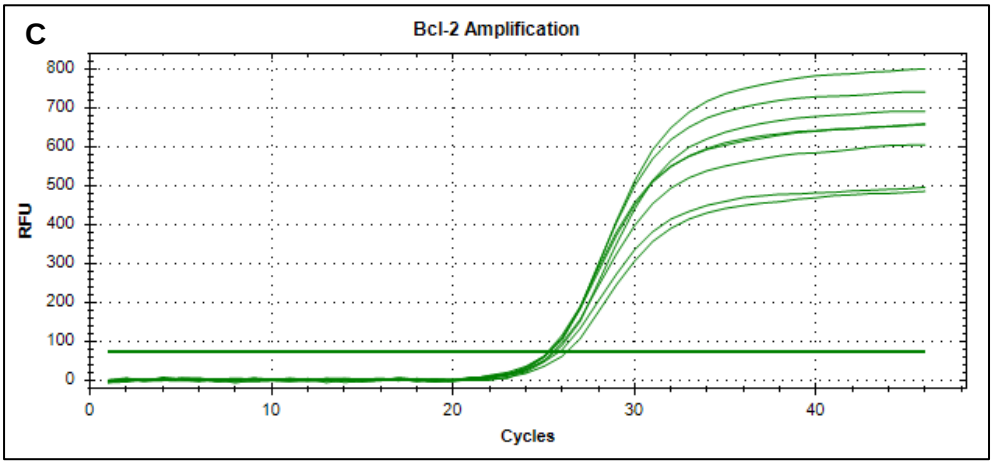

Bcl-2	
Ta	**Cq**
60.0ºC	25.89
59.7ºC	25.28
59.2ºC	25.24
58.2ºC	25.53
57.0ºC	25.32
56.0ºC	25.63
55.3ºC	25.34
55.0ºC	26.29

Appendix B2: Standard curves

Standard curves for **(A)** *GAPDH*, **(B)** *RBBP6*, **(C)** *p53* and **(D)** *Bcl-2* primers after a 1:10 serial dilution

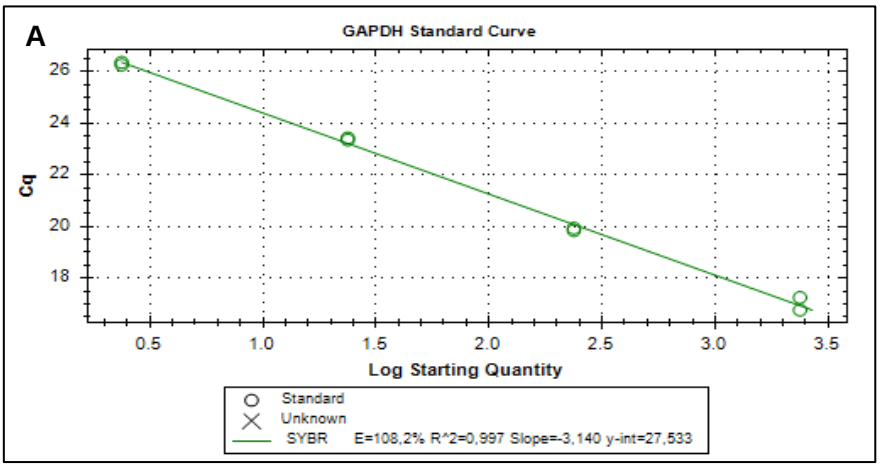

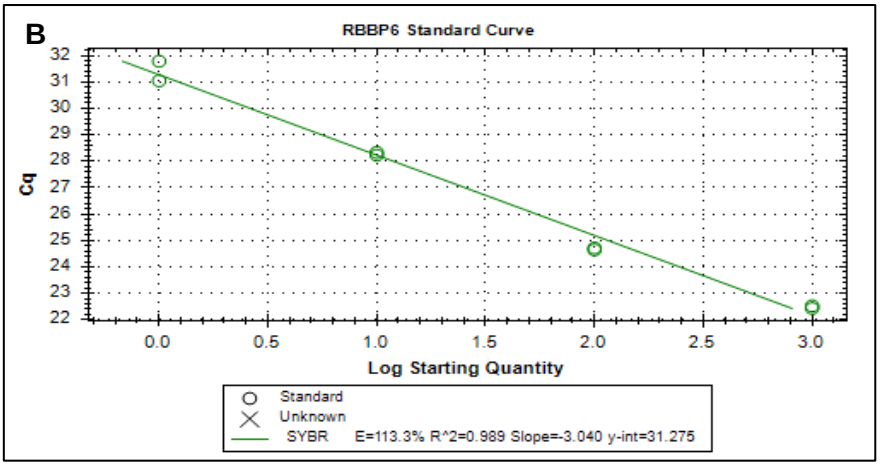

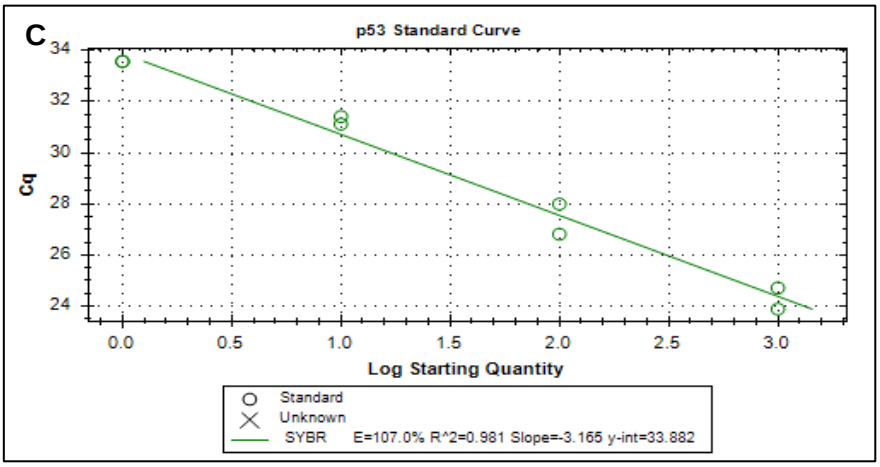

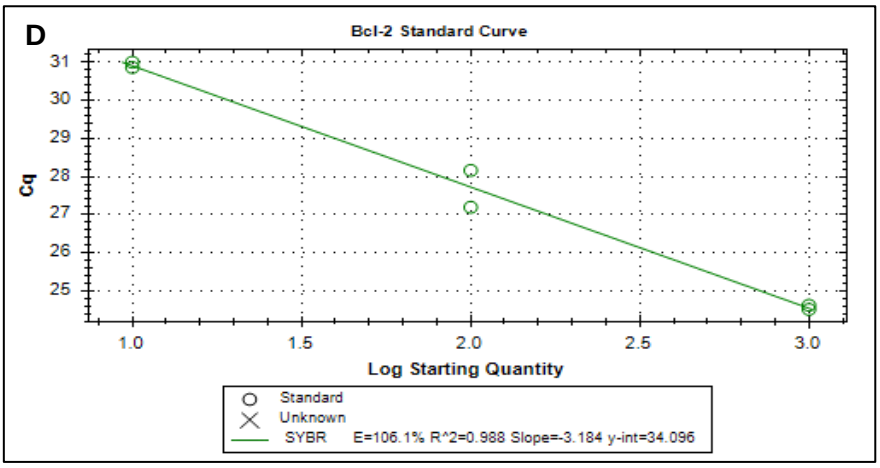
D
Bcl-2 Standard Curve
Cq
31
30
29
28
27
26
25
1.0
1.5
2.0
2.5
3.0
Log Starting Quantity
Standard
Unknown
SYBR E=106.1% R^2=0.988 Slope=-3.184 y-int=34.096

Appendix B3: Melting curves

Melting curves for **(A)** *GAPDH*, **(B)** *RBBP6*, **(C)** *p53* and **(D)** *Bcl-2* primers

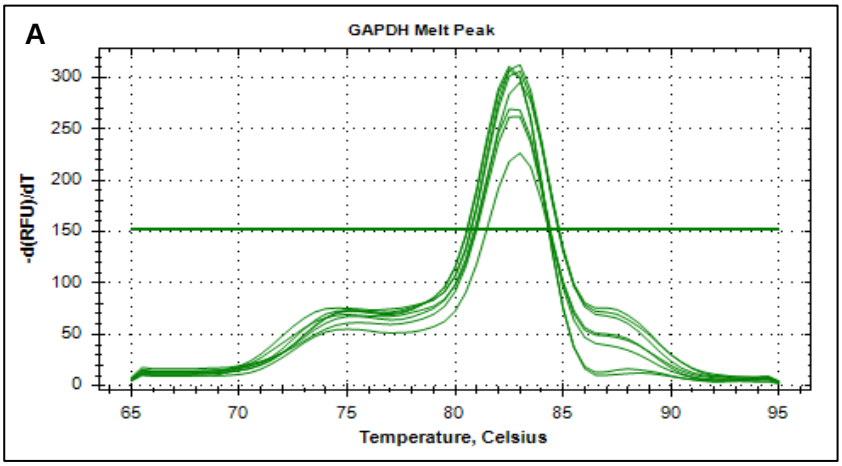

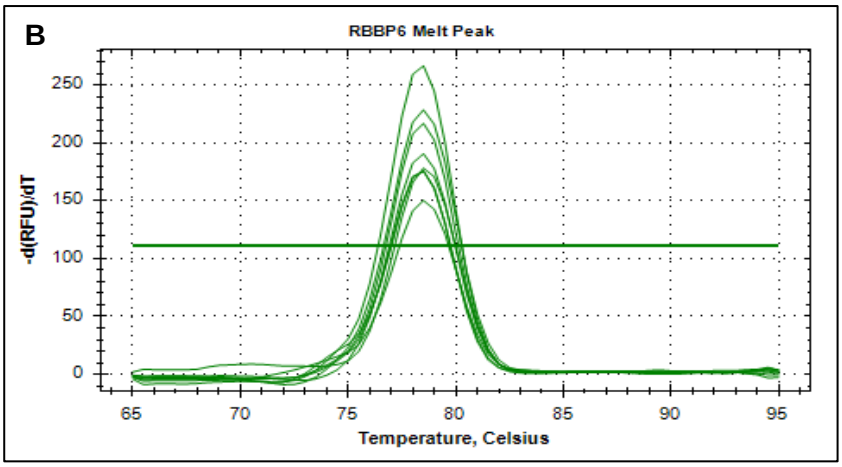

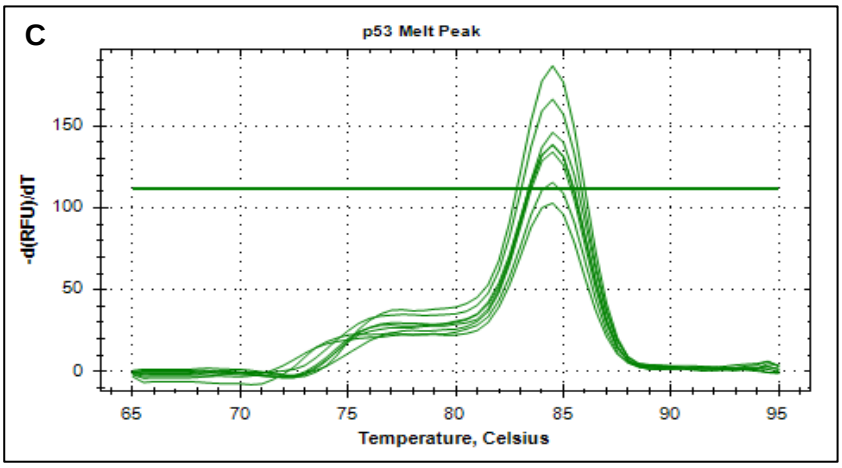

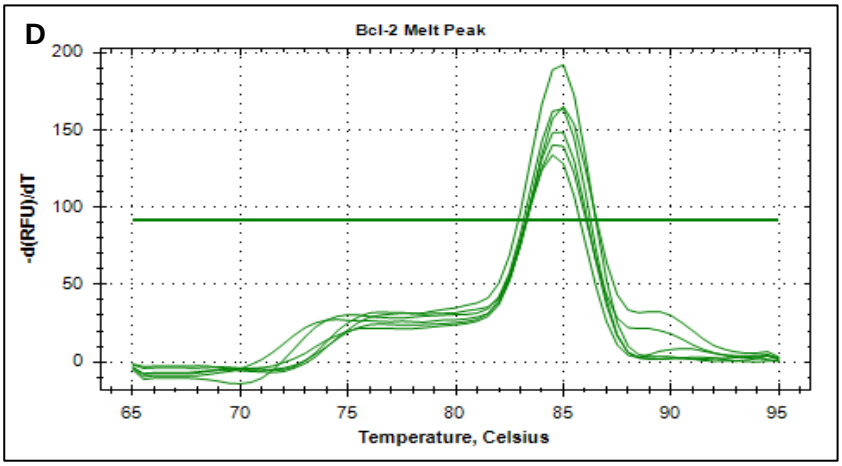
D
Bcl-2 Melt Peak
200
150
100
50
0
-d(RFU)/dT
65
70
75
80
85
90
95
Temperature, Celsius

TURNITIN REPORT

MSc Dissertation

ORIGINALITY REPORT

14%	13%	12%	%
SIMILARITY INDEX	INTERNET SOURCES	PUBLICATIONS	STUDENT PAPERS

PRIMARY SOURCES

1	Repository.up.ac.za Internet Source	2%
2	www.ncbi.nlm.nih.gov Internet Source	1%
3	Pontsho Moela, Mpho M.S. Choene, Lesetja R. Motadi. "Silencing RBBP6 (Retinoblastoma Binding Protein 6) sensitises breast cancer cells MCF7 to staurosporine and camptothecin-induced cell death", Immunobiology, 2014 Publication	1%
4	wiredspace.wits.ac.za Internet Source	1%
5	hdl.handle.net Internet Source	<1%
6	Felicia Paulraj, Faridah Abas, Nordin Lajis, Iekhsan Othman, Sharifah Hassan, Rakesh Naidu. "The Curcumin Analogue 1,5-Bis(2-hydroxyphenyl)-1,4-pentadiene-3-one Induces Apoptosis and Downregulates E6 and E7	<1%